AD-779 494

LAUNCH TUBE AND ROCKET INTERACTION FOR AN AERODYNAMICALLY NEUTRAL SPIN-STABILIZED FREE ROCKET

Joe W. Reece, et al

Auburn University

Prepared for:

Army Missile Command

April 1974

Unclassified

Security Classification

DOCUMENT CONTROL DATA - R & D AD-779 494

(Security classification of title, body of abstract and indexing annotation must be entered when the overall report is classified)

1. ORIGINATING ACTIVITY (Corporate author)	2a. REPORT SECURITY CLASSIFICATION
School of Engineering (ME Dept.) Auburn University Auburn, Alabama 36830	Unclassified
	2b. GROUP

3. REPORT TITLE

Launch Tube and Rocket Interaction for An Aerodynamically Neutral Spin-Stabilized Free Rocket

4. DESCRIPTIVE NOTES (Type of report and inclusive dates)

Technical (October 15, 1972 - October 15, 1973)

5. AUTHOR(S) (First name, middle initial, last name)

Joe W. Reece, Gerry A. Lindholm, and William A. Tomb

6. REPORT DATE	7a. TOTAL NO. OF PAGES	7b. NO. OF REFS
April 1974	133	18

8a. CONTRACT OR GRANT NO.	9a. ORIGINATOR'S REPORT NUMBER(S)
DAAH01-73-C-0226 b. PROJECT NO.	
c.	9b. OTHER REPORT NO(S) (Any other numbers that may be assigned this report)
d.	

10. DISTRIBUTION STATEMENT

Distribution of this document is unlimited

11. SUPPLEMENTARY NOTES	12. SPONSORING MILITARY ACTIVITY
	Army Missile Command

13. ABSTRACT

A linearized model is developed for the dynamics of a spinning, unbalanced, rigid rocket during the tip-off phase of launch. Mallaunch rates for the rocket are obtained for the short time interval from tip-off to end of guidance. The results show that tip-off should not be a major cause of mallaunch for very high spin rates and short tip-off times.

Rocket flexibility is modelled for the launch phase. The model accounts for bearing clearances, a variable stiffness motor section and allows for the 3-D motion of a rigid warhead. The phenomenon of whirling is investigated and the bent configuration of the rocket is calculated for synchronous whirling. The resulting mallaunch rates agree with reported range data.

Dynamical equations of motion are developed for a multitube launcher assembly for a spin-stabilized rocket. A parametric study is performed to minimize the mallaunch rates affecting missile flight. The results show that prudent selection of specific structural parameters can minimize mallaunch rates.

DD FORM 1 NOV 68 1473 (PAGE 1)

S/N 0101-807-6801

I

Unclassified

Security Classification

14 KEY WORDS	LINK A		LINK B		LINK C	
	ROLE	WT	ROLE	WT	ROLE	WT
Spinning Rocket Dynamics						
Flexible Body Dynamics						
Rocket Launch Dynamics						
Rocket Launcher Dynamics						
Rocket Mallaunch						
Rocket Malaim						
Tip-off						
Whirling of Flexible Rockets						

TECHNICAL REPORT

LAUNCH TUBE AND ROCKET INTERACTION FOR AN AERODYNAMICALLY NEUTRAL SPIN-STABILIZED FREE ROCKET

by

Reece, Joe W.
Lindholm, G.
and
Tomb, W. A.

under contract with

U. S. ARMY MISSILE COMMAND
REDSTONE ARSENAL
Contract Number DAAH01-73-C-0226

AUBURN UNIVERSITY
SCHOOL OF ENGINEERING

ENGINEERING EXPERIMENT STATION

Mechanical Engineering Department

April 1974

TABLE OF CONTENTS

PREFACE

This report presents results of a study designed to investigate the dynamics of a spin-stabilized free rocket during the launch phase of motion. The models developed are applicable for the case of very high spin rates similar to those achieved by ANSSR, an aerodynamically neutral spin-stabilized rocket developed by Emerson Electric Company for the U. S. Army [1]*. This 105 mm rocket is pre-spun in its launcher by four auxiliary motors thrusting tangentially at the rear of the round. The boost phase of the flight does not begin until these motors have been exhausted. Thus, the rocket exits the launcher with spin rates (10,000 rpm) considerably greater than those considered by previous investigators [2]. A double-diameter launcher tube is used to minimize tip-off effects.

The design objective for the ANSSR system has been to utilize the stabilizing effect of the extremely high spin rate in lieu of fins to decrease the overall wind sensitivity of the weapon. A factor affecting the accuracy of any free rocket is mallaunch (that component of the rocket angular rate vector not aligned with the launcher bore axis at the instant of release). Mallaunch values observed with optical lever and camera techniques at Redstone Arsenal were higher than expected [3]. This investigation has addressed the problem of mallaunch due to

---

* Numbers in square brackets refer to references at the end of the preface.

- tip-off effects
- in-tube rocket bending
- launcher motion caused by rocket excitation

This report is presented in three distinct sections. Each section is complete with its own list of symbols, figures, tables and references. Results obtained are discussed at the end of each section and will not be belabored here. However, we will mention that the results show

- that tip-off should not be a major cause of mallaunch
- that body bending can be a major cause of mallaunch
- that the launcher support system can be designed so as to minimize mallaunch

The diligent efforts of the project leader's co-workers Messrs. Lindholm and Tomb is hereby acknowledged. The calculations were made with the help of Mr. John B. Hill. Also, the skill and extreme good humor of Mrs. Dianne Fretwell along with Mr. Robert Sullivan and Mr. Robert Young were indispensable in preparing the manuscript.

The research team, during the course of this investigation, has enjoyed the cooperation of the Aeroballistic Directorate of Redstone

Arsenal and particularly that of Messrs. Conard and Vest of the Systems Evaluation Branch.

Joe W. Reece
Project Leader

PREFACE REFERENCES

1. Bauman, R., "ANSSR Flight Test Program," Volume I, Technical Report, Emerson Electric Company Report No. 2362, 18 February 1972.

2. Bullock, R. C. and Harrington, W. J., "Summary Report on Study of the Gun-Boosted Rocket System," Contract No. DA-01-009 ORD-1022, North Carolina State Final Report, Copy No. 101, 15 December 1962.

3. Pell, K. M. and Vest, C. L., "A Study of Selected Problems based on ANSSR Flight Tests, RD-72-25, U. S. Army Missile Command, Redstone Arsenal, Alabama, 1972.

MASTER LIST OF FIGURES

SECTION I

SECTION II

SECTION III

MASTER LIST OF TABLES

SECTION I

MALLAUNCH DUE TO TIP-OFF

ABSTRACT

A linearized model is developed for the dynamics of a spinning, unbalanced, rigid rocket during the tip-off phase of launch. Mallaunch rates for the rocket are obtained for the short time interval from tip-off to end of guidance. The results show that tip-off should not be a major cause of mallaunch for very high spin rates and short tip-off times.

LIST OF SYMBOLS

X,Y,Z	ground reference
$\hat{i},\hat{j},\hat{k}$	unit vectors of X,Y,Z
x,y,z	body reference
$\bar{e}_1,\bar{e}_2,\bar{e}_3$	unit vectors of x,y,z
ψ,θ	Euler Angles
$\underset{\sim}{\omega}^{g}_{R}$	angular rotation vector of x,y,z with respect to X,Y,Z
$\underset{\sim}{\omega}^{g}_{R}$	angular rotation vector of the rocket with respect to X,Y,Z
$\bar{\Omega}$	angular rotation vector of the rocket with respect to x,y,z (spin rate of rocket)
$\bar{H}_o$	angular momentum vector of the rocket with respect to the origin of x,y,z
$\bar{M}_o$	external moment vector with respect to the origin of x,y,z
I_{xx},I_{yy},I_{zz}	principle moments of inertia of the rocket with respect to x,y,z
$\bar{R}$	front bearing reaction vector
$\bar{T}$	thrust vector
$\bar{F}_I$	inertia load vector
m	rocket mass
E	distance of rocket mass center from y-axis

$\bar{r}$	position vector of the c.m. of the rocket with respect to x,y,z
M_{xo}, M_{yo}, M_{zo}	components of $\bar{M}_o$ expressed in x,y,z
g	32.2 ft/sec^2
Θ, Ψ	transfer functions of Θ and Ψ
S	eigenvalues of the system
$\lvert\bar{\omega}_p\rvert$	magnitude of the pitch mallaunch rate
$\lvert\bar{\omega}_y\rvert$	magnitude of the yaw mallaunch rate
V	approximate rocket velocity at the end of guidance
a	average rocket acceleration from boost motor ignition until the end of guidance
s	guidance length
δ	bearing mismatch - longitudinal
t	total tip-off time

A. INTRODUCTION

A possible source of mallaunch for the ANSSR Rocket is due to what has come to be called the "tip-off" effect. This phenomenon occurs in the time period after the rocket's rear bearing has lost its launcher tube support while the front bearing retains its support. Due to the extremely small time of contact it is possible to obtain a closed form solution for a linearized dynamical model of the rocket motion during "tip-off". The process of analysis allows the capability of treating both static and dynamic unbalances. The mallaunch rates, caused solely by tip-off, which are predicted by this model are the pitch and yaw rotation rates for the rocket immediately after the front bearing has lost its launch tube support, i.e., as the rocket becomes free. These rates are depicted in Figure 1.

The spinning, unbalanced, rigid (i.e., no bending) rocket during the tip-off phase is open to the same sort of dynamic analysis usually applied to the classical dropped gyro [1]. A significant difference is the inclusion of the pertubation of the rocket motion due to static and dynamic mass unbalances. As a result, this analysis yields a set of linearized equations of motion rather than the more general solution utilizing elliptic functions [1].

Shown in Figure 2 is the configuration of the rocket in the tip-off phase. In the analysis, the rocket is assumed to be simply supported by its front bearing. These simple supports are aligned with the

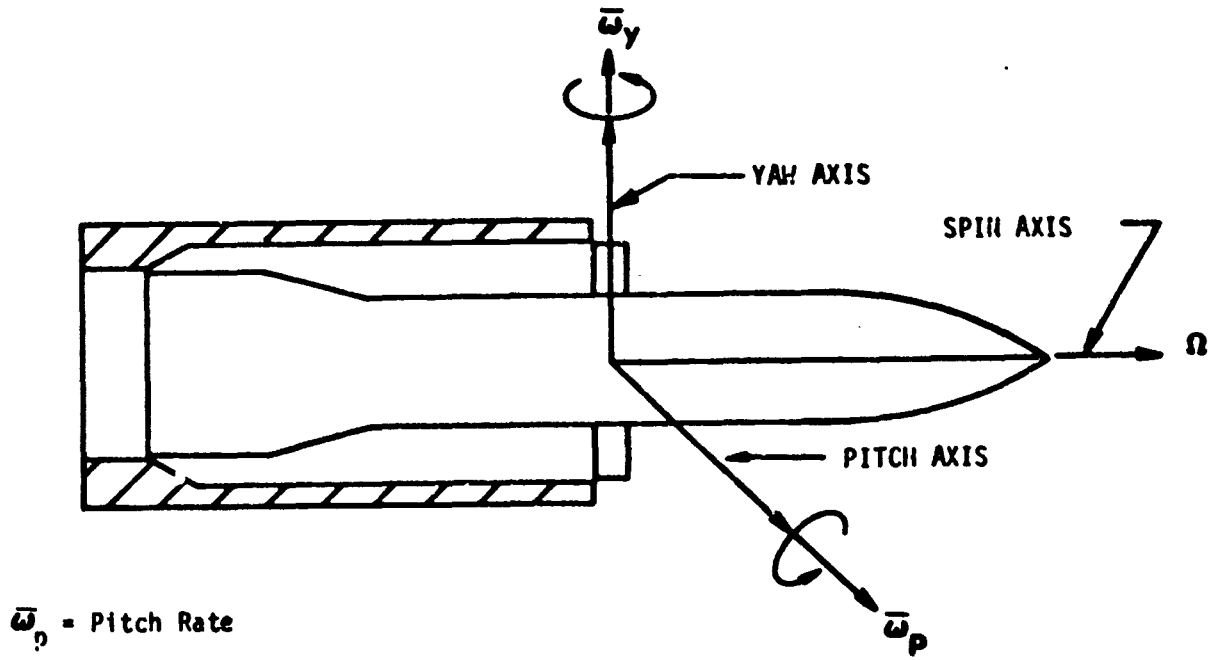

$\bar{\omega}_p$ = Pitch Rate

$\bar{\omega}_y$ = Yaw Rate

Figure 1. Depiction of pitch and yaw mallaunch rates

geometric center of the front bearing. At "time zero", (i.e., when the rear bearing has lost its launcher tube support) the position of the rocket is as shown in Figure 2.

The physical characteristics used in this analysis are presented in Table I.

Rocket Mass (Slug)	Traverse M.I. (Slug-ft^2)	Axial M.I (Slug-ft^2)	*C.M. Location (ft)
1.54	2.2	0.03	2.058

TABLE I. Rocket Characteristics (ANSSR II)

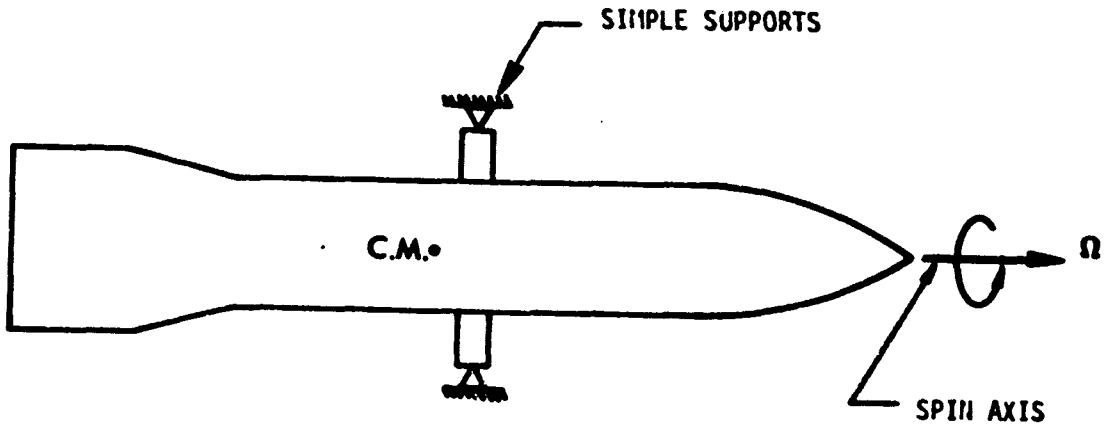

Figure 2. Rocket configuration in the tip-off phase

B. ANALYSIS

The position of the rocket in space can, at any time, be described by the two independent Euler angles shown in Figure 3.

The coordinate systems and Euler angles used in the analysis are defined as follows:

- Ground Reference: Ground reference is (X,Y,Z) with respective unit vectors $(\hat{i},\hat{j},\hat{k})$. The origin is fixed at the geometric center of the front bearing. The Y axis is taken positive going out of the launcher tube's longitudinal axis. The Z axis is taken positive up and parallel to the local vertical. The X axis completes a right hand system. All equations of motion will be written with respect to this coordinate system. This can be done as the acceleration of point "o" is essentially parallel to the acceleration of the rocket C.M. for the short time period involved. This frame will be designated as "frame g".

- Body Reference: Body reference is (x,y,z) with respective unit vectors $(\bar{e}_1,\bar{e}_2,\bar{e}_3)$. The origin (point "o") of this frame is fixed coincident with that of frame g. At time zero this frame is aligned with frame g (i.e., $\psi = \theta = 0.0$). At any time, the position of the body reference with respect to frame g is defined by the Euler angles ψ and θ as in Figure 3. This frame will be designated as "frame b".

It is important to note that x and z do not spin with the rocket, i.e., the rocket spins about the y axis of frame b.

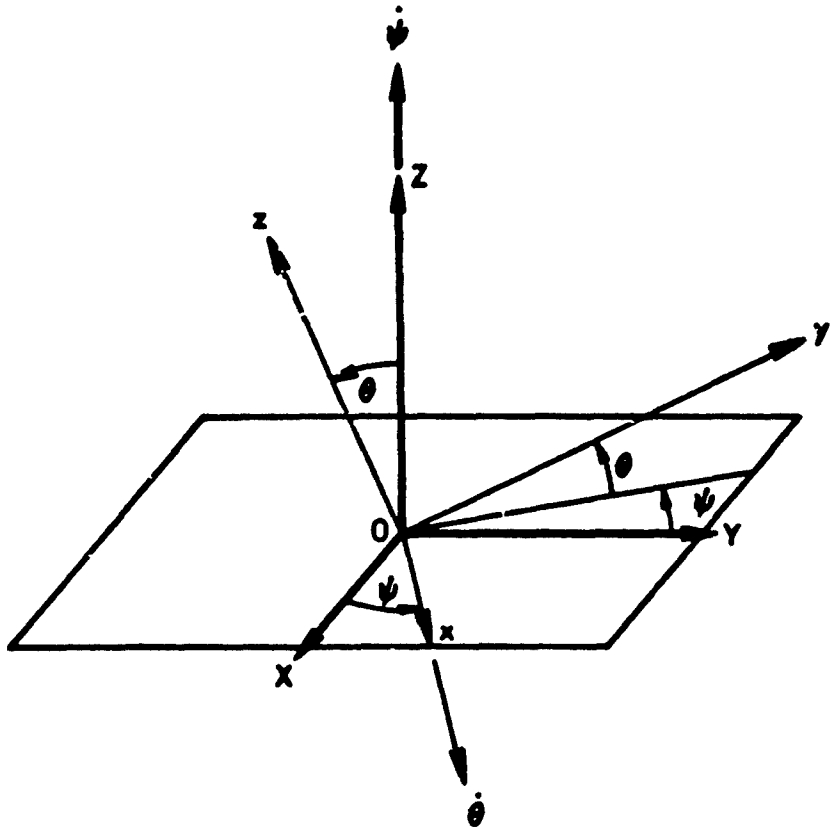

Figure 3. Rocket Euler Angles and Coordinate Systems

• System Euler Angles: The two independent Euler angles that describe the position of frame b with respect to frame g are ψ and θ. ψ is the first angle of rotation about Z and θ is the second angle of rotation about x. Both angles and their rates are expressed in rad and rad/sec respectively.

The relation between the coordinates of frame b and those of frame g is:

$$\begin{bmatrix} x \\ y \\ z \end{bmatrix} = [A] \cdot \begin{bmatrix} X \\ Y \\ Z \end{bmatrix} \qquad (1)$$

with matrix [A] defined as:

$$[A] = \begin{bmatrix} 1 & 0 & 0 \\ 0 & C\theta & S\theta \\ 0 & -S\theta & C\theta \end{bmatrix} \cdot \begin{bmatrix} C\psi & S\psi & 0 \\ -S\psi & C\psi & 0 \\ 0 & 0 & 1 \end{bmatrix} \qquad (2)$$

where $C\theta$ is taken to be $\cos(\theta)$, etc.

Now:

$\underline{\omega}^{g}_{b}$ = the angular rate of frame b with respect to frame g ($\underline{\omega}^{d}$ rad/sec).

$\underline{\omega}^{g}_{R}$ = the angular rate of the rocket with respect to frame g ($\underline{\omega}^{d}$ rad/sec).

$\bar{\Omega}$ = the angular rate of the rocket with respect to frame b ($\underline{\omega}^{d}$ rad/sec).

The above angular rates are given by the following equations:

$$\underline{\omega}^{g}_{b} = \dot{\theta}\,\bar{e}_1 + \dot{\psi}S\theta\,\bar{e}_2 + \dot{\psi}C\theta\,\bar{e}_3 \qquad (3)$$

$$g_{\bar{\omega}}R = \dot{\theta}\,\bar{e}_1 + (\dot{\psi}S\theta + \Omega)\,\bar{e}_2 + \dot{\psi}C\theta\,\bar{e}_3 \qquad (4)$$

$$\bar{\Omega} = \Omega\,\bar{e}_2 \qquad (5)$$

It follows that the angular momentum vector of the rocket expressed in frame b is:

$$\bar{H}_o = I_{xx}\dot{\theta}\,\bar{e}_1 + I_{yy}(\dot{\psi}S\theta + \Omega)\,\bar{e}_2 + I_{zz}\dot{\psi}C\theta\,\bar{e}_3 \qquad (6)$$

The sum of all external moments about point "0" must be equal to the first time derivative of $\bar{H}_o$ with respect to frame g. So:

$$\bar{M}_o = \frac{d}{dt}(\bar{H}_o) \qquad (7)$$

or

$$\bar{M}_o = \dot{\bar{H}}_o\Big|_{\text{frame b}} + g_{\bar{\omega}}{}^{b} \times \bar{H}_o \qquad (8)$$

If it is assumed that for the time period of interest, θ, ψ and their respective time derivatives are very small (on the order of milliradians), all second order terms, such as $I_{zz}\dot{\psi}S\theta C\theta$, that result from the evaluation of equation (8) can be ignored as $|\bar{\Omega}|$ is large. If $S\theta = \theta$ and $C\theta = 1$, equation (8) reduces to

$$\left.\begin{aligned} M_{xo} &= I_{xx}\ddot{\theta} - I_{yy}\Omega\dot{\psi} \\ M_{yo} &= 0 \\ M_{zo} &= I_{zz}\dot{\psi} + I_{yy}\Omega\dot{\theta} \end{aligned}\right\} \qquad (9)$$

These equations are similar in form to those presented in [2] for the analysis of the two-axis gyroscope.

The only forces acting on the rocket during the tip-off configuration, Figure 4, are rocket weight, inertia loads due to static and dynamic mass unbalances, thrust, and front bearing reactions. Of these, only the rocket weight and inertia loads exert any moment about point "0". This is true because the rocket is assumed to be rigid (i.e., no bending) and point "0" is located at the geometric center of the front bearing. It is known, that if the rocket is bent during tip-off, that a component of the thrust vector will create a moment about point "0". The question of the degree of bending that the rocket experiences is treated in Section II of this report.

$\bar{R}$ = front bearing reaction. This force always acts in the z - x plane and is assumed to act, at all time, on a line through point "0" ($\frac{d}{=}$ lb).

$\bar{T}$ = rocket thrust vector. This force always acts along y. ($\frac{d}{=}$ lb).

$-mg\hat{k}$ = rocket weight. This force always acts at the rocket c.m. and is always parallel to Z. ($\frac{d}{=}$ lb). Note, g = 32.2 ft/sec^2.

$\bar{F}_I$ = inertia load due to static and dynamic mass unbalances. This force is assumed to act through the rocket c.m. and always in a plane parallel to the z-x plane. The rate of rotation of $\bar{F}_I$ is assumed to be that of the rocket (i.e., 987 rad/sec) and its location with respect to an arbitrary reference axis in its plane of rotation will be given by the quantity Ωt where Ω = 987 rad/sec and t = tim ($\frac{d}{=}$ sec). The magnitude of $\bar{F}_I$ is given by:

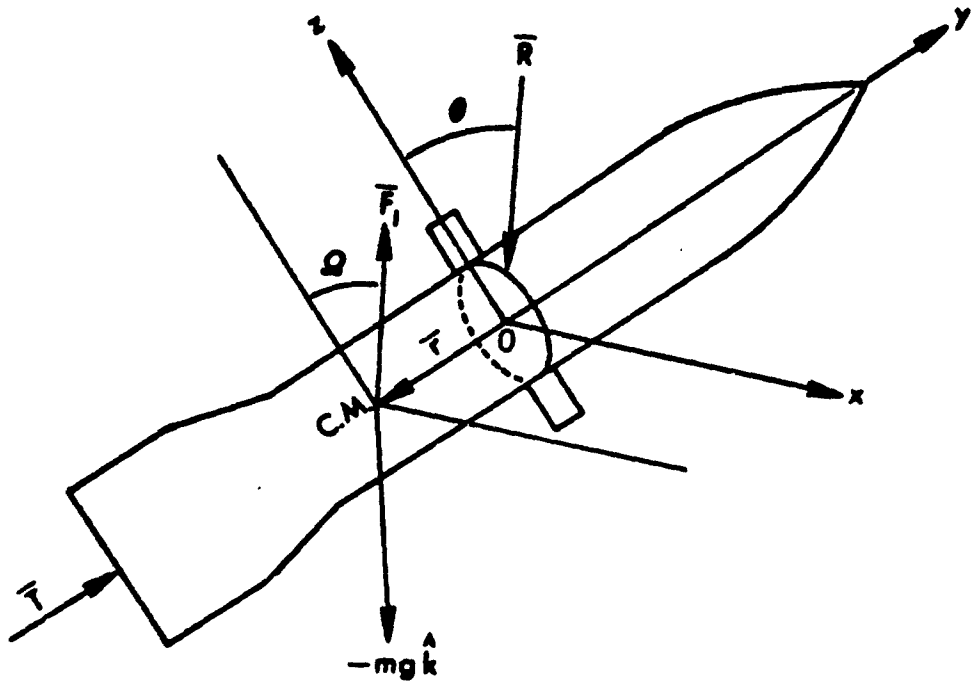

Figure 4. Free body diagram of the rocket during tip-off

$$|\bar{F}_I| = mE\Omega^2 \tag{10}$$

where:

m = rocket mass ($\stackrel{d}{=}$ slug)

E = distance of m from y ($\stackrel{d}{=}$ ft)

= rocket spin rate ($\stackrel{d}{=}$ rad/sec)

$\bar{r}$ = the position vector of the c.m. with respect to frame b. This vector is always parallel to y. ($\stackrel{d}{=}$ ft).

Now:

$$\bar{M}_o = \bar{r} \times \bar{F} \tag{11}$$

with

$$\bar{F} = \bar{F}_I - mg\hat{k} \tag{12}$$

as

$$C\theta = 1,$$

$$M_{xo} = mgr - mE\Omega^2 r \cos(\Omega t)$$

$$M_{yo} = o \tag{13}$$

$$M_{zo} = mE\Omega^2 r \sin(\Omega t)$$

Equations (13) represent the external moments about point "O" during tip-off. Note also that equations (13) assume that at time zero $\bar{F}_I$ is aligned with +Z.

Substitution of equations (13) into equations (9) yields:

$$I_{xx}\ddot{\theta} - I_{yy}\Omega\dot{\psi} = mgr - mE\Omega^2 r\cos(\Omega t)$$
$$I_{zz}\ddot{\psi} - I_{yy}\dot{\theta} = mE\Omega^2 r\sin(\Omega t) \qquad (14)$$

Since the rocket is symmetric (i.e., $I_{xx} = I_{zz}$) the following terms are defined:

$$\omega = \frac{I_{yy}}{I_{xx}}\Omega$$
$$M_1 = \frac{mgr}{I_{xx}} \qquad (15)$$
$$M_2 = \frac{ME\Omega^2 r}{I_{xx}}$$

Note that the term ω is the natural frequency of the system ($\frac{d}{=}$ rad/sec). If equations (15) are substituted into equations (14) then the equations of motion take on the following form:

$$\ddot{\theta} - \omega\dot{\psi} = M_1 - M_2\cos(\Omega t)$$
$$\ddot{\psi} + \omega\dot{\theta} = M_2\sin(\Omega t) \qquad (16)$$

The equations of motion for the system are a pair of second order, coupled, linear, non-homogeneous, ordinary differential equations in θ and ψ.

Equations (16) can be modified for the case of $\bar{F}_I$ being initially aligned with the -Z axis at time zero and have the form:

$$\ddot{\theta} - \omega\dot{\psi} = M_1 + M_2\cos(\Omega t)$$
$$\ddot{\psi} + \omega\dot{\theta} = -M_2\sin(\Omega t) \qquad (17)$$

The Laplace transform method [2] was used to solve equations (16). The transformed equations have the form:

$$\begin{bmatrix} S^2 & -S\omega \\ S\omega & S^2 \end{bmatrix} \begin{bmatrix} \Theta \\ \Psi \end{bmatrix} = \begin{bmatrix} \frac{M_1}{S} - \frac{M_2 S}{S^2+\Omega^2} \\ \frac{M_2 \Omega}{S^2+\Omega^2} \end{bmatrix} \qquad (18)$$

where the S's are the eigenvalues of (16).

The response functions for Θ and Ψ can be obtained from (18) and are of the form:

$$\Theta = \frac{M_1}{S(S^2+\omega^2)} - \frac{SM_2}{(S^2+\omega^2)(S^2+\Omega^2)} + \frac{M_2\Omega\omega}{S(S^2+\omega^2)(S^2+\omega^2)}$$

$$\Psi = \frac{M_2(\Omega+\omega)}{(S^2+\omega^2)(S^2+\Omega^2)} - \frac{M_1\omega}{S^2(S^2+\omega^2)} \qquad (19)$$

By use of the partial fraction method and tables in [2] the inverse transforms of Θ and Ψ are found and the time responses for a Θ and Ψ during tip-off are:

$$\theta(t) = \cos(\Omega t)\left[\frac{M_2}{\Omega(\Omega-\omega)}\right] - \cos(\omega t)\left[\frac{M_1}{\omega^2} + \frac{M_2}{\omega(\Omega-\omega)}\right] + \frac{M_1}{\omega^2} + \frac{M_2}{\omega\Omega}$$

$$\psi(t) = \sin(\omega t)\left[\frac{M_1}{\omega^2} + \frac{M_2}{\omega(\Omega-\omega)}\right] - \sin(\Omega t)\left[\frac{M_2}{\Omega(\Omega-\omega)}\right] - \frac{M_1}{\omega} t$$

With the first time derivatives of equations (19) and the projection of these quantities onto frame g the magnitudes of the pitch and yaw mallaunch rates are found to be:

$$|\bar{\omega}_p| = \dot{\theta}\cos(\Psi)$$
$$|\bar{\omega}_y| = \dot{\Psi} \qquad (21)$$

Figure 9 was obtained by assuming that both the thrust and the mass are constant from boost motor ignition until the end of guidance. An average thrust for this time was computed as 4808.367 lb [4]. With a rocket mass of 1.54 slug an average acceleration of 3122.316 ft/sec^2 can be calculated. As the initial velocity of the rocket is zero the velocity at the end of guidance can be calculated from:

$$V = \sqrt{2as} \qquad (22)$$

and has a value of 1246.96 in/sec.

a = average acceleration up to the end of guidance ($\stackrel{d}{=}$ ft/sec^2)

s = guidance length (20.75 in.) [4]

If the velocity of the rocket is assumed to be constant during tip-off then the following relation exists between velocity, bearing mismatch, and total time of tip-off:

$$t = \delta/V \qquad (23)$$

where

δ = bearing mismatch ($\stackrel{d}{=}$ in.)

t = total tip-off time ($\stackrel{d}{=}$ sec.)

V = average velocity of the rocket during tip-off (1246.96 in/sec)

Thus, for any specified amount of bearing mismatch the total tip-off time can be calculated.

A typical dynamic unbalance at the front bearing (before balancing) has been measured as 0.45 oz-in and reported in [3]. This is equivalent to an effect caused by a D'Alembert's force at the center of mass and expressed by equation (10). For a rocket mass of 1.54 slugs and Ω of 987 rad/sec, the equivalent E will be 5.015×10^{-5}ft.

In order to obtain the mallaunch rates, the amount of bearing mismatch must be specified. If the bearing mismatch is as much as a tenth of an inch then the total tip-off time is 8.0×10^{-5} sec (Figure 9).

With the aforementioned conditions and for the case where $\bar{F}_I$ is initially aligned with -Z the pitch and yaw mallaunch rates of 0.048×10^{-2} rad/sec and -0.0136×10^{-3} rad/sec respectively (Figures 7 and 8). These two values yield by a vector sum a total mallaunch rate of 0.48×10^{-3} rad/sec due to the .10 inch mismatch.

The shaded area on Figures 5, 6, 7, and 8 depict the range of mallaunch for 0.0 to 0.02 oz-in of mass unbalance as reported in [3]. For a bearing mismatch of 0.23 in and total tip-off time of 20×10^{-5} sec, a mass unbalance of 0.02 oz-in yields pitch and yaw mallaunch rates of 0.0598×10^{-2} rad/sec and 0.0123×10^{-3} rad/sec respectively if $\bar{F}_I$ is assumed to be initially aligned with the -Z axis. These two values yield by a vector sum a total mallaunch rate of 0.598×10^{-3} rad/sec due to the 0.23 inch mismatch.

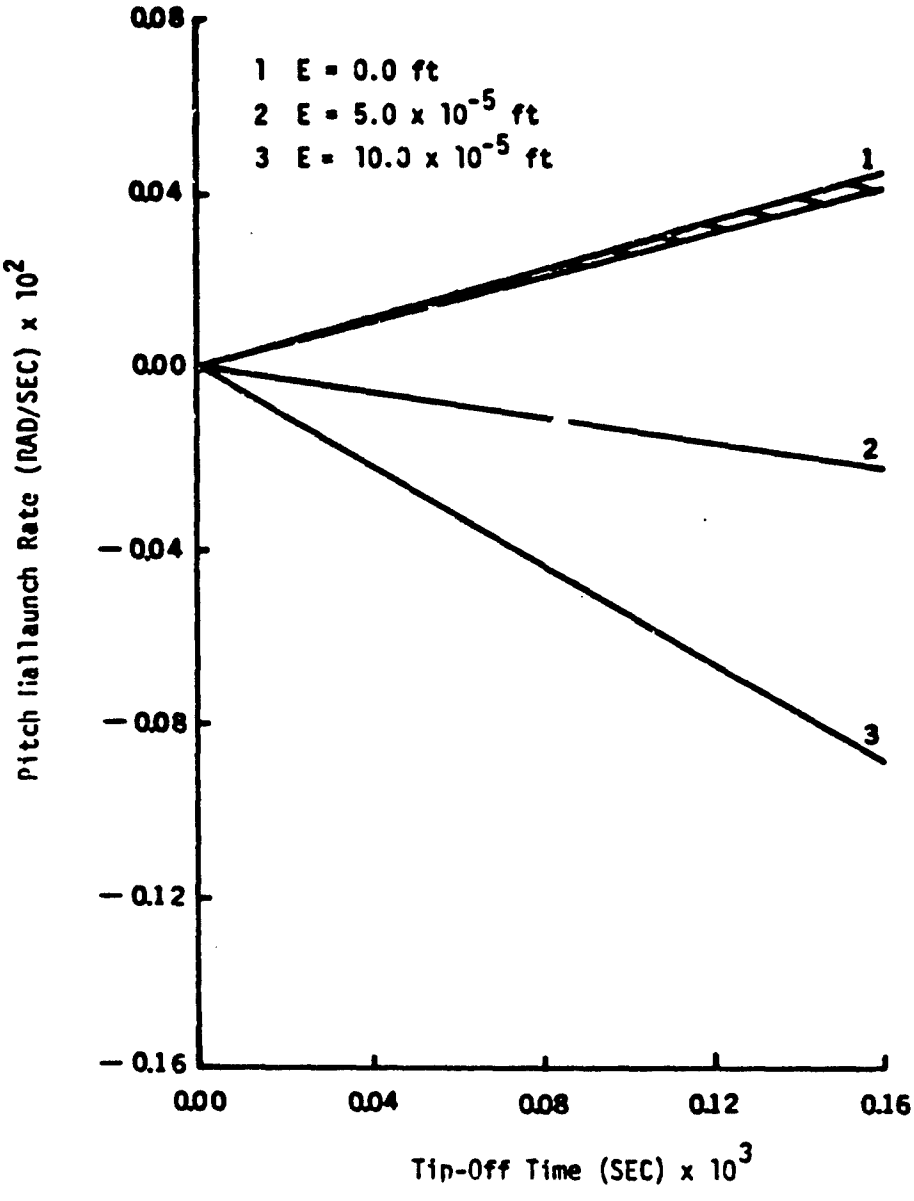

Figure 5. Pitch Hallaunch Rate Versus Tip-Off Time with $\bar{F}_I$ Initially Aligned with +Z

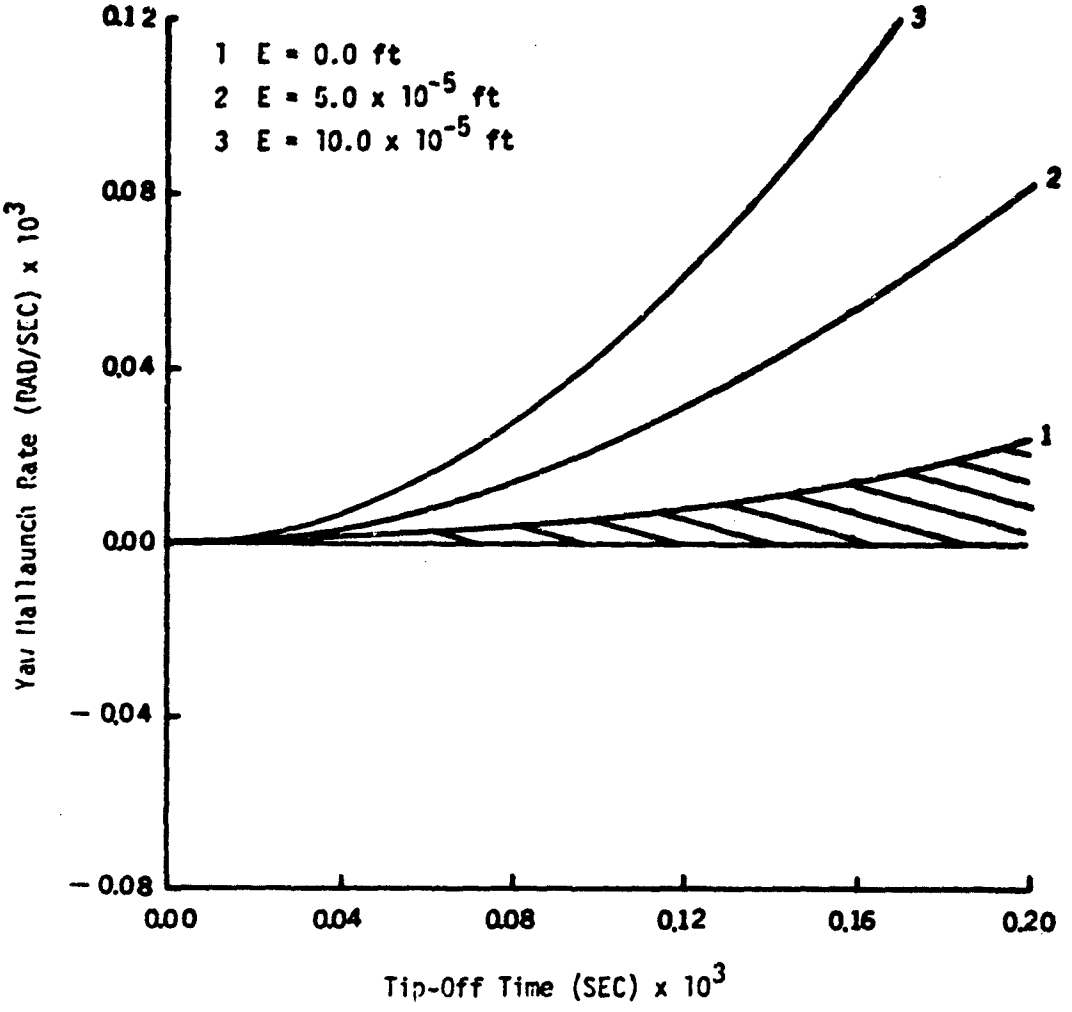

Figure 6. Yaw Hallaunch Rate Versus Tip-Off Time with $\bar{F}_I$ Initially Aligned with +Z

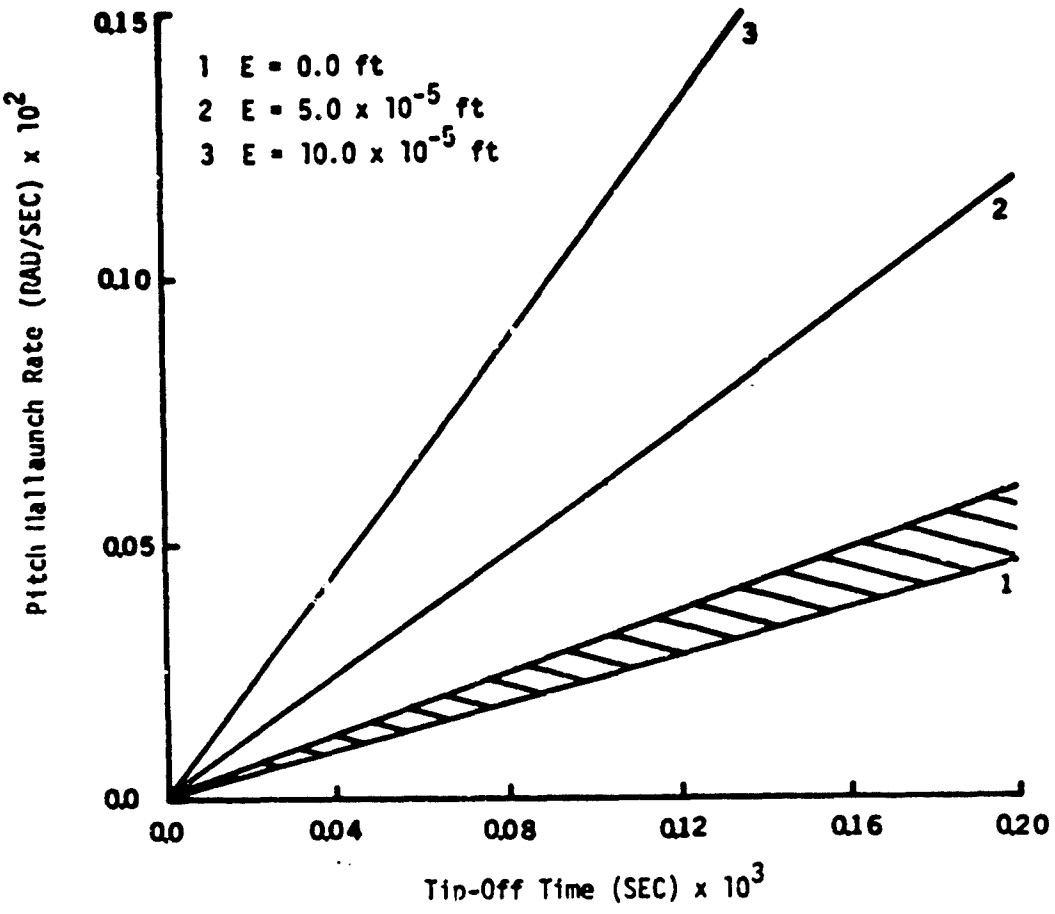

Figure 7. Pitch Mallaunch Rate Versus Tip-Off Time with $\bar{F}_I$ Initially Aligned with -Z

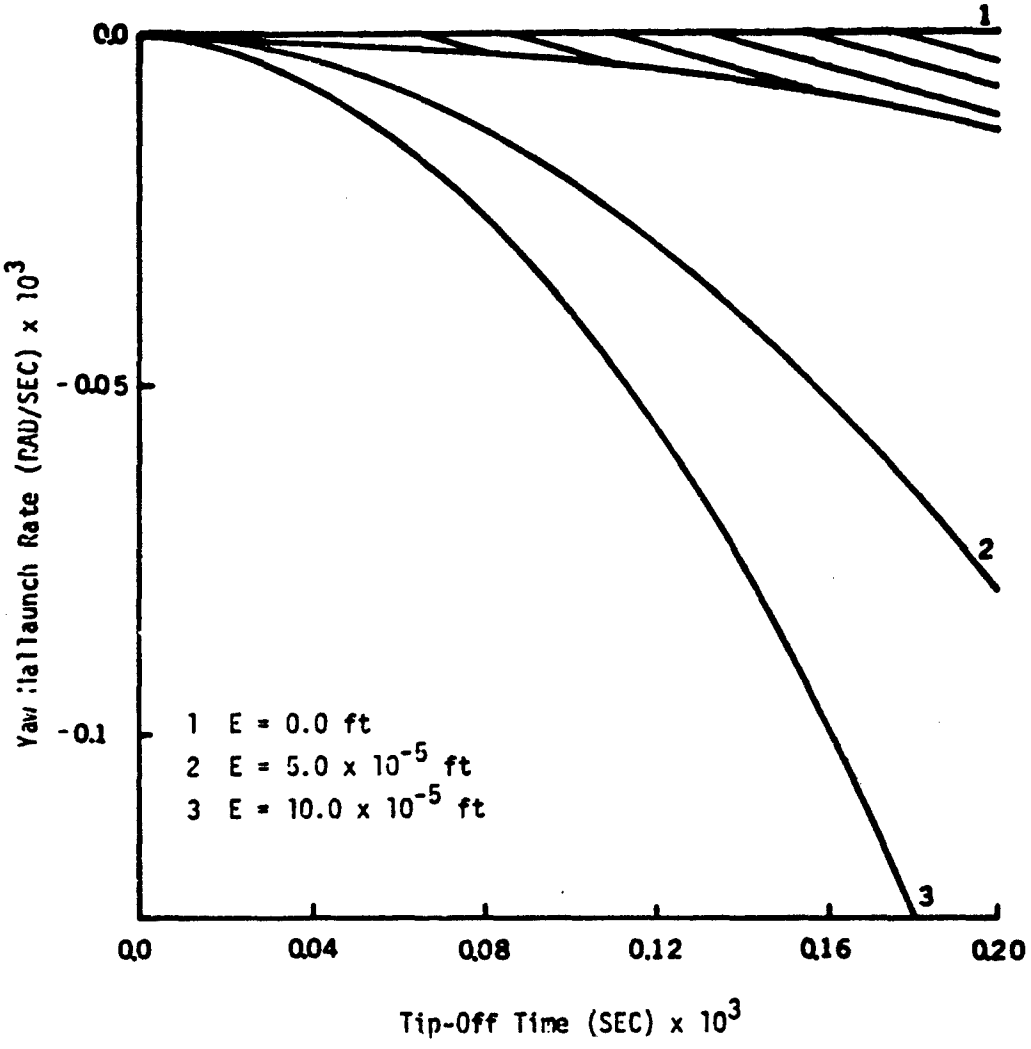

Figure 8. Yaw Hallaunch Rate versus Tip-Off Time with $\overline{F}_I$ Initially Aligned with -Z

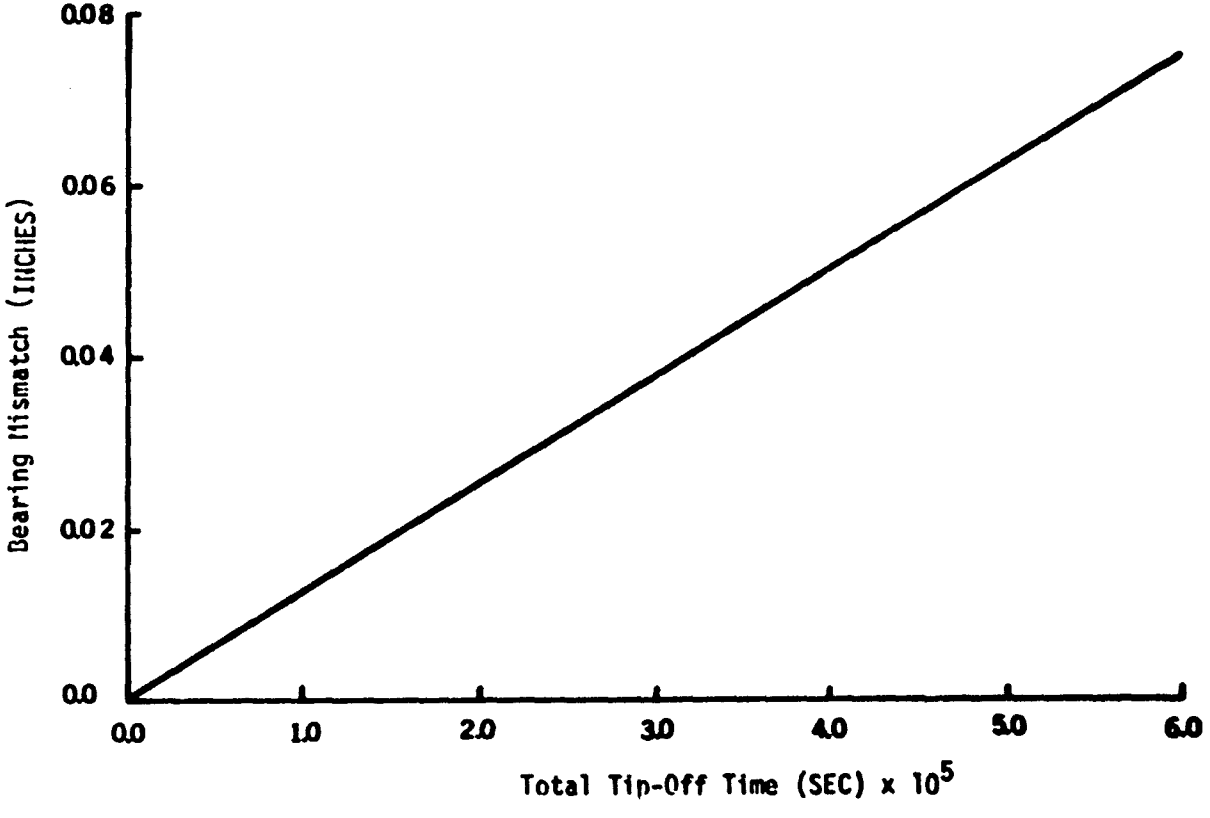

Figure 9. Bearing Mismatch Versus Total Tip-Off Time

C. LIST OF REFERENCES

1. Arnold and Maunder, Gyrodynamics and Its Engineering Applications, Academic Press, New York and London, 1961.

2. Cannon, R. H., Jr., Dynamics of Physical Systems, McGraw-Hill, Inc., 1967.

3. Rubert, Flight Tests of An Aerodynamically Neutral, Spin Stabilized Rocket (ANSSR), RT-TR-72-17, U. S. Army Missile Command, Redstone Arsenal, Alabama, 1972.

4. Pell, K. M., Vest, C. L. and Donovan, J. C., ANNSR Flight Test Simulation and Selected Problem Investigation, RD-72-30, U. S. Army Missile Command, Redstone Arsenal, Alabama, 1972.

SECTION II

MALLAUNCH DUE TO IN-TUBE ROCKET BENDI!IG

ABSTRACT

Rocket flexibility is modelled for the launch phase. The model accounts for bearing clearances, a variable stiffness motor section and allows for the 3-D motion of a rigid warhead. The phenomenon of whirling is investigated and the bent configuration of the rocket is calculated for synchronous whirling. The resulting mallaunch rates agree with reported range data.

LIST OF SYMBOLS

$\bar{a}$	acceleration of payload center of mass with respect to X,Y,Z
$\bar{a}_T$	longitudinal (along launch tube) acceleration of rocket due to engine thrust
$\bar{e}_1, \bar{e}_2, \bar{e}_3$	unit vectors in x,y,z
$\bar{H}$	moment of momentum vector
$\hat{i}, \hat{j}, \hat{k}$	unit vectors in X,Y,Z
I_{ij}	Inertia tensor of rocket
k	dynamic stiffness
K	stiffness (as to bending)
L	length between bearing centers
m	mass
$\bar{M}$	bending moment
$\bar{r}$	position vector of center mass of payload section with respect to X,Y,Z
x,y,z	body reference
X,Y,Z	ground reference
α	bending angle
β_i	rocket section deviation angle for ith section
ϵ_1, ϵ_2	bearing clearances
ϕ	angle between longitudinal axes of launch tube and unbent rocket
ψ, θ	Euler Angles
Ψ	Laplace transform of ψ
Θ	Laplace transform of θ

$\bar{\omega}$ body frame spin rate with respect to X,Y,Z

ω_{MAL} Mallaunch or component of rocket spin vector not along launch tube axis

ω_R angular rate vector of rocket with respect to X,Y,Z

$\bar{\Omega}$ angular rate vector of rocket with respect to x,y,z

A. INTRODUCTION

The objective of this section of the report is to develop an analytical model that will predict the whirling and mallaunch rates of ANSSR II. The motor section of the rocket will be modelled as a variable EI beam that is simply supported between its front and rear bearings while the payload section will be considered rigid. The basis of these assumptions is Figure 25 of [1].

The analysis will be divided into four parts. The bending and deflection equations of the motor section subjected to the loading condition shown in Figure 1 will be developed first. A general motion analysis of the payload section, coupled with the bending equations, will then be carried out and will yield a whirling rate for ANSSR II that is within 18 to 20 percent of the observed whirling rate. A prescribed motion analysis of the payload section, taking into account the rocket's bearing clearances, is also coupled with the bending equations yielding the degree of "in-tube" bending for ANSSR II. The degree of bending predicted by this model will be in agreement with bending data that is presented in Figure 22 and Figure 23 of [1]. Once the degree of "in-tube" bending is known then the mass center of the bent rocket and its PLAI with respect to its mass center are both found via a lumped parameter model. Thus, knowing the bent rocket's PLAI, the mallaunch rate of ANSSR II is easily found.

The majority of the above analysis is carried out in one of the transverse planes of the rocket as complete symmetry of rocket motion in its perpendicular transverse planes is assumed.

B. BENDING AND DEFLECTION EQUATIONS OF THE MOTOR SECTION

The motor section of ANSSR II is considered to be a variable EI beam as shown in Figure 1. The coordinate system used in this analysis is $(\bar{X},\bar{Y},\bar{Z})$. The origin is located at the center of the rear bearing. The $\bar{Y}$ axis is taken positive going from the rear of the rocket towards the nose and is parallel to the unbent rocket's longitudinal axis. The $\bar{X}$ and $\bar{Z}$ axes are normal to $\bar{Y}$ and form a right hand system. The sign convention that will be used is that a negative moment, applied as in Figure 1, will cause a positive displacement.

The bending and deflection equations for the various sections of the motor section are represented as;

$$\alpha_{\bar{x}i} = -\frac{M_{\bar{x}}}{2\,EI_i\,L}\bar{y}^2 + \frac{C_i}{EI_i} \tag{1}$$

and

$$z_i = -\frac{M_{\bar{x}}}{6\,EI_i\,L}\bar{y}^3 + \frac{C_i}{EI_i}\bar{y} + \frac{K_i}{EI_i} \tag{2}$$

where,

i = 1, 2, and 3 and represents the beam sections:

$$0 \le \bar{y}\ L_1,\ L_1 \le \bar{y} \le L_2,\ L_2 \le \bar{y} \le L$$

respectively,

$M_{\bar{x}}$ = A moment applied in the negative $\bar{X}$ direction as shown in Figure 1 ($\frac{d}{=}$ ft lb),

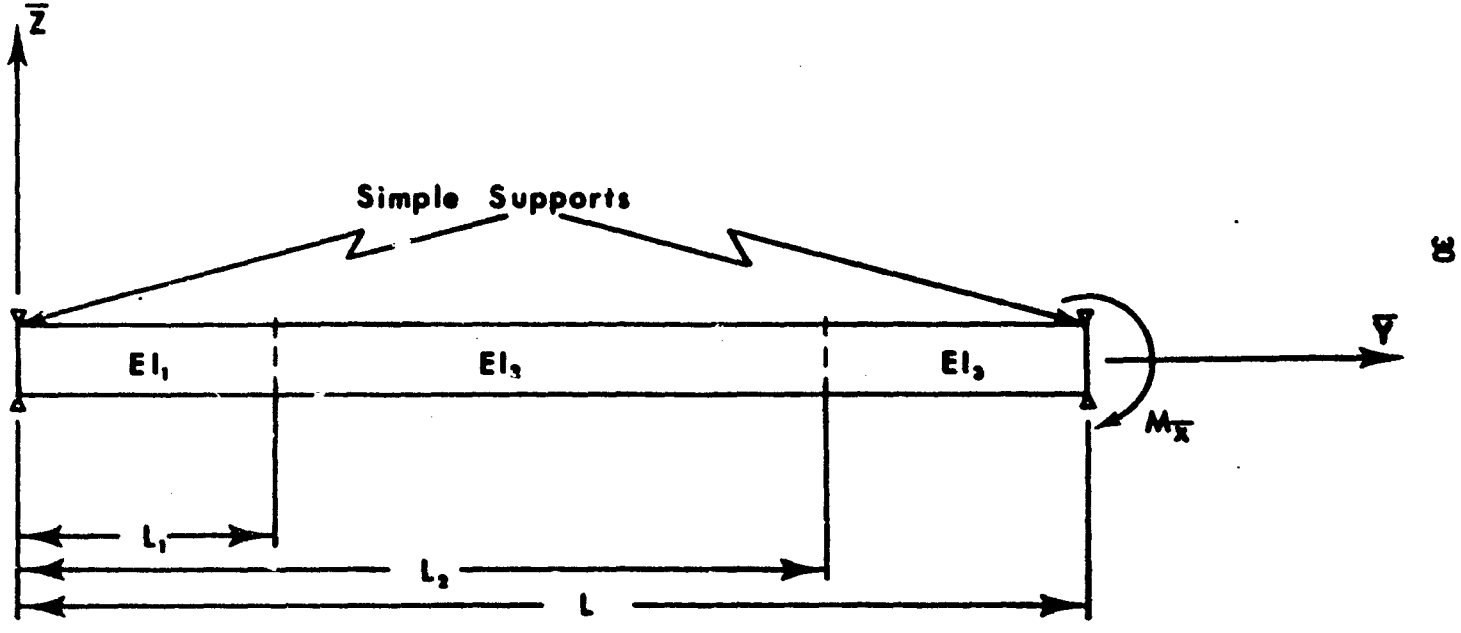

Figure 1: Loading Condition and Coordinate System Definition for Motor Section

EI_i = the EI of the ith section of the motor section, see Figure 1 ($\stackrel{d}{=}$ lb ft^2),

L = the length of the motor section ($\stackrel{d}{=}$ ft)

C_i and K_i = constants of integration of the ith motor section ($\stackrel{d}{=}$ lb ft^2 and lb ft respectively).

The constants C_i and K_i can be evaluated due to the following boundary conditions:

At $\bar{y} = 0$, $z = 0$;

At $\bar{y} = L_1$, $\alpha_{\bar{x}1} = \alpha_{\bar{x}2}$, and $z_1 = z_2$;

At $\bar{y} = L_2$, $\alpha_{\bar{x}2} = \alpha_{\bar{x}3}$, and $z_2 = z_3$;

At $\bar{y} = L$, $z_3 = 0$

Upon evaluation of the boundary conditions the C_i and K_i are found to be:

$$C_1 = -\left[\frac{EI_1}{EI_3} - \frac{EI_1}{EI_2}\right]\left[\frac{M_x L_2^2}{2L} - \frac{M_x L_2^3}{3L^2}\right] - \left[\frac{EI_1}{EI_2} - 1\right]\left[\frac{M_x L_1^2}{2L} - \frac{M_x L_1^3}{3L^2}\right] + \frac{M_x L EI_1}{6EI_3} \quad (3)$$

$$C_2 = -\frac{M_x L_1^2}{2L}\left[\frac{EI_2}{EI_1} - 1\right] + \frac{EI_2}{EI_1} C_1 \quad (4)$$

$$C_3 = -\frac{M_x L_2^2}{2L}\left[\frac{EI_3}{EI_2} - 1\right] - \frac{M_x L_1^2}{2L}\left[\frac{EI_3}{EI_1} - \frac{EI_3}{EI_2}\right] + \frac{EI_3}{EI_1} C_1 \quad (5)$$

$$K_1 = 0 \quad (6)$$

$$K_2 = -\frac{M_x L_1^2}{3L}\left[1 - \frac{EI_2}{EI_1}\right] \quad (7)$$

$$K_3 = -\frac{M_x L_2^3}{3L}\left[1 - \frac{EI_3}{EI_2}\right] - \frac{M_x L_1^3}{3L}\left[\frac{EI_3}{EI_2} - \frac{EI_3}{EI_1}\right] \tag{8}$$

The degree of bending in both transverse planes of the motor section at the front bearing can be found by combining equations (1) and (5). The equations are of the following form;

$$\alpha_{\bar{X}3} = \frac{1}{\bar{K}} M_{\bar{X}} \tag{9}$$

and

$$\alpha_{\bar{Z}3} = \frac{1}{\bar{K}} M_{\bar{Z}} \tag{10}$$

where

$$\frac{1}{\bar{K}} = \frac{L_2^3}{3L^2}\left[\frac{1}{EI_3} - \frac{1}{EI_2}\right] - \frac{L_1^3}{3L^2}\left[\frac{1}{EI_1} - \frac{1}{EI_2}\right] - \frac{L}{3EI_3} \tag{11}$$

The quantity $\bar{K}$ can be thought of as the bending stiffness of the motor section at the front bearing to a mument applied as shown in Figure 1.

The numerical values of L_1, L_2, L and EI_i used in this report are presented in Table I.

C. GENERAL MOTION ANALYSIS OF THE PAYLOAD SECTION

As stated, the payload section of the rocket will be assumed to be rigid. The position of the payload section in the space can be described by two independent Euler angles as shown in Figure 2.

The coordinate systems and Euler angles used in this portion of the analysis are defined as follows:

- Ground Reference: Ground reference is (X,Y,Z) with respective unit vectors $(\hat{i},\hat{j},\hat{k})$. The origin is fixed at the center of the front bearing. The Y axis is taken positive going out of the launch tube longitudinal axis. The Z axis is taken positive up and parallel to the local vertical. The X axis completes the right hand system.

- Body Reference: Body reference is (x,y,z) with respective unit vectors $(\bar{e}_1, \bar{e}_2, \bar{e}_3)$. The origin (CM_p) is located at the mass center of the payload section. If the angles ψ and θ were both zero then the body reference axes would be parallel to the corresponding ground reference axes.

It is important to note that x and z do not spin with the rocket, i.e., the rocket spins about the y axis of the body frame.

- System Euler Angles: The two independent Euler angles that describe the position of the body reference (or frame) with respect to the ground reference are ψ and θ.-ψ is the first rotation about z and -θ is the second angle of rotation about x'. Note that x' is parallel to x. Both angles and their time derivatives are expressed in rad and rad per second respectively.

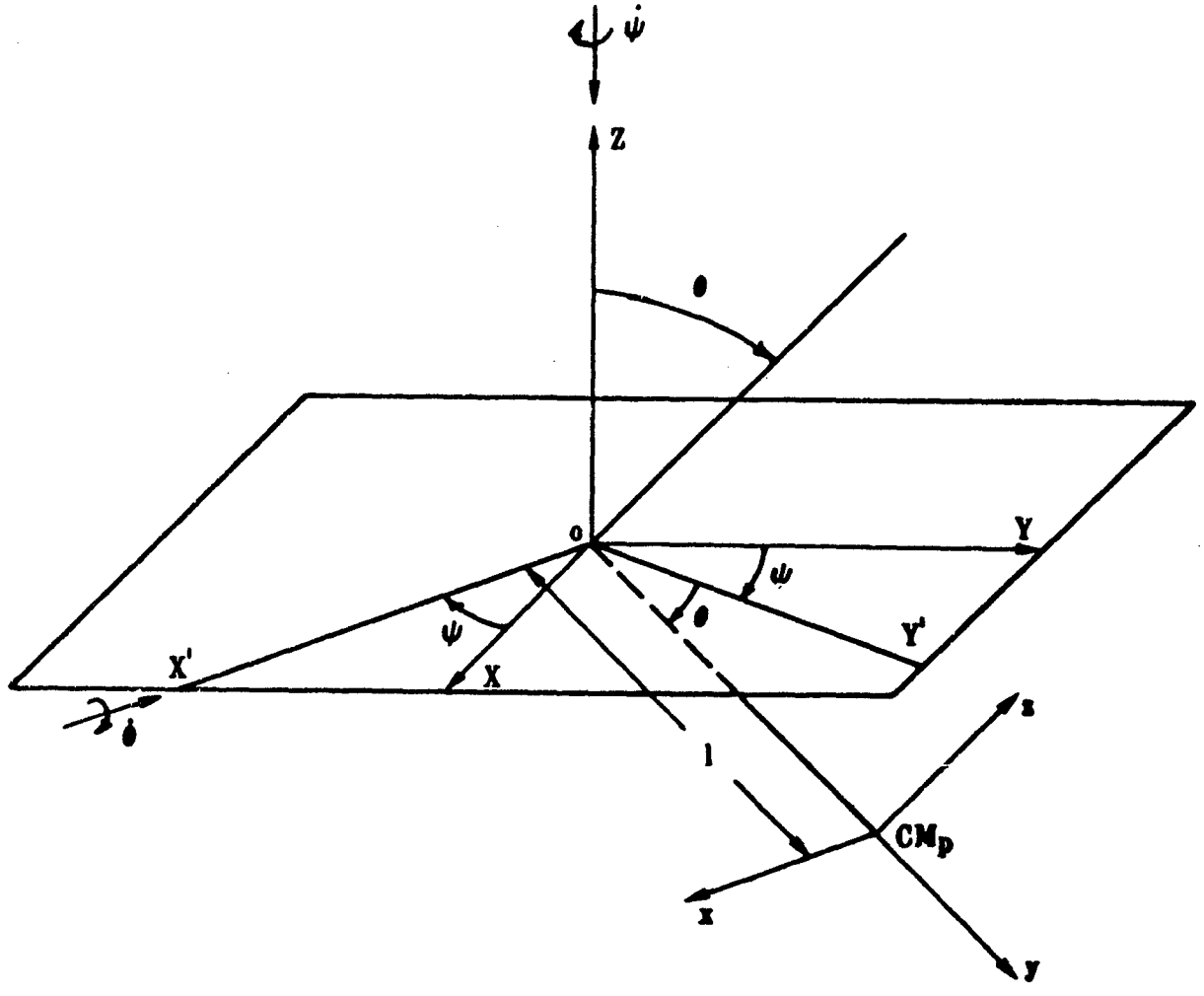

Figure 2: Coordinate Systems and Euler Angles Used in the General Motion Analysis of the Payload Section.

The relation between the coordinates of the body frame and those of the ground reference is:

$$\begin{bmatrix} x \\ y \\ z \end{bmatrix} = [B] \cdot \begin{bmatrix} X \\ Y \\ Z \end{bmatrix} \tag{12}$$

with the matrix [B] defined as,

$$[B] = \begin{bmatrix} 1 & 0 & 0 \\ 0 & C\theta & -S\theta \\ 0 & S\theta & C\theta \end{bmatrix} \cdot \begin{bmatrix} C\phi & -S\phi & 0 \\ S\phi & C\phi & 0 \\ 0 & 0 & 1 \end{bmatrix} \tag{13}$$

or, the relation may also have the following form:

$$\begin{bmatrix} X \\ Y \\ Z \end{bmatrix} = [C] \cdot \begin{bmatrix} x \\ y \\ z \end{bmatrix} \tag{14}$$

with the matrix [C] defined as,

$$[C] = \begin{bmatrix} C\phi & S\phi & 0 \\ -S\phi & C\phi & 0 \\ 0 & 0 & 1 \end{bmatrix} \cdot \begin{bmatrix} 1 & 0 & 0 \\ 0 & C\theta & S\theta \\ 0 & -S\theta & C\theta \end{bmatrix} \tag{15}$$

where $C\theta$ is taken to be COS(θ), etc.

Now:

$\bar{\omega}$ = the angular rate vector of the body frame with respect to the ground reference ($\underline{\underline{d}}$ rad/sec).

$\bar{\omega}_R$ = the angular rate vector of the rocket with respect to the ground reference ($\underline{\underline{d}}$ rad/sec).

$\bar{\Omega}$ = the angular rate vector of the rocket with respect to the body frame, i.e., the rocket spin rate ($\underline{\underline{d}}$ rad/sec).

The above angular rate vectors are given by the following equations:

$$\bar{\omega} = -\dot{\theta}\bar{e}_1 + \dot{\psi}\,S\theta\,\bar{e}_2 - \dot{\psi}\,C\theta\,\bar{e}_3 \tag{16}$$

$$\bar{\omega}_R = -\dot{\theta}\bar{e}_1 + (\dot{\psi}\,S\theta + \Omega)\bar{e}_2 - \dot{\psi}\,C\theta\,\bar{e}_3 \tag{17}$$

$$\bar{\Omega} = \Omega\bar{e}_2 \tag{18}$$

It follows that the angular momentum vector of the payload section with respect to its mass center, expressed in the body frame is [2]:

$$\bar{H}_{cmp} = -I_{xx}\dot{\theta}\bar{e}_1 + I_{yy}(\dot{\psi}S\theta + \Omega)\bar{e}_2 - I_{zz}\dot{\psi}\,C\theta\,\bar{e}_3 \tag{19}$$

The sum of all external moments about the mass center of the payload section must be equal to the first time derivative of $\bar{H}_{cmp}$ with respect to the ground reference. Therefore,

$$\bar{M}_{cmp} = \frac{d}{dt}\left[(\bar{H}_{cmp})\right]_{\substack{\text{Body}\\\text{frame}}} + \bar{\omega} \times \bar{H}_{cmp} \tag{20}$$

A constant spin rate of 987 rad/sec will be used in this analysis. This value was obtained by averaging the spin rates (excluding flights 1, 2, and 3) presented in Table 6 of [3]. As 987 rad/sec is a very large number, all second order terms, such as $I_{zz}\,\dot{\psi}^2\,S\theta\,C\theta$, that result from the evaluation of equation (20) can be ignored. Because the degree of

"in-tube" bending has been observed to be very small, [1 or 2], the substitution of $S\theta = \theta$, $S\psi = \psi$, $C\theta = 1$, and $C\psi = 1$ into equation (20) yields:

$$\bar{H}_{cmp} = (I_{yy}\,\Omega\,\dot{\psi} - I_{xx}\,\ddot{\theta})\bar{e}_1 - (I_{zz}\ddot{\psi} + I_{yy}\,\Omega\,\dot{\theta})\bar{e}_3 \qquad (21)$$

where

$I_{xx} = I_{zz}$ = the transverse mass moments of inertia of the payload section with respect to its mass center ($\frac{d}{=}$ slug ft^2).

I_{yy} = the longitudinal mass moment of inertia of the payload section with respect to its mass center ($\frac{d}{=}$ slug ft^2).

Equation (21) can be expressed in the ground reference with the use of equations (14) and (15). Therefore,

$$\bar{H}_{cmp} = (I_{yy}\,\Omega\,\dot{\psi} - I_{xx}\,\ddot{\theta})\hat{i} - (I_{zz}\ddot{\psi} + I_{yy}\,\Omega\,\theta)\hat{k} \qquad (22)$$

The only external forces that create a moment about the mass center of the payload section are the reaction forces acting at point "O" as shown in Figure 3. These forces can be evaluated with the use of Newton's Second Law, i.e.,

$$\bar{F}_{cmp} = M_p\,\bar{a} \qquad (23)$$

where

M_p = the mass of the payload section ($\frac{d}{=}$ slug).

$\bar{a}$ = the acceleration of the mass center of the payload section with respect to the ground reference ($\frac{d}{=}$ ft/sec^2).

Now, $\bar{a}$ can be found due to the fact that,

$$\bar{a} = \frac{d^2}{dt^2}(\bar{r}) \qquad (24)$$

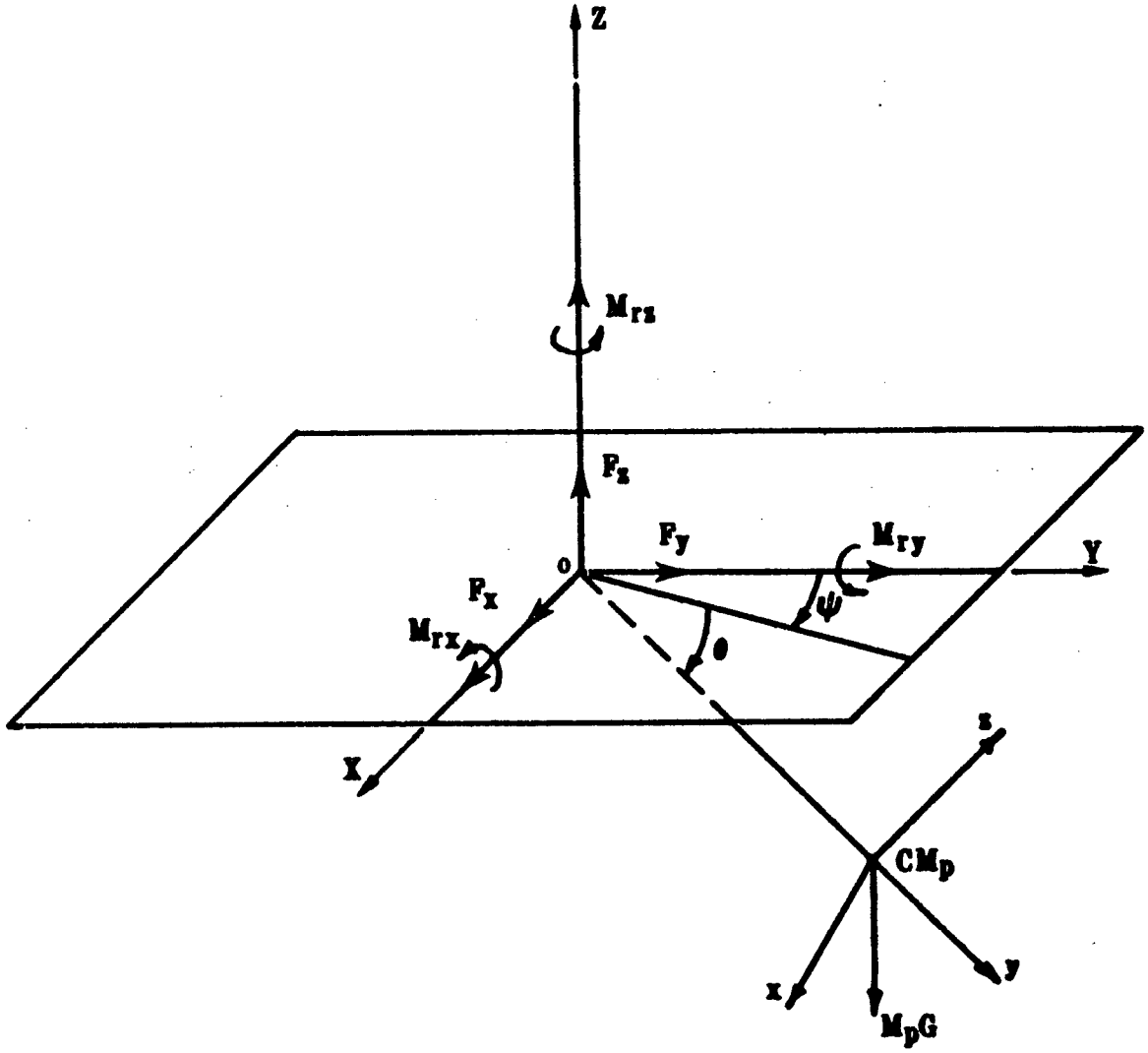

Figure 3: Freebody Diagram of Payload Section

where

$\bar{r}$ = the position vector of the mass center of the payload section with respect to the ground reference ($\overset{d}{=}$ ft) and is of the form,

$$\bar{r} = \ell\psi\hat{i} + \ell\,\hat{j} - \ell\theta\hat{k} \tag{25}$$

where

ℓ = the linear distance between the point "cm_p" and the point "0", see Figure 2 ($\overset{d}{=}$ ft). If equation (25) is combined with equation (24) then the following expression is found,

$$\bar{a} = \ell\ddot{\psi}\hat{i} - \ell\ddot{\theta}\hat{k} \tag{26}$$

As the rocket is also accelerating in the positive Y direction due to the thrust provided by the main engine, equation (26) can be modified to be of the form,

$$\bar{a} = \ell\ddot{\psi}\hat{i} + a_T\,\hat{j} - \ell\ddot{\theta}\hat{k} \tag{27}$$

where

a_T = the longitudinal acceleration of the rocket due to the thrust of the main engine ($\overset{d}{=}$ ft/sec^2).

The mass of the rocket and the thrust are assumed constant from boost motor ignition until the end of guidance. An average thrust for this time was computed as 4808 lb [4]. With a rocket mass of 1.54 slug [5] an average acceleration (a_T) of 3122 ft/sec^2 can be calculated.

The only external moments that act on the payload section are the reaction moments acting at point "0", see Figure 3. These moments can be evaluated with the use of the following equation,

$$\bar{M}_R - (\bar{r} \times \bar{F}_{cm_p}) = \bar{M}_{cm_p} \tag{28}$$

where

$\bar{M}_R$ = the reaction moments acting on the payload section at point "O" ($\frac{d}{=}$ ft lb).

An expression for $\bar{M}_R$ can be found by substituting equations (22), (23), (25), and (27) into equation (28). This substitution yields a vector equation for $\bar{M}_R$ which can be represented by the following scalar equations:

$$M_{RX} = -\ddot{\theta}(I_{xx} + \ell^2 M_p) + \psi \ell M_p a_T + \dot{\psi}\Omega I_{yy} \tag{29}$$

$$M_{RY} = 0$$

$$M_{RZ} = \ddot{\psi}(I_{xx} + \ell^2 M_p) + \psi \ell M_p a_T - \dot{\theta}\Omega I_{yy} \tag{31}$$

The above equations are the components of the reaction moment, acting on the payload section at point "O", that enables the payload section to move as depicted in Figure 2. An equal, but opposite, moment must act on the motor section and is of the form,

$$M_X = \ddot{\theta}(I_{xx} + \ell^2 M_p) - \theta \ell M_p a_T - \dot{\psi}\Omega I_{yy} \tag{32}$$

$$M_Y = 0 \tag{33}$$

$$M_Z = \ddot{\psi}(I_{xx} + \ell^2 M_p) - \psi \ell M_p a_T + \dot{\theta}\Omega I_{yy} \tag{34}$$

If the unbent rocket is placed in the tube such that the $(\bar{X},\bar{Y},\bar{Z})$ axes are parallel to their respective (X,Y,Z) axes, and equations (9) and (10) are re-written as:

$$M_{\bar{X}} = K \alpha_{\bar{x}3} \tag{9a}$$

and

$$M_Z = K\,\alpha_{Z3} \tag{10a}$$

then the following expressions result:

$$K\,\alpha_{\bar{X}3} = \ddot{\theta}(I_{xx} + \ell^2 M_p) - \theta \ell\, M_p\, a_T - \dot{\psi}\Omega\, I_{yy} \tag{35}$$

$$K\,\alpha_{\bar{Z}3} = \ddot{\psi}(I_{xx} + \ell^2 M_p) - \psi \ell\, M_p\, a_T + \dot{\theta}\Omega\, I_{yy} \tag{36}$$

As θ and ψ are $\alpha_{\bar{X}3}$ and $\alpha_{\bar{Z}3}$, to the first order, respectively, equations (35) and (36) become

$$\ddot{\theta}(I_{xx} + \ell^2 m_p) - \theta(\ell\, m_p\, a_T + K) - \dot{\psi}\,\Omega\, I_{yy} = 0 \tag{35a}$$

and

$$\ddot{\psi}(I_{xx} + \ell^2 m_p) - \psi(\ell\, m_p\, a_T + K) + \dot{\theta}\,\Omega\, I_{yy} = 0 \tag{36a}$$

The term $\ell\, m_p\, a_T \ll K$ and can be ignored in this analysis. If

$$A = \frac{K}{I_{xx} + \ell^2 m_p} \tag{37}$$

and

$$B = \frac{\Omega\, I_{yy}}{I_{xx} + \ell^2 m_p} \tag{38}$$

then equations (35a) and (36a) become,

$$\ddot{\theta} - A\theta - B\dot{\psi} = 0 \tag{35b}$$

and

$$\ddot{\psi} - A\psi + B\dot{\theta} = 0 \tag{36b}$$

The above procedure, i.e., the combination of general dynamics equations and bending equations is similar to a procedure that is presented in [6].

The Laplace Transform Method [7] can be used to put equations (35b) and (36b) into the following form:

$$\begin{bmatrix} (S^2 - A) & - & BS \\ BS & & (S^2 - A) \end{bmatrix} \cdot \begin{bmatrix} \Theta \\ \Psi \end{bmatrix} = [C] \tag{39}$$

where

S = the eigenvalues of (35) and (36) ($\frac{d}{=}$ rad/sec).

Θ and Ψ = the transfer functions of θ and ψ respectively.

$[C]$ = A matrix that is a function of S and the initial values of θ, ψ, $\dot{\theta}$, and $\dot{\psi}$ [7]. Its particular form is of no importance to this analysis.

The eigenvalues, or natural frequencies of whirl, of equations (35) and (36) can be found by setting the determinant of the matrix

$$\begin{bmatrix} (S^2 - A) & - & BS \\ BS & & (S^2 - A) \end{bmatrix} \tag{40}$$

equal to zero. This yields the characteristic equation of equations (35) and (36) whose roots are the eigenvalues. The characteristic equation is

$$(S^2 - A)^2 + B^2 S^2 = 0 \tag{41}$$

The physical properties of the motor section and the payload section (Tables I and II) and the spin rate of the rocket (987 rad/sec)

are all that is needed to evaluate equation (41). The resulting roots of (41) are $\pm$ j 810 rad/sec and $\pm$ j 749 rad/sec, where the j denotes an imaginary number. These values are within 18 to 20 percent, respectively, of the rocket spin rate of 987 rad/sec.

That the whirling rate during the spin-up phase is less than the rocket spin rate has been documented previously, e.g., see Figure 22 of [1]. However, no explanation for the discrepancy was given. Examination of this data shows that the whirling rate is about 406 rad/sec while the spin rate is about 510 rad/sec. This ratio of whirling rate to spin rate of .796 agrees very well with theoretical results obtained in this study. In fact, the average value of the two whirling rates, 810 rad/sec and 749 rad/sec, ratioed to the spin rate of 987 rad/sec gives .794.

Other range data indicates that, when the spin motors are exhausted, the rocket settles into a state of synchronous whirl. Strain gage data from hard mounted launchers support this contention.

D. PRESCRIBED MOTION ANALYSIS OF THE PAYLOAD SECTION

This section of the report will be an analysis of a more prescribed "in tube" rocket motion. It will also take into account the actual front and rear bearing clearances of ANSSR II. The basic bent, in-tube rocket shape is shown in Figure 4 where ϵ_1 and ϵ_2 are the rear and front bearing clearances respectively. As shown in Figure 4, α is the angle between the unbent rocket axis, ϕ is the angle between the longitudinal axis of the launch tube and the bent rocket axis. Nominal values of ϵ_1 and ϵ_2 can be found to be 0.003155 inches and 0.002075 inches respectively [5]. If L, the length between bearing centers, is 2.1625 ft [5] then the angle ϕ can be found and is 2.0154×10^{-4} rad.

Experimental strain gauge and optical lever data [1 or 2] strongly indicates that the in-tube motion is one of synchronous whirl, i.e., the rocket spins about its bent axis with a rate of 987 rad/sec and it whirls around the launch tubes longitudinal axis at the rate of 987 rad/sec simultaneously. This means that there is no flexing of the motor section and thus no shear forces due to flexure. Thus, a somewhat less complex model can be used than the Timoshenko beam [8] model that is needed to account for shear due to flexure.

So, even though the general motion analysis of the payload section yielded a whirling rate within 18 to 20 percent of the actual rocket spin rate, this portion of the report, due to the strong experimental evidence previously cited, will assume the rocket to have a whirling frequency equal to the spin frequency, i.e., a synchronous whirling situation prevails.

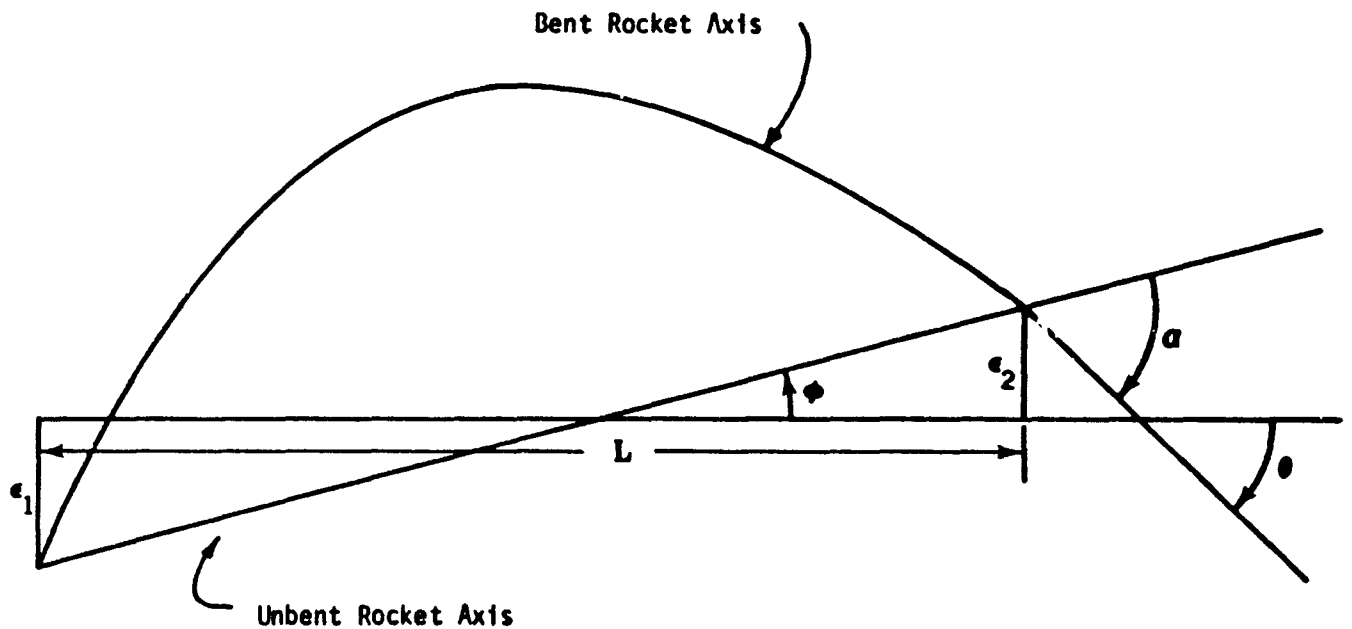

Figure 4: Basic, Bent, In-Tube Rocket Shape

Once again, the payload section is assumed to be rigid. This analysis, due to symmetry, is an instantaneous one and the particular configuration in space is depicted by Figure 5.

The ground and body reference definitions remain the same as in the previous section (noting the addition of the front bearing clearance, Figure 5).

The Euler angles definitions also remain the same but are placed under the constraints that $\psi = \dot{\psi} = \dot{\theta} = 0$ and ϑ is a constant.

The relation between the coordinates of the body frame and those of the ground reference can be found by using equations (12), (13), (14) and (15) subject to the above constraints.

The terms $\bar{\omega}$, $\bar{\omega}_R$, and $\bar{\Omega}$ are as previously defined and their respective values are

$$\bar{\omega} = C\theta\,\omega\bar{e}_2 + S\theta\,\omega\bar{e}_3 \tag{42}$$

$$\bar{\omega}_R = (\Omega + C\theta\,\omega)\bar{e}_2 + S\theta\,\omega\bar{e}_3 \tag{43}$$

$$\Omega = \Omega\bar{e}_2 \tag{44}$$

The angular momentum vector of the payload section with respect to its mass center is of the form:

$$\bar{H}_{cm_p} = I_{yy}\,(\Omega + C\theta\,\omega)\bar{e}_2 + I_{zz}\,S\theta\,\omega\bar{e}_3 \tag{45}$$

where

ω = the magnitude of the whirling rate vector, 987 rad/sec.

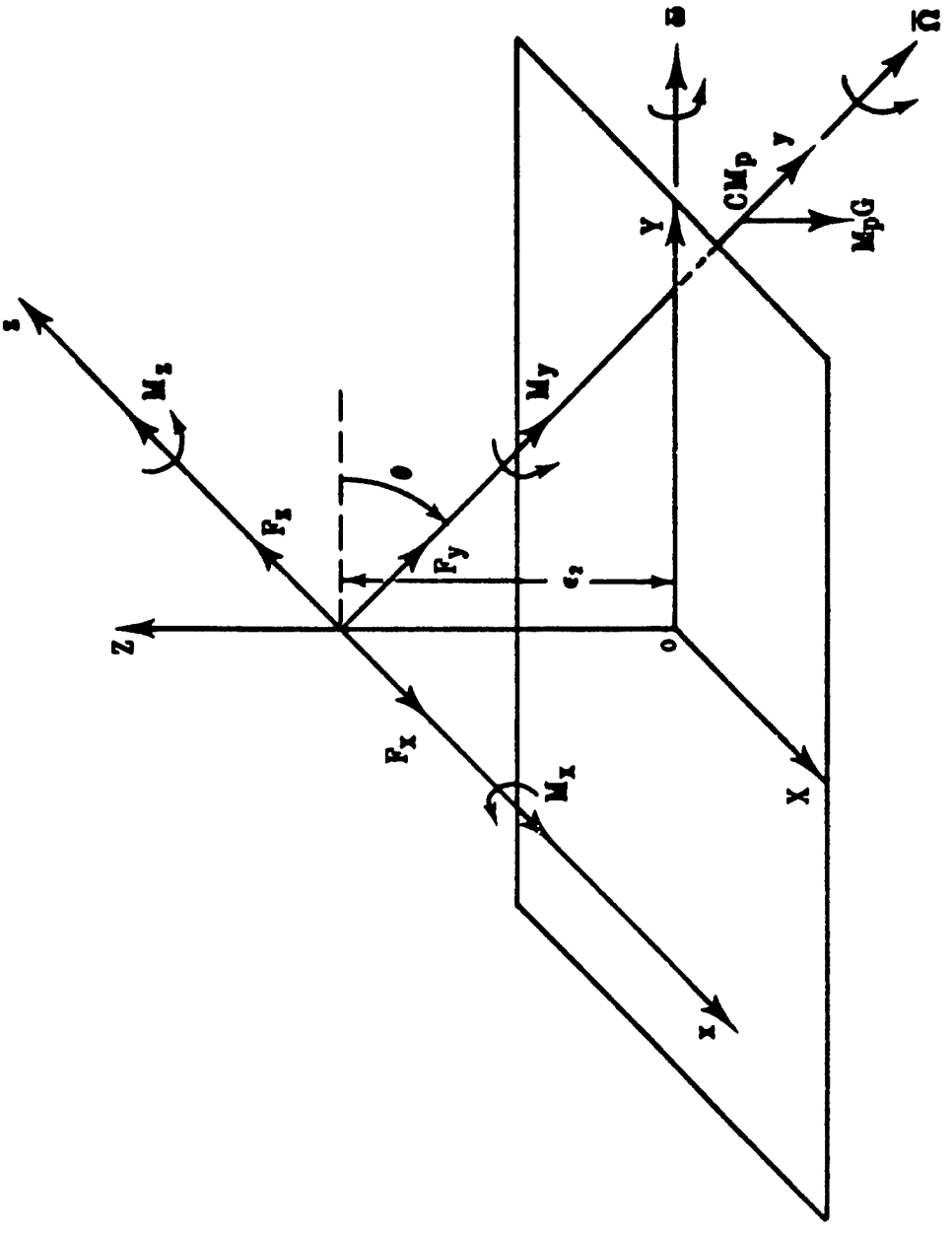

Figure 5: Freebody Diagram and Particular Configuration of Payload Section

The sum of all external moments about the payload sections mass center can be found by substituting equations (42) and (45) into equation (20). The resulting expression for the moment vector is

$$\bar{M}_{cm_p} = [\omega^2 S\theta C\theta (I_{zz} - I_{yy}) - I_{yy}\, \omega\, \Omega\, S\theta]\, \bar{e}_1 \qquad (46)$$

As in the general motion analysis, a constant spin rate of 987 rad/sec will be used, second order terms are ignored, and small angles are assumed.

The external forces that create a moment about the mass center of the payload section are shown in Figure 5. These forces can be found with the use of equation (23). The definitions of m_p, $\bar{a}$, and r will remain the same but the expression for $\bar{a}$ and $\bar{r}$ will be written as

$$\bar{a} = \bar{\omega} \times (\bar{\omega} \times \bar{r}) \qquad (47)$$

and

$$\bar{r} = (\ell - S\theta\epsilon_2)\, \bar{e}_2 + C\theta\epsilon_2\, \bar{e}_3 \qquad (48)$$

Note that

ℓ = the linear distance between the point "cmp" and point "P" (ℓ ft).

The resulting expression for $\bar{a}$ can be found by substituting equations (42) and (48) into equation (47),

$$\bar{a} = \omega^2 (S\theta\epsilon_2 - S^2\theta\, \ell)\bar{e}_2 - \omega^2(C\theta\epsilon_2 - S\theta C\theta\, \ell)\bar{e}_3 \qquad (49)$$

It has been demonstrated that the thrust of the rocket engine has little effect on the problem so this section of the report will not include it.

The external moments acting on the payload section are also shown in Figure 5 and can be evaluated by substituting equations (23), (46), (48) and (49) into equation (28). Thus, the following expression is found for the reaction moments at point "P",

$$\bar{M}_R = - [M \ell \omega^2 \epsilon_2 + \omega^2 (I_{yy} - I_{zz} - m_p \ell^2) \theta] \bar{e}_1 \tag{50}$$

An equal, but opposite, moment must act on the motor section and since at this instant the x axis and X axis are parallel, this moment is of the following scalar form:

$$M_X = M \ell \omega^2 \epsilon_2 + \omega^2 (I_{yy} - I_{zz} - m_p \ell^2) \tag{51}$$

By aligning $\bar{X}$ and X, and by noting that α (Figure 4) is equal to $\alpha_{\bar{X}3}$ then equations (9a) and (51) can be combined to form,

$$K\alpha = M \ell \omega^2 \epsilon_2 + \omega^2 (I_{yy} - I_{zz} - m_p \ell^2) \theta \tag{52}$$

If a dynamic stiffness is defined as

$$k = \omega^2 (I_{yy} - I_{zz} - m_p \ell^2) \tag{53}$$

and it is observed that

$$\theta = \alpha - \phi \tag{54}$$

then the following expression can be written:

$$\alpha = \frac{m_p \ell \omega^2 \epsilon_2 - k\phi}{K - k} \tag{55}$$

This equation results in a direct computation for α. If a rocket length of 48.24 inches is used and the rest of the needed physical char-

acteristics are obtained from Tables I and II then the resulting value of α is 1.123 millirad. A value of θ can now be found from equation (54) and is 0.922 millirad. Once it is realized that θ is the "in-tube" pitch angle of the payload section, it is seen that the presented value is in excellent agreement with the experimental data presented in [1 or 2].

E. MASS CENTER AND PLAI OF THE BENT ROCKET

This section of the report deals with the calculation of the mass center and the PLAI (Principal Linear Axis of Inertia) of the bent rocket. Both will be found via a lumped parameter model.

The analysis will be divided into two parts: first, the mass center of the bent rocket will be found, and then the PLAI will be found with respect to the launcher axis. In both parts, the physical characteristics of the rocket will be lumped in four sections: the motor assembly, the first and second halves of the shell section, and the payload section as in Figure 6. The resulting PLAI will give a mallaunch rate that is about halfway between the mallaunch rates of 200 millirad/sec and 300 millirad/sec reported in [1] and [2].

The mass of the entire shell section can be found using a shell length (L_s) of 1.871 ft., a shell thickness of 0.038 in., an inside shell radius of 2.0 in., mild steel shell (density equal to 15.23 slug/ft^3), a fuel density of 3.28 slug/ft^3, an inside fuel radius of 1.0 in., and a fuel thickness of 1.0 in [9]. The resulting shell and fuel mass (m_s) is 0.4992 slug. As the entire mass of the motor section is 0.7689 slug, Table II, the resulting motor assembly mass (m_m) is 0.2697 slug. Note that the motor section is made up of the motor assembly and both shell sections.

The distance of the mass center of the motor assembly (cm_m) from the rear of the rocket (d),(see Figure 7), can be found using the following equation,

$$d = \frac{m_m L_{cm} + m_s (L_{cm} - L_m - 1/4\, L_s)}{m_m} \qquad (56)$$

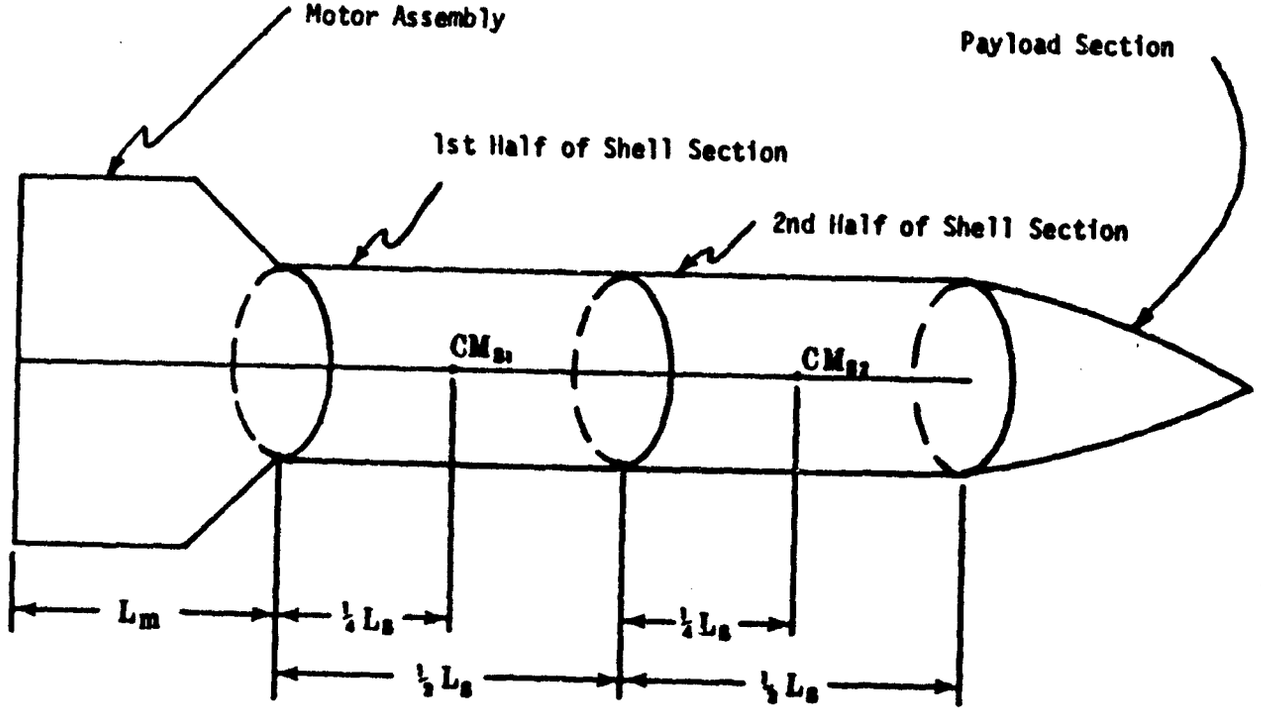

Figure 6: The Four Sections of the Rocket

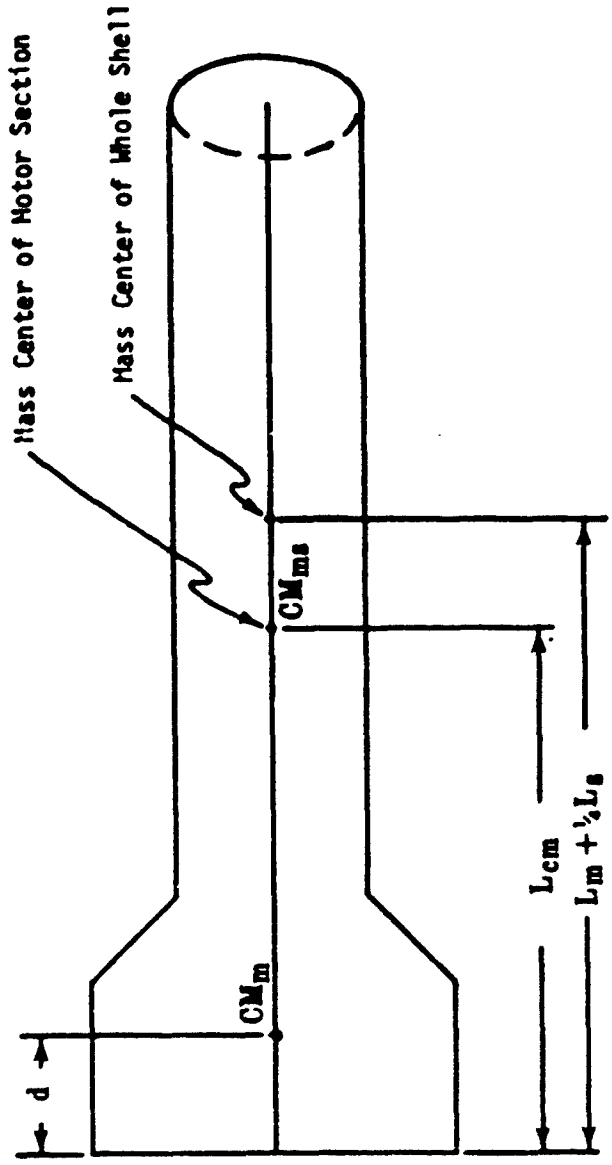

Figure 7: Location of cm_m with Respect to the Rear of the Rocket

where

L_{cm} = the distance of the mass center of the motor section from the rear of the rocket (0.9133 ft).

The resulting numerical value of d is 0.2556 ft.

Figure 8 shows the geometry of the four rocket sections in their bent configuration. The following symbols will be defined to clarify Figure 8,

z_1 = the value of the i = 1 deflection equation evaluated at $\bar{y}$ = 0.333 ft. The numerical value of z_1 is 2.5313×10^{-4}ft.

z_2 = the value of the i = 2 deflection equation evaluated at $\bar{y}$ = 1.269 ft. The numerical value of z_2 is 6.5677×10^{-4}ft.

β_m = the angle between the longitudinal axis of the motor assembly and the unbent axis of the rocket (0.795 millirad).

β_{s1} = the angle between the front half of the longitudinal axis of the shell section and the unbent axis of the rocket (0.4312 millirad).

β_{s2} = the angle between the second half of the longitudinal axis of the shell section and the unbent axis of the rocket (0.7021 millirad).

β_p = α = the angle between the longitudinal axis of the payload section and the rocket's unbent axis (1.1236 millirad).

Figure 9 shows the locations of the mass centers of the four rocket section with respect to the (X,Y,Z) coordinate system. The mass center of the motor assembly is described by coordinate pairs (y_m,z_m). Each remaining section has its respective coordinate pairs of (y_{s1},z_{s1}), (y_{s2},z_{s2}), and (y_p,z_p). The numerical values of each of these pairs are:

y_m = 0.2557 ft. $\qquad$ $z_m = 1.942 \times 10^{-4}$ft

y_{s1} = 0.8010 ft. $\qquad$ $z_{s1} = 4.551 \times 10^{-4}$ft.

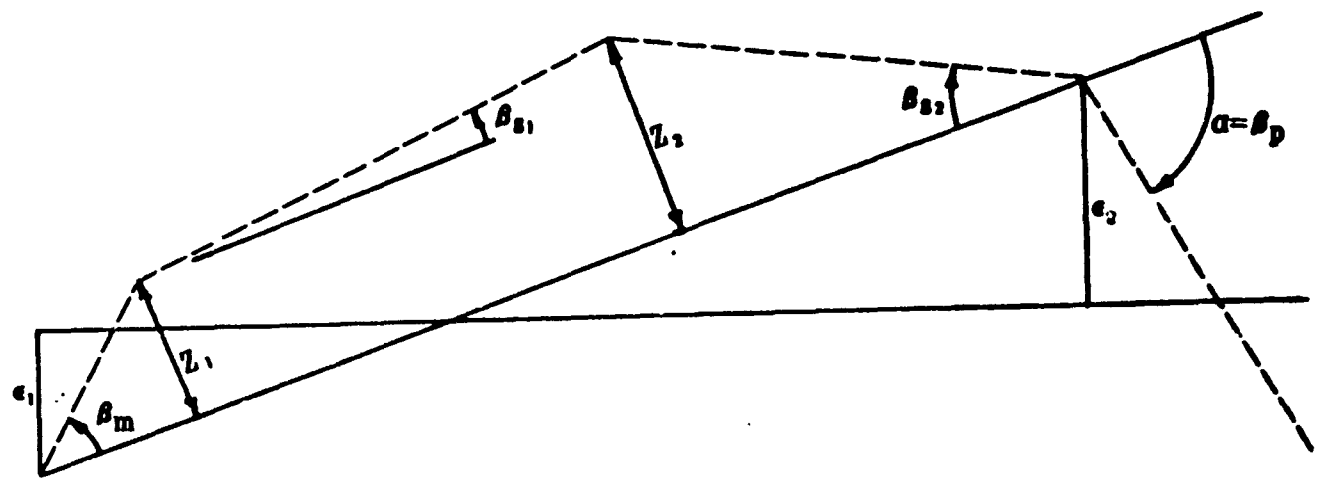

Figure 8: Rocket Sections Bent Configuration

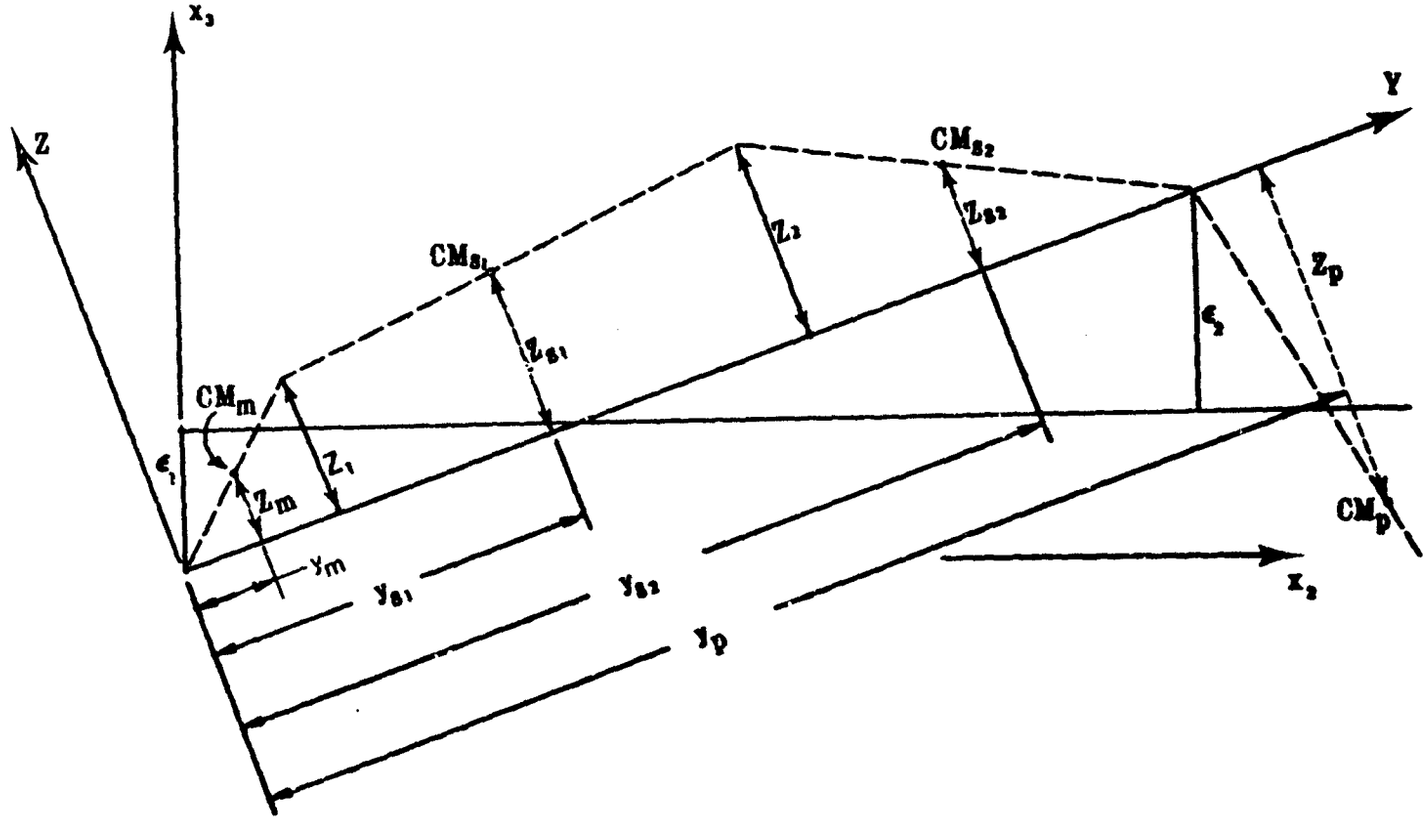

Figure 9: Rocket Sections Mass Center Locations

y_{s2} = 1.7365 ft. $\quad z_{s2} = 3.2838 \times 10^{-4}$ ft.

y_p = 2.9834 ft. $\quad z_p = 8.7548 \times 10^{-4}$ ft.

The mass center of the rocket can now be found with the use of the following equations,

$$y_{cm} = \frac{\sum y_n m_n}{\sum m_n} \tag{57}$$

$$z_{cm} = \frac{\sum z_n m_n}{\sum m_n} \tag{58}$$

where

y_{cm} = the y coordinate of the mass center of the bent rocket in the (X,Y,Z) system ($\stackrel{d}{=}$ ft)

z_{cm} = the z coordinate of the mass center of the bent rocket in the (X,Y,Z) system ($\stackrel{d}{=}$ ft)

N = m, s1, s2, and p and represents the motor assembly, the first half of the shell section, the second half of the shell section, and the payload section respectively.

y_n = the y coordinate of the nth section's mass center in the (X,Y,Z) system ($\stackrel{d}{=}$ ft)

z_n = the z coordinate of the nth section's mass center in the (X,Y,Z) system ($\stackrel{d}{=}$ ft)

m_n = the mass of the nth section ($\stackrel{d}{=}$ slug).

The resulting numerical values for y_{cm} and z_{cm} upon evaluation of equations (57) and (58) on 1.951 ft. and -2.781×10^{-4} ft. respectively.

The coordinate system (X_1,X_2,X_3) is shown in Figure 9. The relationship between the coordinates of the (X_1,X_2,X_3) system and those of the (X,Y,Z) system is,

$$\begin{bmatrix} X_1 \\ X_2 \\ X_3 \end{bmatrix} = [D] \cdot \begin{bmatrix} X \\ Y \\ Z \end{bmatrix} \tag{59}$$

where the matrix [D] is defined as,

$$[D] = \begin{bmatrix} 1 & 0 & 0 \\ 0 & C\phi & -S\phi \\ 0 & S\phi & C\phi \end{bmatrix} \tag{60}$$

Note that ϕ is defined by Figure 4 and has a value of 0.2015 milliradians for the bearing clearances given previously.

If X_2^{cm} and X_3^{cm} represent the coordinates of the rocket's mass center in the (X_1,X_2,X_3) system, their values, via equations (59) and (60), are 1.951 ft. and 1.1512×10^{-4} ft. respectively.

The coordinate pairs (X_2^N, X_3^N) can also be found with the use of equations (59) and (60) and their values are,

$X_2^m = 0.2557$ ft $\qquad X_3^m = 2.4573 \times 10^{-4}$ ft.

$X_2^{s1} = 0.8010$ ft. $\qquad X_3^{s1} = 6.1654 \times 10^{-4}$ ft.

$X_2^{s2} = 1.7365$ ft. $\qquad X_3^{s2} = 6.7835 \times 10^{-4}$ ft.

$X_2^p = 2.9834$ ft. $\qquad X_3^p = -2.742 \times 10^{-4}$ ft.

Now that the geometry and mass center locations are known for the four rocket sections and for the entire rocket, the task of finding the inertia tensor of the rocket can be undertaken. The inertia tensor of each rocket section will be found with respect to the principal axis system that is located at its own mass center, e.g., see Figure 10. Then the inertia tensor of each section is found in a coordinate system at its mass center, that is parallel to the (X_1,X_2,X_3) system. Next, the entire inertia tensor of the rocket will be found at a coordinate system located at the rocket's mass center and parallel to (X_1,X_2,X_3). The final step is to diagonalize this inertia tensor and thus find the bent rocket's PLAI.

The longitudinal mass moment of inertia of the first half of the shell section with respect to its principal axis system can be found from the following equation,

$$s_1 Iy'y' = 1/2(m_1 r^2_o - m_2 r^2_1) + 1/2 (m_{f1} r^2_{fo} - m_{f2} r^2_{f1}) \qquad (61)$$

where,

r_o = the outside shell radius ($\underline{\underline{d}}$ ft),

r_1 = the inside shell radius ($\underline{\underline{d}}$ ft),

r_{fo} = the outside fuel radius ($\underline{\underline{d}}$ ft),

r_{f1} = the inside fuel radius ($\underline{\underline{d}}$ ft),

and the quantities m_1, m_2, m_{f1}, and m_{f2} are given by the following equations,

$$m_1 = 1/2\ \rho\ \pi\ L_s\ r^2_o \qquad (62)$$

$$m_2 = 1/2\ \rho\ \pi\ L_s\ r^2_1 \qquad (63)$$

$$m_{f1} = 1/2\ \rho_f \pi\ L_s\ r^2_{fo} \qquad (64)$$

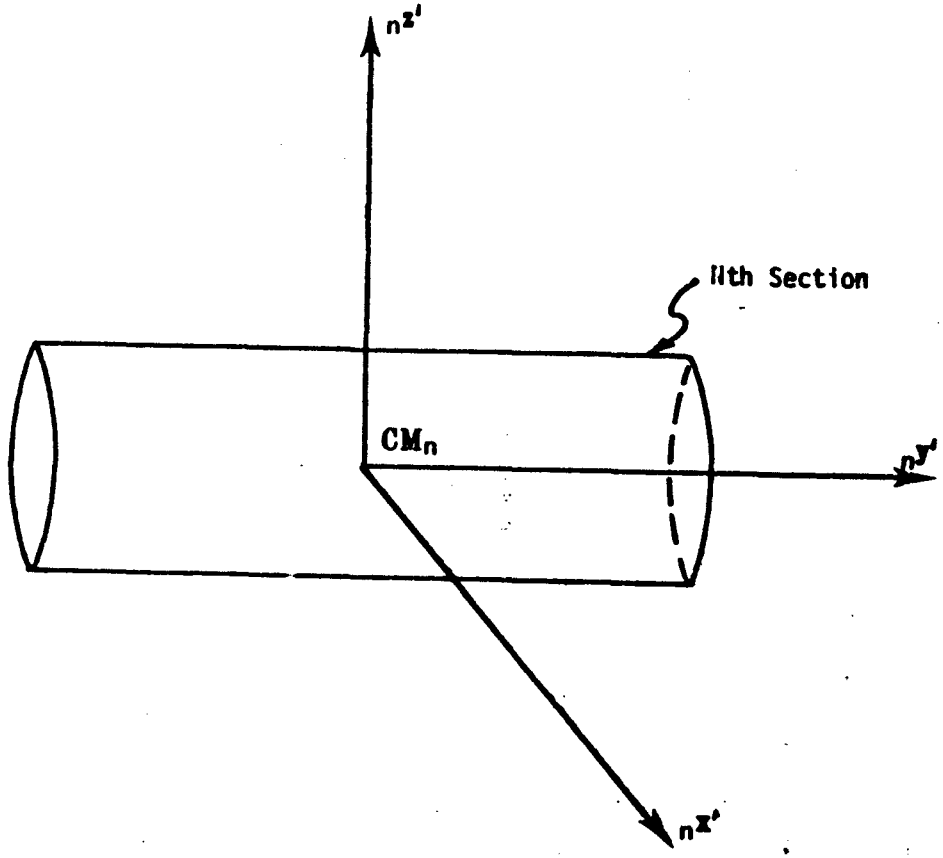

Figure 10: Definition of Principal Axis System of Nth Section

$$m_{f2} = 1/2\ \rho_f\ \pi\ L_s\ r^2_{f1} \tag{65}$$

where

ρ = the mass density of mild steel ($\frac{d}{=}$ slug/ft^3),

ρ_f = the mass density of the fuel ($\frac{d}{=}$ slug/ft^3).

The transverse mass monent of inertia of the first half of the shell section with respect to its principal axes can be found from the following equation,

$$_{s1}I_{x'x'} = {}_{s1}I_{z'z'} = 1/12\ [3(m_1 r^2_o - m_2 r^2_1) + (1/2\ L_s)^2(m_1 - m_2)]$$

$$+ 1/12\ [3(m_{f1} r^2_{fo} - m_{f2} r^2_{fo}) + (1/2\ L_s)^2(m_{f1} - m_{f2})] \tag{66}$$

The numerical values of $_{s1}I_{y'y'}$ and $_{s1}I_{x'x'}$ are 4.8731×10^{-3} slug/ft^2 and 0.0206 slug/ft^2 respectively. As the physical dimensions of the first and second halves of the shell section are the same, their mass moments of inertia are the same.

The principal axis system of the motor section (x',y',z') is shown in Figure 11. The values of d_m, d_{s1} and d_{s2} are 0.6577 ft., 0.1123 ft., and 0.8231 ft. respectively. The values of the principal longitudinal, and transverse ($I_{y'y'}$ and $I_{x'x'} = I_{z'z'}$) mass moments of inertia of the motor section with respect to (x',y',z') are 0.01837 slug/ft^2 and 0.43900 slug ft^2 (Table II) respectively.

The longitudinal mass moment of inertia ($_mI_{y'y'}$) of the motor assembly with respect to its own principal axis system, $_m$(x',y',z'), can be found from the following equation,

$$_mI_{y'y'} = I_{y'y'} - {}_{s1}I_{y'y'} - {}_{s2}I_{y'y'} \tag{67}$$

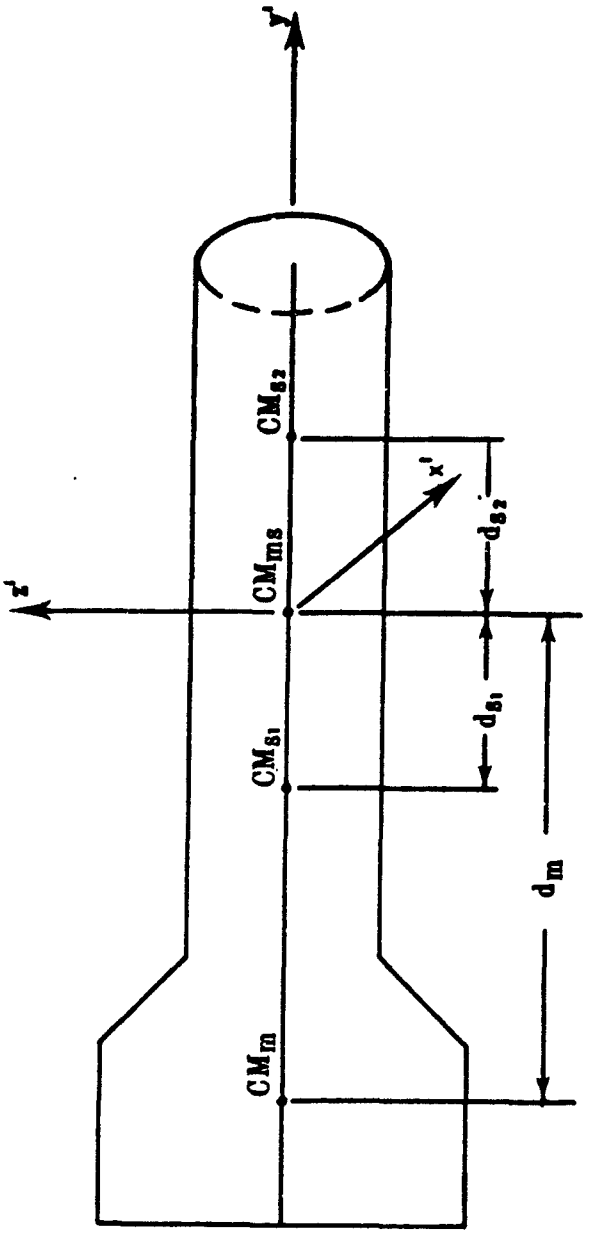

Figure 11: Principal Axis System of Motor Section

Also, the transverse mass moment of inertia (${}_{m}I_{x'x'} = {}_{m}I_{z'z'}$) of the motor assembly with respect to the same system is expressed by,

$$ {}_{m}I_{x'x'} = {}_{m}I_{z'z'} = I_{x'x'} - {}_{s1}I_{x'x'} - m_{s1}(d_{s1})^2 - {}_{s2}I_{x'x'} - m_{s2}(d_{s2})^2 - m_{m}(d_{m})^2 \qquad (68) $$

The resulting values of ${}_{m}I_{y'y'}$ and ${}_{m}I_{x'x'}$ are 8.6264×10^{-3} slug/ft^2 and 0.1087 slug/ft^2 respectively.

The inertia characteristics of the payload section are in Table 2. The values of ${}_{p}I_{y'y'}$ and ${}_{p}I_{x'x'}$ are 0.0108 slug/ft^1 and 0.20423 slug/ft^2 respectively.

The coordinate systems ${}_{N}(x_1,x_2,x_3)$ and ${}_{cm}(x_1,x_2,x_3)$ are shown in Figure 12. The ${}_{N}(x_1,x_2,x_3)$ system is at the mass center of the Nth section and parallel to the (x_1,x_2,x_3) system. The ${}_{cm}(x_1,x_2,x_3)$ system is located at the mass center of the bent rocket and is also parallel to the (x_1,x_2,x_3) system.

Figures 13, 14, 15 and 16 show the geometric relationship between the ${}_{N}(x',y',z')$ systems and the ${}_{N}(x_1,x_2,x_3)$ systems.

The inertia tensor of each section can be found in its respective (x_1,x_2,x_3) system by the transformation properties of the inertia terms (See Section 16.5 of [10]).

The resulting inertia tensor for each section with respect to its own (x_1,x_2,x_3) system is for the following motor assembly;

$$ {}_{m}I_{x_1x_1} = {}_{m}I_{x_3x_3} = 0.1087 \text{ slug ft}^2 $$

$$ {}_{m}I_{x_2x_2} = 9.6265 \times 10^{-3} \text{ slug ft}^2 $$

$$ {}_{m}I_{x_1x_2} = {}_{m}I_{x_2x_3} = 0 $$

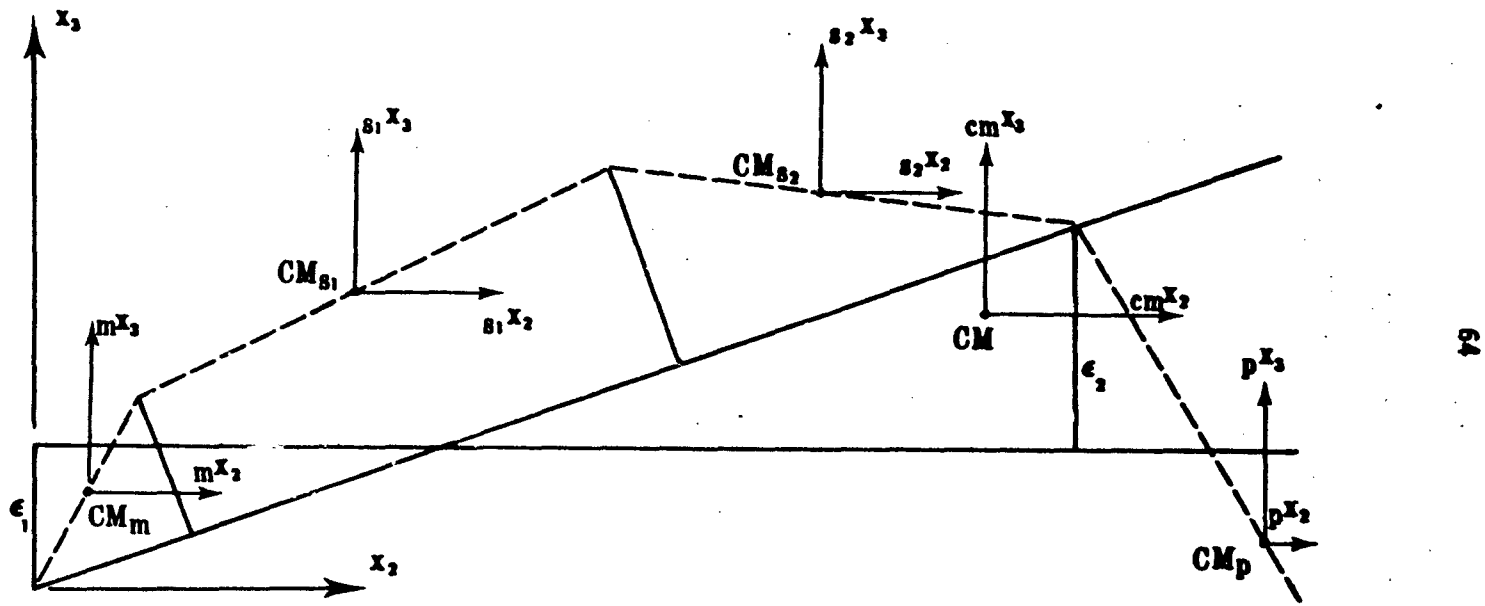

Figure 12: Definitions of $N(X_1, X_2, X_3)$ and $_{cm}(X_1, X_2, X_3)$

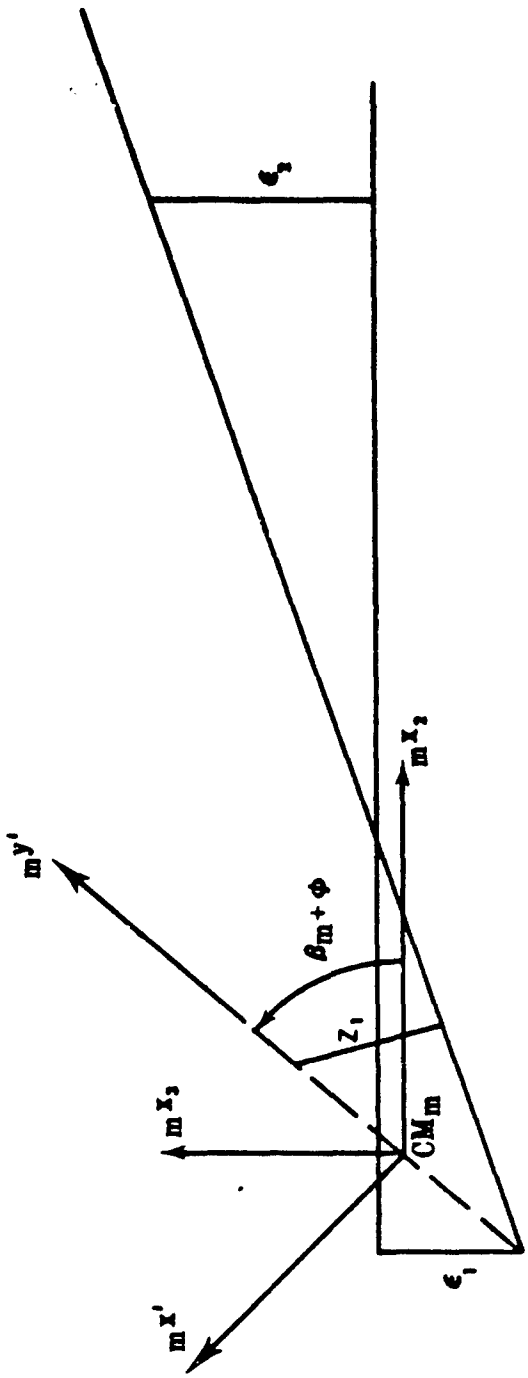

Figure 13: Geometric Relationship Between $_m(x', y', z')$ and $_m(x_1, x_2, x_3)$.

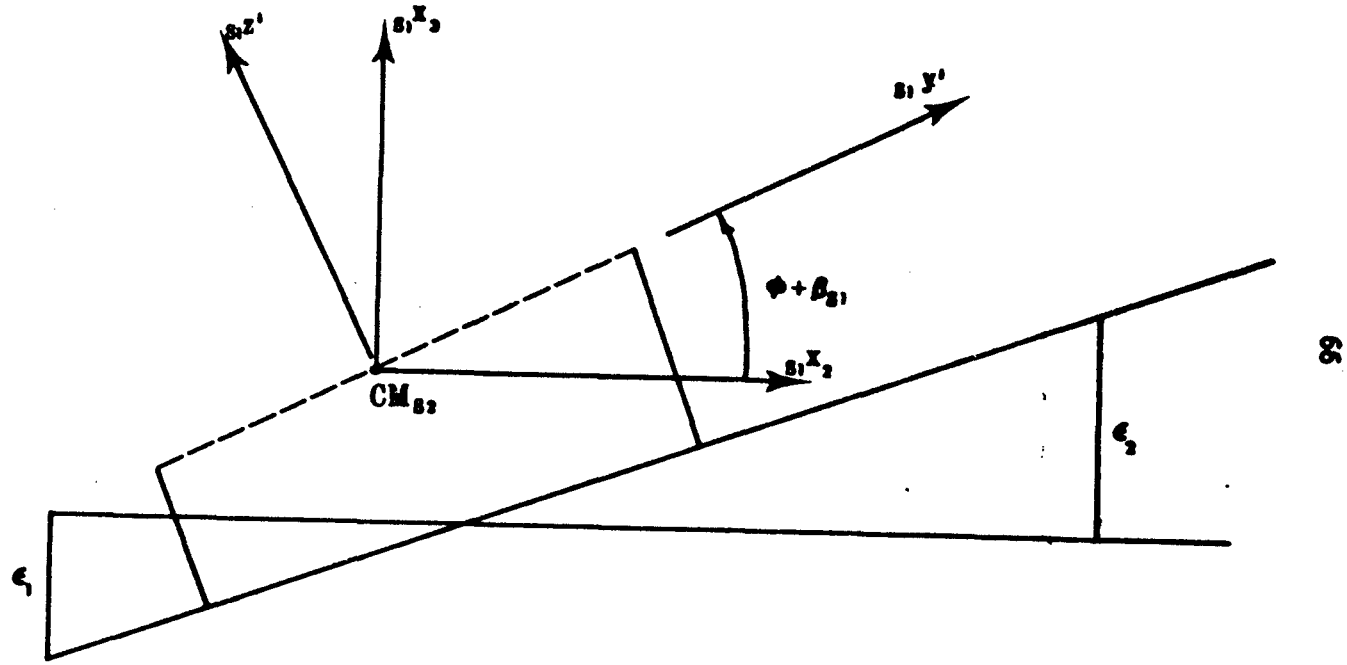

Figure 14: Geometric Relationship Between $_{s1}(X',Y',Z')$ and $_{s1}(X_1,X_2,X_3)$

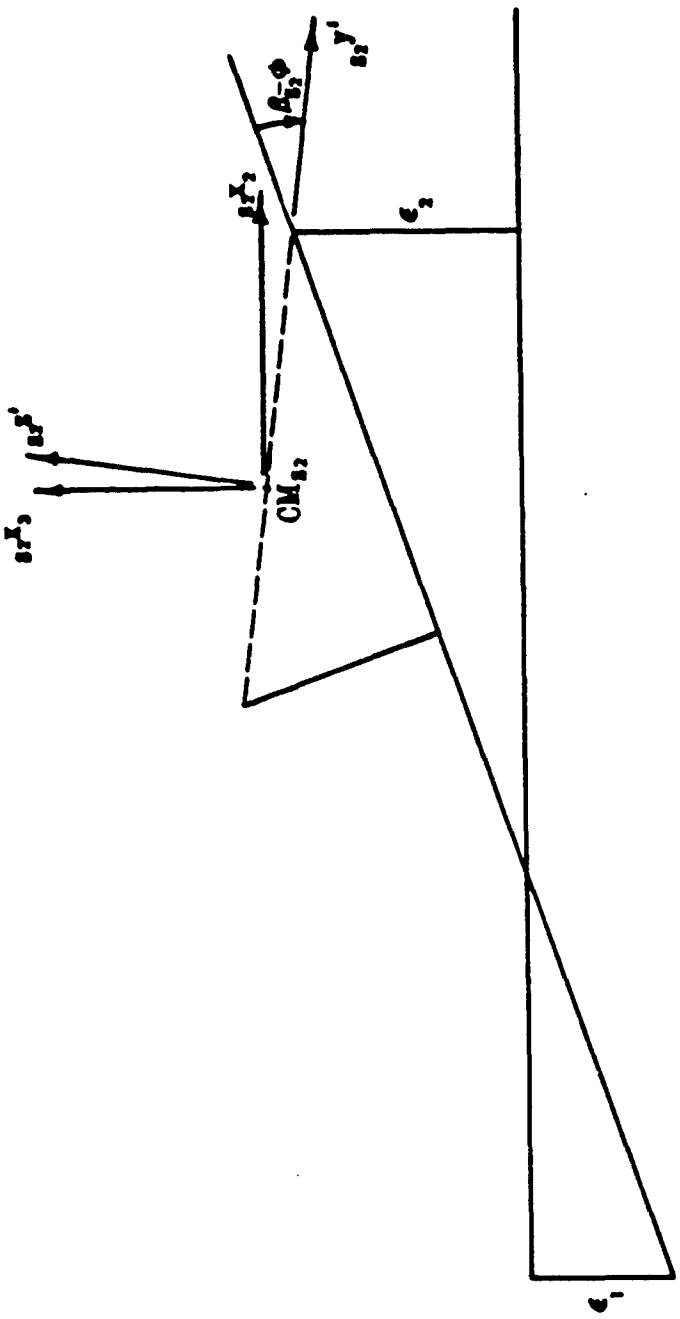

Figure 15: Geometric Relationship Between $_{s1}(X', Y', Z')$ and $_{s1}(X_1, X_2, X_3)$

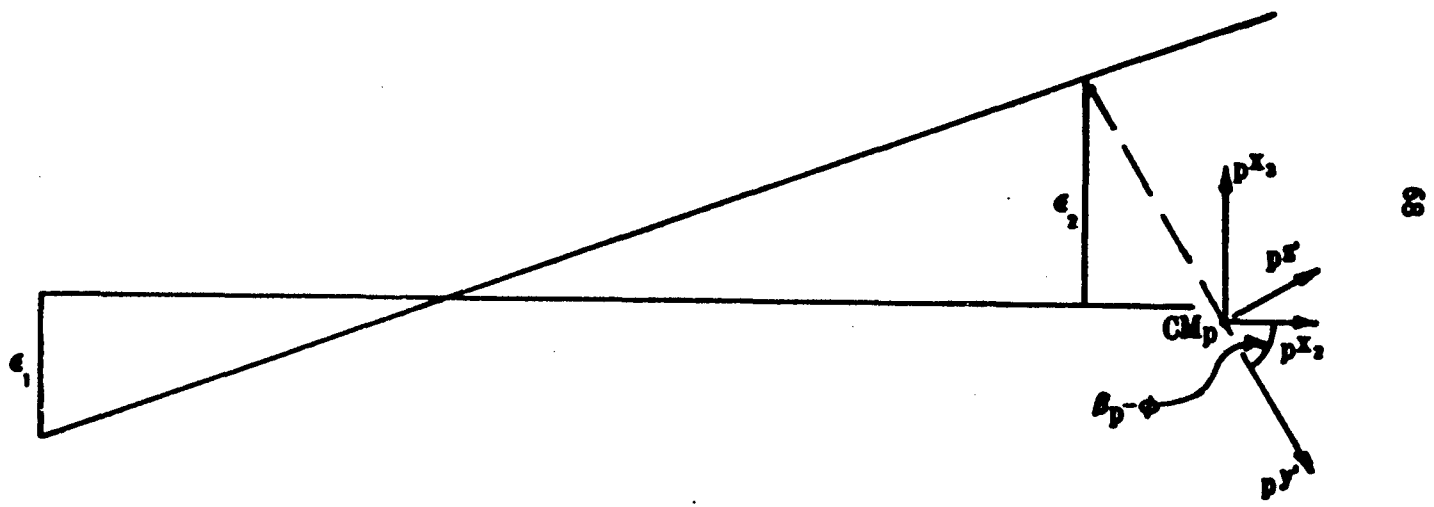

Figure 16: Geometric Relationship Between $_p(X', Y', Z')$ and $_p(X_1, X_2, X_3)$

$$m^I_{x_1x_1} = m^I_{x_3x_3} = 0.1087 \text{ slug ft}^2$$

$$m^I_{x_2x_2} = 8.6265 \times 10^{-3} \text{ slug ft}^2$$

$$m^I_{x_1x_2} = m^I_{x_1x_3} = 0$$

$$m^I_{x_2x_3} = 9.6223 \times 10^{-5} \text{ slug ft}^2$$

for the first half of the shell section

$$s1^I_{x_1x_1} = s1^I_{x_3x_3} = 0.02064 \text{ slug ft}^2$$

$$s1^I_{x_2x_2} = 4.8731 \times 10^{-3} \text{ slug ft}^2$$

$$s1^I_{x_1x_2} = s1^I_{x_1x_3} = 0$$

$$s1^I_{x_2x_3} = 9.98 \times 10^{-6} \text{ slug ft}^2$$

for the second half of the shell section

$$s2^I_{x_1x_1} = s2^I_{x_3x_3} = 0.02064 \text{ slug ft}^2$$

$$s2^I_{x_1x_2} = s2^I_{x_1x_3} = 0$$

$$s2^I_{x_2x_3} = -3.9575 \times 10^{-9} \text{ slug ft}^2$$

for the payload section

$$p^I_{x_1x_1} = p^I_{x_3x_3} = 0.20423 \text{ slug ft}^2$$

$$p^I_{x_2x_2} = 0.010833 \text{ slug ft}^2$$

$$p^I_{x_1x_2} = p^I_{x_1x_3} = 0$$

$$p^I_{x_2x_3} = -1.783 \times 10^{-4} \text{ slug ft}^2$$

The total inertia tensor of the bent rocket with respect to its $_{cm}(x_1,x_2,x_3)$ system can be found with the following equations,

$$_{cm}I_{x_2x_2} = m^I_{x_2x_2} + s1^I_{x_2x_2} + s2^I_{x_2x_2} + p^I_{x_2x_2} + m_m(x_3^{cm} - x_3^m)^2 + m_{s1}(x_3^{cm} - x_3^{s1})^2 + m_{s2}(x_3^{cm} - x_3^{s2})^2 + m_p(x_3^{cm} - x_3^p)^2 \quad (69)$$

$$_{cm}I_{x_3x_3} = m^I_{x_3x_3} + s1^I_{x_3x_3} + s2^I_{x_3x_3} + p^I_{x_3x_3} + m_m(x_2^{cm} - x_2^m)^2 + m_{s1}(x_2^{cm} - x_2^{s1})^2 + m_{s2}(x_2^{cm} - x_2^s)^2 + m_p(x_2^{cm} - x_2^p)^2 \quad (70)$$

$$_{cm}I_{x_1x_1} = m^I_{x_1x_1} + s1^I_{x_1x_1} + s2^I_{x_1x_1} + p^I_{x_1x_1} + m_m[(x_2^{cm} - x_2^m)^2 + (x_3^{cm} - x_3^m)^2] + m_p[(x_2^{cm} - x_2^p)^2 + (x_3^{cm} - x_3^p)^2] + m_{s1}[(x_2^{cm} - x_2^3)^2 + (x_2^{cm} - x_2^{s2})^2 + (x_3^{cm} - x_3^s)^2] \quad (71)$$

As $(x_3^{cm} - x_3^N)^2 << (x_2^{cm} - x_2^N)^2$, then ${}_{cm}I_{x_1x_1} = {}_{cm}I_{x_3x_3}$.

$$ {}_{cm}I_{x_1x_2} = {}_{cm}I_{x_1x_3} = 0 \tag{72} $$

$$ {}_{cm}I_{x_2x_3} = {}_{m}I_{x_2x_3} + {}_{s1}I_{x_2x_3} + {}_{s2}I_{x_2x_3} + m_m\, r_2^m\, r_3^m + m_{s1}\, r_2^{s1}\, r_3^{s1} + m_{s2}\, r_2^{s2}\, r_3^{s2} + m_p\, r_2^p\, r_3^p \tag{73} $$

where the quantities r_2^N and r_3^N are defined in the following equations

$$ \bar{r}_N = r_2^N\, \hat{j} + r_3^N\, \hat{k} \tag{74} $$

and $\bar{r}_N$ is the position vector of the mass center of the Nth section with respect to ${}_{cm}(x_1,x_2,x_3)$, [10]. The resulting numerical values are:

$${}_{cm}I_{x_2x_2} = 0.02921 \text{ slug ft}^2$$

$${}_{cm}I_{x_1x_1} = {}_{cm}I_{x_3x_3} = 2.2949 \text{ slug ft}^2$$

$${}_{cm}I_{x_2x_3} = -6.1663 \times 10^{-4} \text{ slug ft}^2$$

The angle between the PLAI axis and the ${}_{cm}x_2$ axis, Figure 17, is given by

$$ \text{TAN}(2\beta_{PLAI}) = \frac{-2\,{}_{cm}I_{x_2x_3}}{{}_{cm}I_{x_2x_3} - {}_{cm}I_{x_3x_3}} \tag{75} $$

The resulting value for β_{PLAI} is -0.2722 millirad.

The instantaneous mallaunch rate that corresponds to this particular geometry can be found from

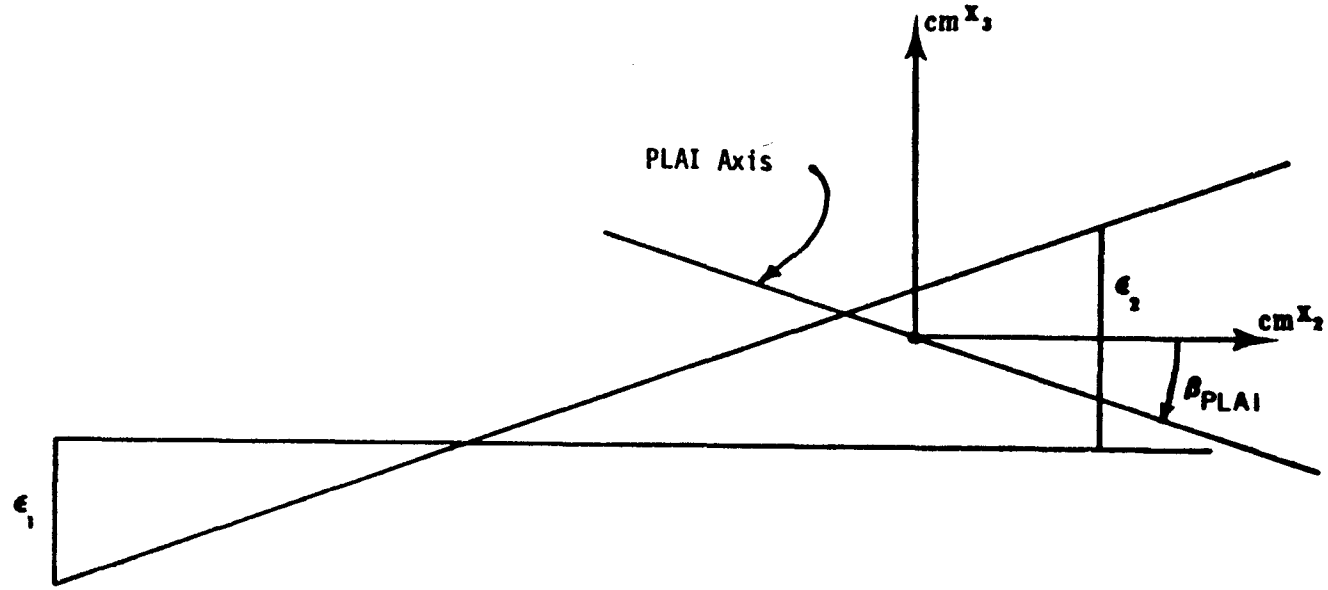

Figure 17: Geometric Relationship Between the PLAI Axis and the cm(X_1, X_2, X_3) System.

$$\omega_{MAL} = \Omega \text{ SIN } (\beta_{PLAI}) \qquad (76)$$

The resulting value of ω_{MAL} is - 267 millirad/sec. As mentioned previously this is about halfway between the values of 200 millirad/sec and 300 millirad/sec presented in [1] and [2] that are predicted to cause the down-range motion of ANSSR II.

L_1	L_2	L_3
0.3333 ft	1.829 ft	2.2042 ft
EI_1	EI_2	EI_3
1,006,944 lb ft^2	208,333 lb ft^2	1,041,667 lb ft^2

TABLE I. Physical Characteristics of the Motor Section

ITEM	Weight (lb)	Center-of-Mass[1] (in)	Transverse[2] Moment of Inertia (lbm-in^2)	Roll Moment of Inertia (lbm-in^2)
Head Assy	12.62	7.70	101.69	16.74
Balance Rings	2.37	12.92	3.75	7.20
Body Assy	4.91	16.34	45.60	15.20
DIM Assy	2.01	20.19	3.64	3.63
Fin Ring Assy	.69	21.85	1.94	.60
Pedestal	2.29	22.86	4.57	6.86
-Payload Section:	24.89	12.70	946.96	50.23
Motor Assy	23.17	36.71	1856.14	76.96
Aft Brg	.80	48.49	2.90	3.00
Skirt	.79	42.76	38.00	6.00
-Motor Section:	24.76	37.28	2035.56	85.96
-Total Rocket:	49.65	24.96	10476.40	136.19
Spin Propellant	.72	47.23	2.31	4.20
-Spin Motor BO:	48.93	24.63	10117.29	131.99
Boost Propellant	11.23	34.53	553.92	19.97
-Boost Motor BO:	37.70	21.68	8136.51	112.02

[1] Station 0.0 at Nose Tip

[2] Inertia about Center-of-Mass

TABLE II. Inertial Characteristics of the ANSSR II Rocket

F. REFERENCES

1. Pell, K. M. and Vest, C. L., "A Study of Selected Problems Based on ANSSR Flight Tests," Internal Technical Note RD-72-25, U. S. Army Missile Command, Redstone Arsenal, August (1972).

2. Greenwood, D. T., Principles of Dynamics, Prentice-Hall, Inc., Englewood Cliffs, New Jersey, (1965).

3. Rubert, et. al., "Flight Tests of An Aerodynamically Neutral, Spin Stabilized Rocket (ANSSR)," Internal Technical Note, RT-TR-72-17, U. S. Army Missile Command, Redstone Arsenal,

4. Pell, K. M., Vest, C. L. and Donovan, J. C., "ANSSR Flight Test Simulation and Selected Problem Investigation," Internal Technical Note RD-72-30, U. S. Army Missile Command, Redstone Arsenal, November, (1972).

5. Emerson Electric Company Drawing No. 638300-1.

6. Arnold, R. N. and Maunder, L., Gyrodynamics, Academic Press, London, (1961).

7. Cannon, R. H., Jr., Dynamics of Physical Systems, McGraw-Hill Book Company, New York, (1967).

8. Thomson, W. T., Mechanical Vibrations, Prentice-Hall, Englewood Cliffs, New Jersey, (1951).

9. Emerson Electric Company Drawing Number 638300-1.

10. Shames, I. H., Engineering Mechanics - Dynamics (Vol II), Prentice-Hall Inc., Englewood Cliffs, New Jersey, (1966).

SECTION III

MALLAUNCH AND MALAIM DUE TO LAUNCHER MOTION

ABSTRACT

Dynamical equations of motion are developed for a multitube launcher assembly for a spin-stabilized rocket. A parametric study is performed to minimize the mallaunch rates affecting missile flight. The results show that prudent selection of specific structural parameters can minimize mallaunch rates.

LIST OF SYMBOLS

A	Constant for the bearing amplitude
a	Average acceleration of the rocket
B	Constant for the bearing amplitude
c	Lateral Stiffness of the supports
d	Translation displacement of rocket along the y-axis after boost ignition
$F_{1,2}$	Vertical stiffness forces
$F_{3,4,5,6}$	Lateral stiffness forces
$F_{7,8}$	Forces due to pitch
$F_{9,10}$	Forces due to yaw
F_i	Reversed inertia force due to the vertical acceleration of launch assembly
F_j	Reversed inertia force due to the lateral acceleration of the launch assembly
I_{xx}	Pitch moment of inertia of launch assembly
I_{xy}	Roll moment of inertia of launch assembly
I_{zz}	Yaw moment of inertia of launch assembly
k	Vertical stiffness of supports
l_1	Distance from aft end of launcher to rear support
l_2	Distance from rear support to front support
l_3	Distance from aft end of launcher to the center of mass

l_4	Center to center distance between rocket bearings
l_5	Vertical distance from top of launcher to the center of mass
m	Mass of the launch assembly
P_B	Magnitude of the rear bearing force
P_F	Magnitude of front bearing force
$\bar{R}_B$	Rear bearing force vector
$\bar{R}_F$	Front bearing force vector
t	Time after boost
x	Displacement in the x-direction
x_c	Distance to the bore axis of the launch tube from the C.M in the x-direction
y	Displacement in the y-direction of launch assembly
z	Displacement in the z-direction of launch assembly
θ	Pitch
ϕ	Roll
ψ	Yaw
ω	Operational spin rate of the rocket

A. INTRODUCTION

The purpose of this section is to present the results of an analytical study of the launch dynamics of a multitube launching assembly for an aerodynamically neutral spin-stabilized rocket.

The system considered in this section has two component parts; the rocket and the multitube launching assembly. The launching assembly is composed of individual tubes that are rigidly mounted together to form a cluster. Each tube contains four guide rails one each on the sides of the tube and one each on the top and bottom of the tube as seen in Figure 1. The stability of the rocket is obtained through gyroscopic effects due to the spinning of the rocket within bearings mounted integrally with the rocket case. This spinning motion is attained before boost (i.e., ignition of the thrust motor) by four spin motors that are mounted on the aft end of the rocket. After the rocket is brought up to the operational spin rate, the thrust motor ignites propelling the rocket out the tube.

If the rocket is rigid (i.e., the rocket case does not bend) and the rocket's center of mass is to be located on the spin axis, then the rocket is theoretically balanced. If either of these conditions are not attained, the rocket will be in a state of unbalance. For the system considered, the unbalance effects are transmitted to the tube guide rails via the rocket's bearings. When the thrust motor is ignited, the rocket will traverse the length of the tube thus causing the unbalance forces to translate along the axis of the launch tube. Due to the spinning motion of the

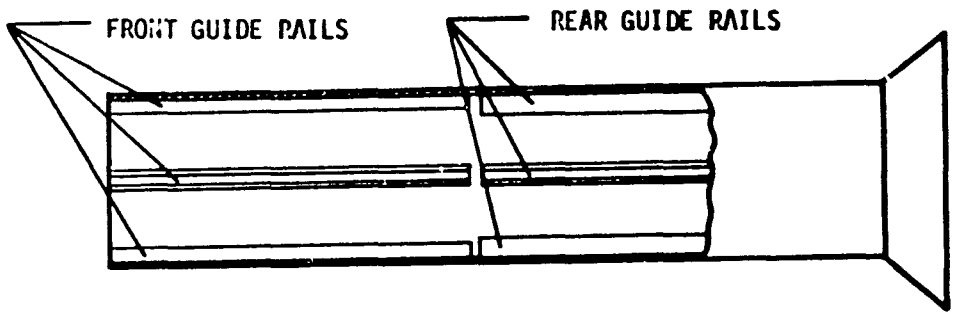

Figure 1. Semi-tactical Launch Tube

rocket, the unbalance forces rotate in a circular path within the launch tube. Thus, the forces applied to the launching system by the rocket are equivalent to a set of spiraling forces out the launch tube. This type of motion by the rocket within the tube can cause the launching assembly to oscillate. If the oscillations are severe enough, they can impart to the rocket a malaim and a mallaunch rate at the end of guidance.

The goal of this investigation is to determine the natural frequencies of the launching system and to determine if the assembly has any undue rotational motions at end of guidance severe enough to disturb missile launch. The theoretical work has been directed toward formulation and solution of the dynamical equations of motion for the multitube launching assembly. The rocket and the assembly are treated as discrete parts with the rocket contributing only to the motion of the assembly by the amplitude and the spin rate of its bearing reactions. In an earlier study it was found that the points of application of the force vectors of the front and rear bearings are 180 degrees out of phase (see Section II). In the mathematical expressions, the system considered is one with two supports equally spaced longitudinally from the center of mass as seen in Figure 2. Each support has a given lateral and vertical stiffness. As the two supports are equally spaced from the center of mass of the launcher assembly, the dynamical equations of motion are decoupled. As a result of this decoupling, mathematical expressions can be developed in a straight forward manner to determine the theoretical position and state of motion of the cluster assembly during launch.

From the mathematical expressions for the natural frequency, the position, and the motion of the assembly, parametric results are obtained

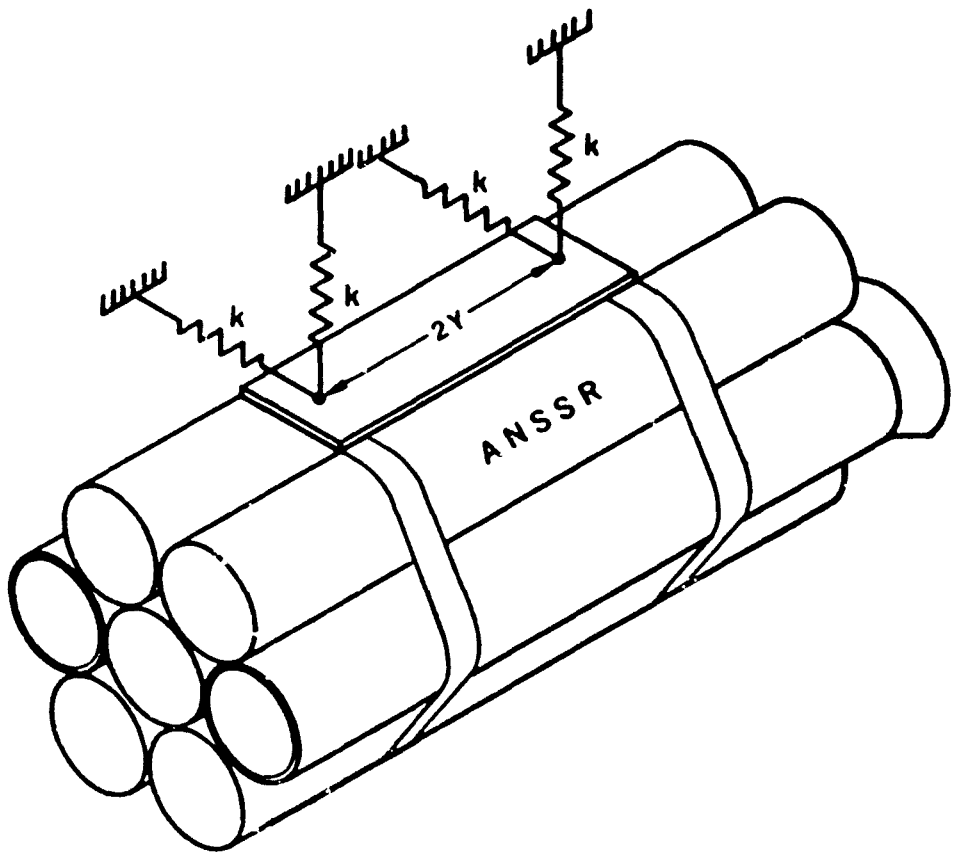

Figure 2. Cluster Assembly with Supports

and are presented in part D of this section. Thus, given certain parameters that affect the stability of the assembly, notably the acceleration of the rocket, the amplitude of the bearing forces the spin rate of the rocket, and the stiffness of the mounting hardware, the malaim and the mallaunch rates at the end of guidance can be determined and accounted for.

B. MATHEMATICAL FORMULATION OF DYNAMICAL EQUATIONS OF MOTION

In developing the differential equations, which describe the motion of the cluster assembly, several physical dimensions are used. For a complete list as to all of these physical dimensions, reference is made to Table I. It is assumed that the individual tubes of the cluster assembly are rigid with respect to one another. The center of the mass is considered fixed and the supports are equally spaced with respect to the center of mass.

The coordinate system to which all motion and position is referred is a right-handed cartesian coordinate system, X,Y,Z, with the origin 0 of the system fixed at the center of mass in such a position that the Y-axis lies parallel to the bore lines of the launch tubes.

From the free body diagrams, Figures 3 and 4, the summation of forces in the negative z-direction gives

$$\sum F_{-z} = 0 = -\bar{R}_B + F_1 + F_i - \bar{R}_F + F_2 \qquad (1)$$

and the summation of forces in the positive x-direction gives

$$\sum F_x = 0 = -\bar{R}_B + F_3 + F_j - \bar{R}_F + F_4 \qquad (2)$$

where F_i and F_j are the reversed inertia forces due to the vertical and lateral stiffness of the launcher assembly such that

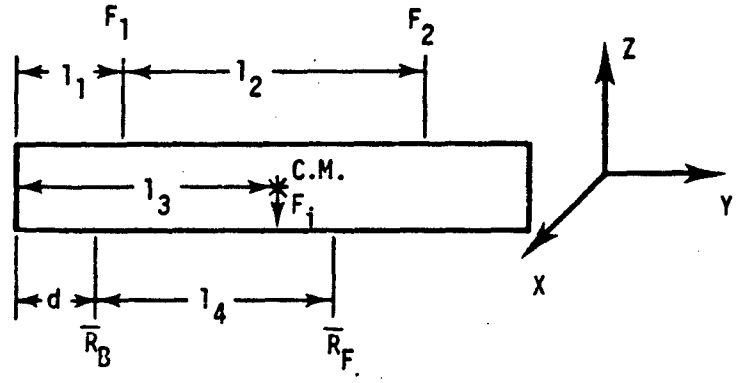

Figure 3. Free Body Diagram Number 1

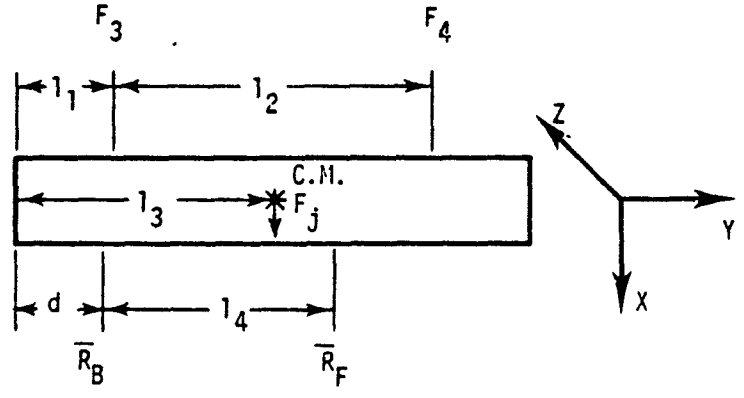

Figure 4. Free Body Diagram Number 2

TABLE I

Physical Dimensions of Launch Tube

l_2	Support Attachment Spacing	14.0 in
l_3	Transverse Distance to Center of Mass Forward of AFT End of Launch Tube	24.495 in
l_4	Rocket Bearing Spacing	25.690 in
I_{xx}	Pitch Moment of Inertia	13.6 slug ft^2
I_{zz}	Yaw Moment of Inertia	13.6 slug ft^2
m	Mass of Launch Assembly	5.49 slugs
a	Average Acceleration of Rocket	3122.316 ft/sec^2
t	Time after Boost Ignition	
ω	Rocket Operational Spin Rate	158 cps

$$F_i = m\ddot{x}$$

and

$$F_j = m\ddot{z}$$

From the free body diagrams, Figure 5,6, and 7, the summation of moments about the center of mass in the positive y-direction yields

$$\sum M_y^* = 0 - I_{yy}\ddot{\phi} + l_5 (F_5 + F_6) - z_c(P_B + P_F) \cos \omega t - x_c(P_B + P_F) \sin\omega t \tag{3}$$

The summation of moments about the center of mass in the x-direction gives

$$\sum M_x^* = 0 = I_{xx}\ddot{\theta} - \tfrac{1}{2} l_2 F_7 + \tfrac{1}{2} l_2 F_8 + (l_3 - d) \bar{R}_B - (l_3 - d - l_4) \bar{R}_F \tag{4}$$

and the summation of moments about the center of mass in the z-direction yields

$$\sum M_z^* = 0 = I_{zz}\ddot{\psi} - \tfrac{1}{2} l_2 F_9 + \tfrac{1}{2} l_2 F_{10} + (l_3 - d) \bar{R}_B - (l_3 - d - l_4) \bar{R}_F \tag{5}$$

From the geometry of the system and the stiffnesses of the supports, the following physical relationships are obtained:

$$F_1 = F_2 = kz \tag{6a}$$

$$F_3 = F_4 = F_5 = F_6 = cx \tag{6b}$$

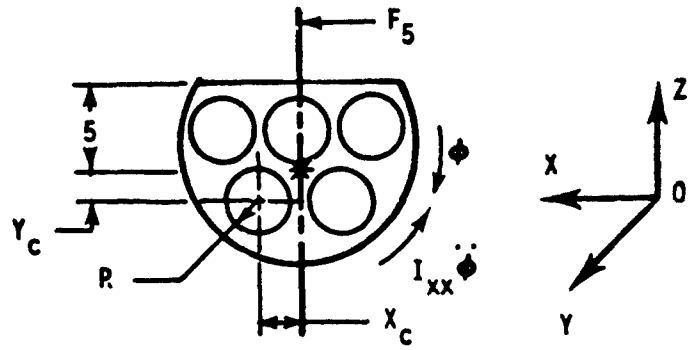

Figure 5. Free Body Diagram Number 3

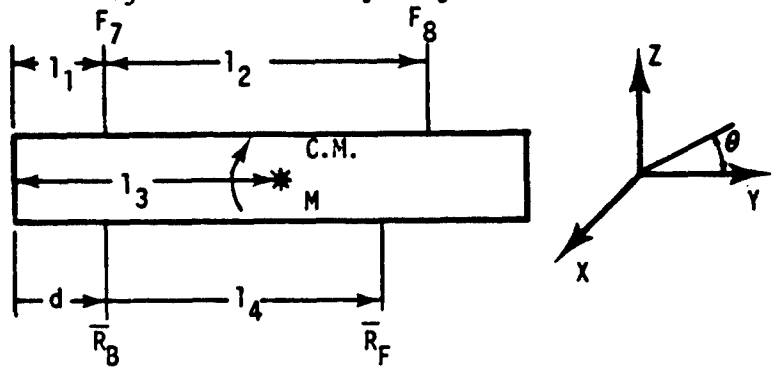

Figure 6. Free Body Diagram Number 4

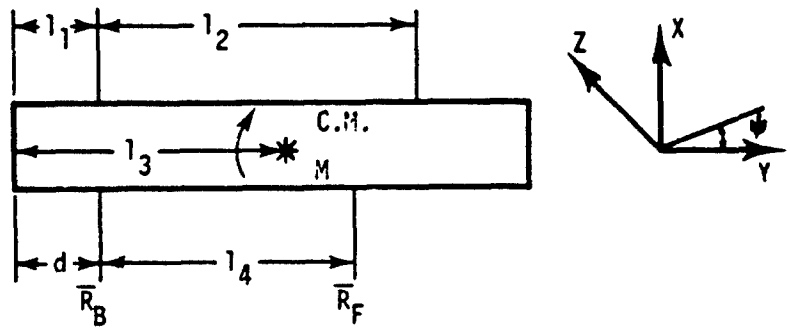

Figure 7. Free Body Diagram Number 5

$$F_7 = k\,(z - \tfrac{1}{2}\, l_2 \sin\theta) \tag{6c}$$

$$F_8 = k\,(z + \tfrac{1}{2}\, l_2 \sin\theta) \tag{6d}$$

$$F_9 = c\,(x - \tfrac{1}{2}\, l_2 \sin\psi) \tag{6e}$$

$$F_{10} = c\,(x + \tfrac{1}{2}\, l_2 \sin\psi) \tag{6f}$$

for small angles of rotation,

$$F_7 = k\,(z - \tfrac{1}{2}\, l_2\, \theta) \tag{6g}$$

$$F_8 = k\,(z + \tfrac{1}{2}\, l_2\, \theta) \tag{6h}$$

$$F_9 = c\,(x - \tfrac{1}{2}\, l_2\, \psi) \tag{6j}$$

$$F_{10} = c\,(x + \tfrac{1}{2}\, l_2\, \psi) \tag{6k}$$

The bearing reactions are cyclic and revolve within the launch tube at a rate approximately equal to the spin rate of the rocket [3]. The front and rear bearing reactors are 180° out of phase. Thus, the bearing reactions can be represented by the sinusoid of functions which results in

$$\overline{R_F} = -P_F \sin\omega t \tag{7a}$$

$$\overline{R_B} = P_B \sin\omega t \tag{7b}$$

where P_F and P_B are the magnitudes of the front and rear bearing reactions respectively and ω is the spin rate of the rocket.

The distance, d, that the rocket has moved out the launch tube is given by the equation

$$d = \tfrac{1}{2} a t^2 \tag{8}$$

where a is the average acceleration of the rocket and t is the elapsed time after boost.

From Newton's second law of motion, the inertia forces associated with the cluster assembly due to acceleration of the center of mass vertically and laterally are

$$F_j = m\ddot{z} \tag{9a}$$

$$F_j = m\ddot{x} \tag{9b}$$

Equations (6a, 6b, 6g-k, 7a, 7b, 8, 9a, 9b) substituted into equations (1-5) result in the dynamical equations of motion.

$$m\ddot{z} + 2kz = (P_B - P_F) \sin \omega t \tag{10}$$

$$m\ddot{x} + 2kz = (P_B - P_F) \sin \omega t \tag{11}$$

$$I_{yy} \ddot{\phi} + 2c l_5 x = (P_B + P_F)(z_c \cos \omega t + X_c \sin \omega t) \tag{12}$$

$$I_{xx} \ddot{\theta} + \tfrac{1}{2} l_2^2 k \theta = -[(l_3 - l_4) P_F + l_3 P_B] + \sin \omega t + \tfrac{1}{2} (P_B - P_F) a t^2 \sin \omega t \tag{13}$$

$$I_{zz} \ddot{\psi} + \tfrac{1}{2} l_2^2 c \psi = -[(l_3 - l_4) P_F + l_3 P_B] + \sin \omega t + \tfrac{1}{2}(P_B + P_F) a t^2 \sin \omega t \tag{14}$$

Equation (12) has two dependent variables, ϕ and x, and one independent

C. SOLUTIONS OF DYNAMICAL EQUATIONS OF MOTION

The solution to the dynamical equations of motion derived in the preceding section will be given in two parts, the first being the natural frequency of the cluster assembly, which will be obtained from the unforced part of the equations of motion. The second solution will be used to obtain the position and motion of the assembly as a function of time during launch.

Part 1

The characteristic equations are obtained by setting the unforced part of the equations of motion equal to zero which yields

$$(ms^2 + 2k)z = 0 \tag{17}$$

$$(ms^2 + 2c)x = 0 \tag{18}$$

$$(I_{yy}s^2 + 2cl_5^2)\phi = 0 \tag{19}$$

$$(I_{xx}s^2 + \tfrac{1}{2}l_2^2k)\theta = 0 \tag{20}$$

$$(I_{zz}s^2 + \tfrac{1}{2}l_2^2c)\psi = 0 \tag{21}$$

The natural frequencies, s, are obtained by a solution of each characteristic equation which gives

$$S_1 = \pm\sqrt{-2k/m} \tag{22}$$

$$S_2 = \pm\sqrt{-2c/m} \tag{23}$$

$$S_3 = \pm\sqrt{-2cl_5^2/I_{yy}} \tag{24}$$

$$S_4 = \pm\sqrt{-l_2^2\ k/2\ I_{xx}} \tag{25}$$

$$S_5 = \pm\sqrt{-l_2^2\ c/2\ I_{zz}} \tag{26}$$

Part 2

Each of the dynamical equations of motion is a second order linear differential equation with constant coefficients. The method of variation of parameters is used to solve the equations. Three different solutions are required due to differences in the forcing functions in the equations of motion. Equations (10) and (11) are of the same form and equations (13) and (14) are of the same form. It is possible to obtain a general solution for each set.

The general form of equations (10) and (11) is

$$m\ddot{y} + ky = A \sin\omega t$$

where m, k, and A are constants. This is a second order linear differential equation with constant coeffients with a sinusoidal forcing function. y is obtained by the method of variation of parameters as

$$y = -\sqrt{\frac{m}{k}}\left(\frac{A\omega}{k-m\omega^2}\right)\sin\sqrt{\frac{k}{m}}\ t + \left(\frac{A}{k-m\omega^2}\right)\sin\omega t \tag{27}$$

z is obtained by a substitution of equation (10) into equation (27) as

$$z = -\sqrt{\frac{m}{2k}}\left(\frac{(P_B - P_F)}{2k - m\omega^2}\right)\sin\sqrt{\frac{2k}{m}}\,t$$

$$+\left(\frac{P_B - P_F}{2k - m\omega^2}\right)\sin\omega t \qquad (28)$$

x is obtained by a substitution of equation (11) into equation (27) as

$$x = \sqrt{\frac{m}{2k}}\left(\frac{(P_B - P_F)}{2c - m\omega^2}\right)\sin\sqrt{\frac{2c}{m}}\,t$$

$$+\left(\frac{P_B - P_F}{2c - m\omega^2}\right)\sin\omega t \qquad (29)$$

Equations (13) and (14) are of the form

$$m\ddot{y} + ky = A\sin\omega t + Bt^2\sin\omega t$$

This equation is also a second order linear differential equation with constant coeffieients. y is again obtained by the method of variation of parameters which yields

$$y = \sqrt{\frac{m}{k}}\left[\frac{A\omega}{k-m\omega^2} + \frac{6Bm\omega}{(k-m\omega^2)^3} + \frac{8Bm^2\omega^3}{(k-m\omega^2)^3}\right]\sin\sqrt{\frac{k}{m}}\,t + \left(\frac{B}{k-m\omega^2}\right)t^2$$

$$\sin\omega t - \frac{4Bm\omega}{(k-m\omega^2)^2}\,t\cos\omega t + \left[\frac{A}{k-m\omega^2} - \frac{2mB}{(k-m\omega^2)} - \frac{8Bm^2\omega^3}{k-m\omega^2)^3}\right]\sin\omega t \qquad (30)$$

θ is obtained by a substitution of the variables and constants of

equation (13) into equation (30) as

$$\theta = \sqrt{\frac{2\,I_{xx}}{l_2^2\,k}}\left[\frac{2\omega[(l_3-l_4)P_F + l_3\,P_B]}{l_2^2\,k - 2\,I_{xx}\omega^2} + \frac{12\,\omega\,I_{xx}a(P_B + P_F)}{(l_2^2\,k - 2\,I_{xx}\omega^2)^2}\right.$$

$$\left. + \frac{32\,I_{xx}^2\,\omega^3\,a(P_B + P_F)}{(l_2^2\,k - 2\,I_{xx}\omega^2)^3}\right]\sin\sqrt{\frac{l_2^2\,k}{2\,I_{xx}}}\,t$$

$$+ \frac{a(P_B + P_F)}{l_2^2\,k - 2\,I_{xx}\omega^2}\,t^2\sin\omega t - \frac{8\,I_{xx}\omega a(P_B + P_F)}{(l_2^2\,k - 2\,I_{xx}\omega^2)^2}\,t\cos\omega t$$

$$- \left[\frac{2[(l_3 - l_4)P_F + l_3\,P_B]}{l_2^2\,k - 2\,I_{xx}\omega^2} + \frac{4\,I_{xx}a(P_B + P_F)}{(l_2^2\,k - 2\,I_{xx}\omega^2)^2}\right.$$

$$\left. + \frac{32\,I_{xx}^2\,\omega^3 a(P_B + P_F)}{(l_2^2\,k - 2\,I_{xx}\omega^2)^3}\right]\sin\omega t \qquad (31)$$

ψ is obtained by a substitution of the variables and constants of equation (14) into equation (30) as

$$\psi = \sqrt{\frac{2\,I_{zz}}{l_2^2\,c}}\left[\frac{2\omega[(l_3-l_4)P_F + l_3\,P_B]}{l_2^2\,c - 2\,I_{zz}\omega^2} + \frac{12\,\omega\,I_{zz}a(P_B + P_F)}{(l_2^2\,c - 2\,I_{zz}\omega^2)^2}\right.$$

$$\left. + \frac{32\,I_{zz}^2\,\omega^3 a(P_B + P_F)}{(l_2^2\,c - 2\,I_{zz}\omega^2)^3}\right]\sin\sqrt{\frac{l_2^2\,c}{2\,I_{zz}}}\,t$$

(Equation continued on next page.)

$$+ \frac{a(P_B + P_F)}{l_2^2 c - 2 I_{zz}\omega^2} t^2 \sin\omega t - \frac{8 I_{zz}\omega a(P_B + P_F)}{(l_2^2 c - 2 I_{zz}\omega^2)^2} t \cos\omega t$$

$$- \left[\frac{2[(l_3-l_4)P_F + l_3P_B]}{l_2^2 c - 2 I_{zz}\omega^2} + \frac{4 I_{zz} a(P_B + P_F)\omega}{(l_2^2 c - 2 I_{zz}\omega^2)^2}\right.$$

$$\left. + \frac{32 I_{zz}^2 \omega^3 a(P_B+P_F)}{(l_2^2 c - 2 I_{zz}\omega^2)^3}\right] \sin\omega t \qquad (32)$$

Equation (16) is of the form

$$m\ddot{y} + ky = A\cos\omega t + B\sin\omega t$$

The same method also serves to obtain a solution for y as

$$y = \sqrt{\frac{m}{k}}\left(\frac{B\omega}{k-m\omega^2}\right)\sin\sqrt{\frac{k}{m}}\,t - \left(\frac{A}{k-m\omega^2}\right)\cos\sqrt{\frac{k}{m}}\,t + \left(\frac{B}{k-m\omega^2}\right)$$

$$\cdot\sin\omega t + \left(\frac{A}{k-m\omega^2}\right)\cos\omega t \qquad (33)$$

ϕ follows by a substitution of equation (16) into equation (33) as

$$\phi = \sqrt{\frac{I_{yy}}{2 c l_5^2}}\left[\frac{X_c (P_B - P_F)}{2 c l_5^2 - I_{yy}\omega^2}\right]\sin\sqrt{\frac{2 c l_5^2}{I_{yy}}}\,t$$

(Equation continued on next page)

$$-\left[\frac{(P_B-P_F)Z_c}{2\,c\,l_5^2 - I_{yy}\omega^2}\right]\cos\sqrt{\frac{2\,c\,l_5^2}{I_{yy}}}\,t + \left[\frac{(P_B - P_F)}{2\,c\,l_5^2 - I_{yy}\omega^2}\right]$$

$$\bullet\,[X_c \sin\omega t + Z_c \cos\omega t] \qquad (34)$$

The stiffness of the mounting hardware is considered such that the lateral stiffness and the vertical stiffness are equal. The equations (31 and 32 are identical except for the principal moments of inertia. If the moments of inertia are approximately equal, then equation (32) becomes identical to equation (31). Equations (28 and 29) are identical as the vertical and lateral stiffness are equal. Thus, substitution of

$$k = c$$

into equations (28, 29, 31, and 32) yields

$$X = Z = -\sqrt{\frac{m}{2k}}\left(\frac{(P_B-P_F)\omega}{2k - m\omega^2}\right)\sin\sqrt{\frac{2k}{m}}\,t + \left(\frac{P_B-P_F}{2k - m\omega^2}\right)\sin\omega t \qquad (35)$$

and

$$\theta = \psi = \sqrt{\frac{2\,I_{xx}}{l_2^2\,k}}\left[\frac{2\omega[(l_3-l_4)P_F + l_3P_B]}{l_2^2\,k - 2\,I_{xx}\omega^2} + \frac{12\omega I_{xx}a(P_B+P_F)}{(l_2^2\,k - 2\,I_{xx}\omega^2)^2}\right.$$

$$\left. + \frac{32\,I_{xx}^2\omega^3 a(P_B+P_F)}{(l_2^2\,k - 2\,I_{xx}\omega^2)^3}\right]\sin\sqrt{\frac{l_2^2\,k}{2\,I_{xx}}}\,t + \frac{a(P_B + P_F)}{l_2^2\,k - 2\,I_{xx}\omega^2}\,t^2\sin\omega t$$

(Equation continued on next page.)

$$- \frac{8\, I_{xx}\omega a(P_B+P_F)}{(l_2^2 k - 2\, I_{xx}\omega^2} - \left[\frac{2[(l_3-l_4)P_F+l_3P_B]}{l_2^2 k - 2\, I_{xx}\omega^2} + \frac{4\, I_{xx}a(P_B+P_F)}{(l_2^2 k - 2\, I_{xx}\omega^2)^2}\right.$$

$$\left. + \frac{32\, I_{xx}^2\omega^3\, a(P_B+P_F)}{(l_2^2 k - 2\, I_{xx}\omega^2)^3}\right]\sin\omega t \qquad (36)$$

For the time rate of change of pitch, $\dot{\theta}$, and displacement,

$$\dot{\theta} = \dot{\psi} = \frac{d}{dt}(\theta) = \left[\frac{2\omega[(l_3-l_4)P_F + l_3P_B]}{l_2^2 k - 2\, I_{xx}\omega^2} + \frac{12\omega I_{xx}a(P_B+P_F)}{(l_2^2 k - 2I_{xx}\omega^2)^2}\right.$$

$$\left. + \frac{32\, I_{xx}^2\omega^3\, a(P_B+P_F)}{(l_2^2 k - 2\, I_{xx}\omega^2)^3}\right]\cos\sqrt{\frac{l_2^2 k}{2\, I_{xx}}}\, t + \frac{2\, a(P_B+P_F)}{l_2^2 k - 2\, I_{xx}\omega^2}\, t$$

$$\cdot\sin\omega t + \frac{a(P_B+P_F)}{l_2^2 k - 2\, I_{xx}\omega^2}\, t^2\cos\omega t + \left[\frac{8\omega I_{xx}a(P_B+P_F)}{(l_2^2 k - 2\, I_{xx}\omega^2)^2}\right]$$

$$\cdot[\omega t\sin\omega t - \cos\omega t] - \left[\frac{2[(l_3-l_4)P_F+l_3P_B)]}{l_2^2 k - 2\, I_{xx}\omega^2} + \frac{4\, I_{xx}\, a(P_B+P_F)}{(l_2^2 k - 2\, I_{xx}\omega^2)^2}\right.$$

$$\left. + \frac{32\, I_{xx}^2\omega^3\, a(P_B+P_F)}{(l_2^2 k - 2\, I_{xx}\omega^2)^3}\right]\omega\cos\omega t \qquad (37)$$

and

$$\dot{x} = \dot{z} = \frac{d}{dt}(x) = \left[\frac{(P_B - P_F)}{2k - m\omega^2}\,\omega\right]\left(\cos\omega t - \cos\sqrt{\frac{2k}{m}}\,t\right) \qquad (38)$$

Equations (35, 36, 37, and 38) give the displacement, malaim, mallaunch, and rate of displacement as a function of the parameters, support stiffness, average acceleration, bearing reactions and spin rate.

D. ANALYSIS AND CONCLUSIONS

From the solution of the dynamical equations of motion, a parametric study has been done to determine the malaim and mallaunch rates at end of guidance. The results of this study are presented in Figures 8 thru 21 for the multitube launcher parameters as listed in Table I.

In this study the following parameters are varied: the average acceleration, the bearing reactions, the support stiffnesses, the operational spin rate and the time from initial boost until end of guidance. The average acceleration was varied from 1000 ft/sec^2 to 4000 ft/sec^2 as shown in Figures 8 and 9. Increasing the average acceleration (i.e., increasing the thrust) decreases the time to end of guidance, but increases the mallaunch rate at end of guidance.

By assuming the front and rear bearing forces to be equal, the displacement, z, and the rate of change of displacement, $\dot{z}$, are zero. Increasing the bearing reactions equally causes the magnitude of the malaim and mallaunch rate to increase as shown in Figures 10 and 11.

Figures 12 and 13 show typical solutions of the dynamical equations of motion for support stiffnesses, $k = 0.0$ to $k = \infty$. As the natural frequency of the cluster assembly approaches the critical spin rate, that is

$$k \longrightarrow \frac{2\, I_{xx}\omega^2}{l_2^2}$$

the magnitude of the malaim and mallaunch rate approaches infinity making the launcher assembly increasingly unstable in these areas. The area of study is confined to

$$k << \frac{2 I_{xx} \omega^2}{l_2^2}$$

Figures 14 and 15 show malaim and mallaunch rates as functions of time for support stiffnesses equal to zero.

The malaim is a finite value for zero stiffness at the end of guidance, but is zero before boost, Figure 16. The mallaunch is also finite at end of guidance, Figure 17, but is zero at time, t = 0.0. After boost, the mallaunch increases negatively then becomes positive at end of guidance. At end of guidance the mallaunch rate tends to become increasingly unstable for large bearing reactions and zero support stiffnesses.

Equations (36) and (37) are periodic functions of the operational spin rate, Figures 18 and 19, hence it is possible to minimize either malaim or mallaunch. The period for mallaunch is approximately 1.4 cycles. The operational spin rate need vary only 0.35 cycles per second at the end of guidance for the mallaunch rate to go from zero to a maximum. For a missile with an operational spin rate of 158 cycles per second, the deviation from zero to maximum mallaunch is 0.22%.

Equations (36) and (37) are also periodic functions of time. The mallaunch rate and the malaim become increasingly large, Figures 20 and 21 as the missile approaches end of guidance. By close selection

of the average acceleration of the rocket, the time at end of guidance may be selected such that the mallaunch rate is zero.

As the mallaunch rate is the time rate of change of malaim, it will not be possible to null both variables at the same time. The malaim affects only the point of impact of a launched missile and can easily be accounted for with initial aim. The mallaunch rate affects the actual trajectory of flight, and hence, should be nulled.

The performance of the missile is very sensitive to any changes in its operational spin rate. The bearing forces increase with the square of the operational spin rate. The time to end of guidance is a direct function of the average acceleration, and hence, the thrust and the operational spin rate of the rocket must be tightly controlled.

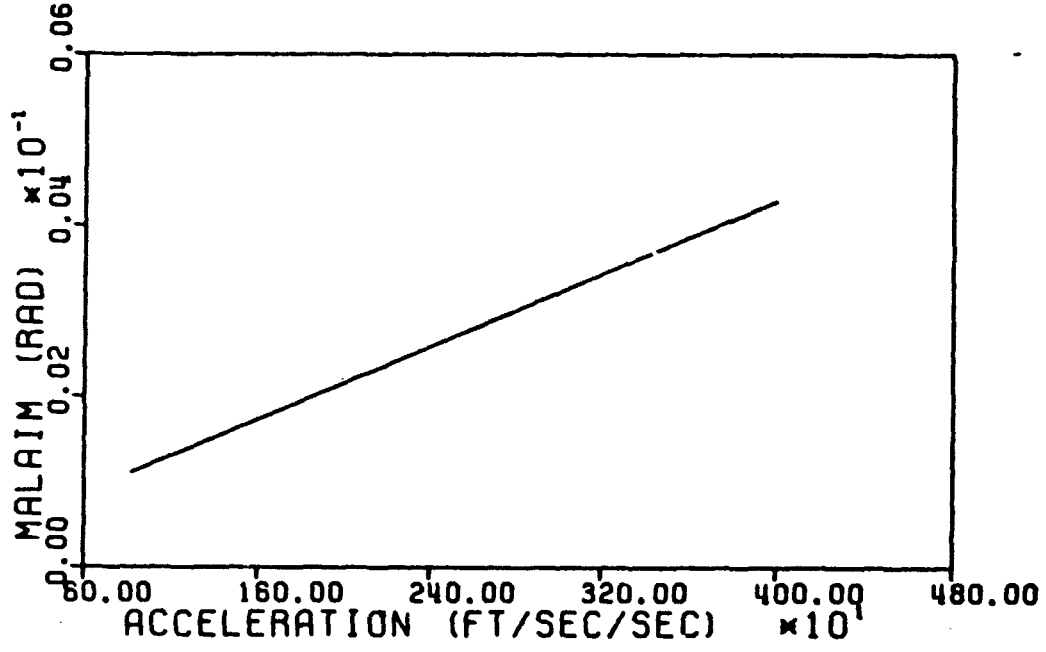

Figure 8. Malaim versus Acceleration
(ω = 158 cps, P_B = 50 lbf)

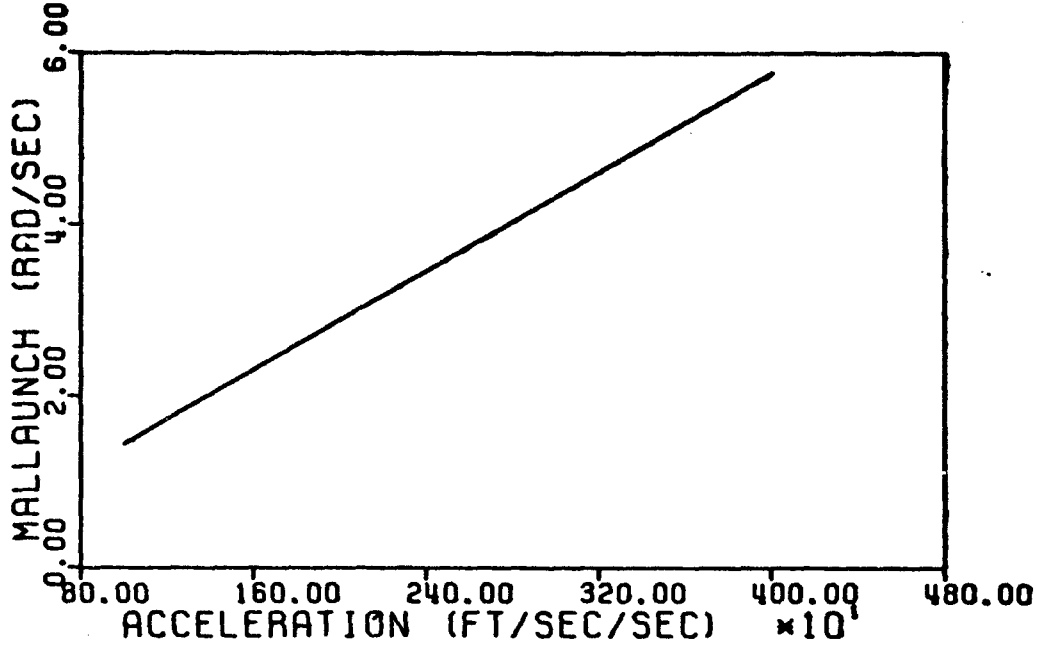

Figure 9. Mallaunch versus Acceleration
(ω = 158 cps, P_B = 50 lbf)

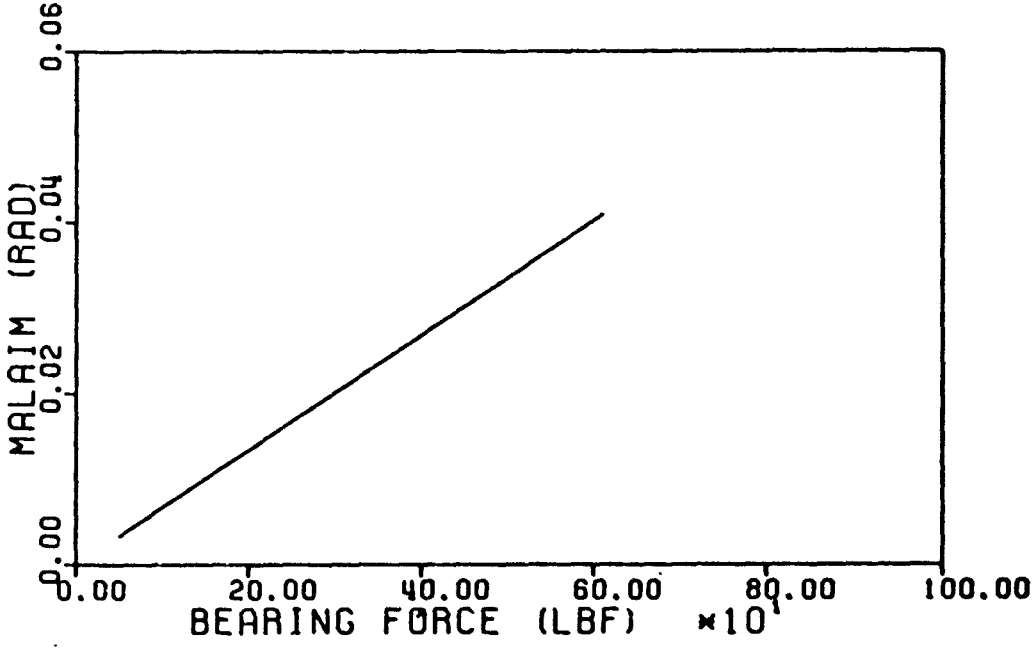

Figure 10. Malaim versus Bearing Reaction
(ω = 158 cps, P_B = 50 lbf)

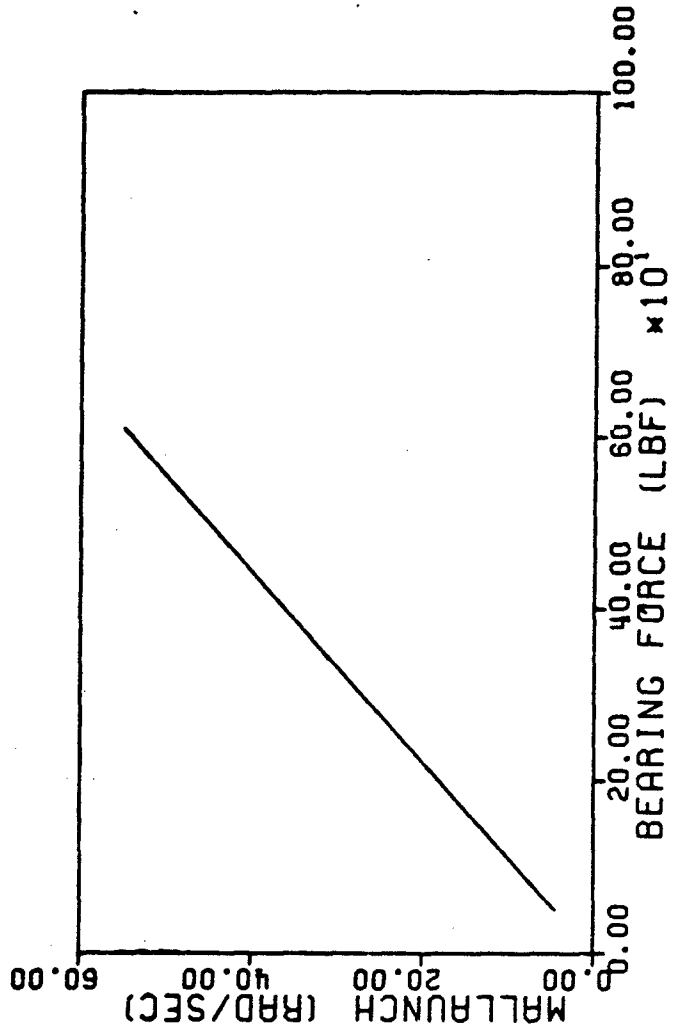

Figure 11. Mallaunch Rate versus Bearing Reaction
(ω = 158 cps, P_B = 50 lbf)

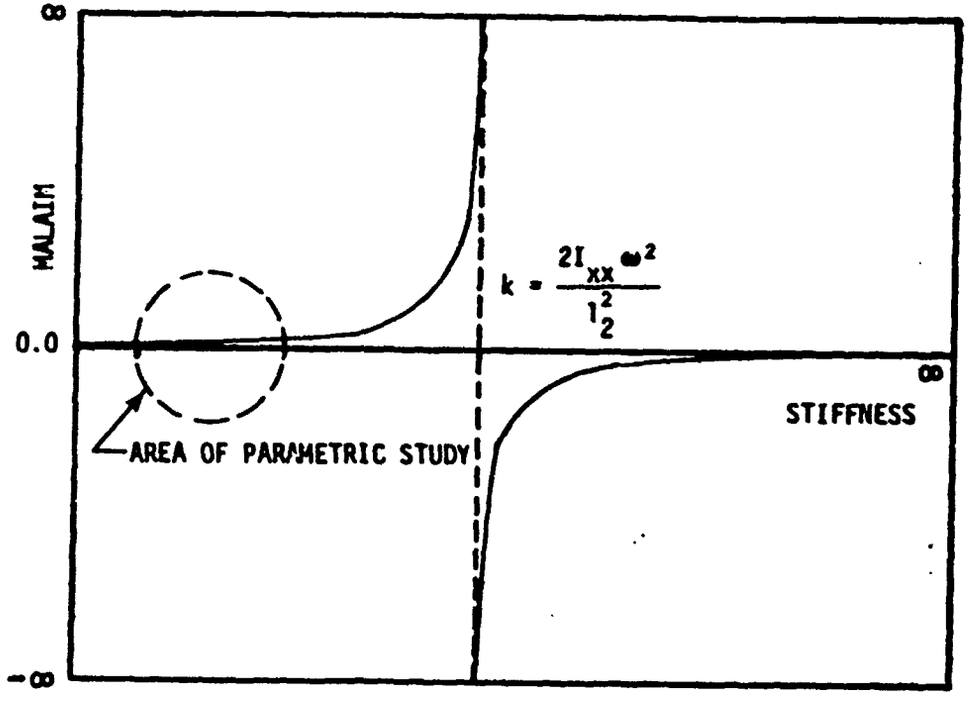

Figure 12. Malaim versus Stiffness at End of Guidance

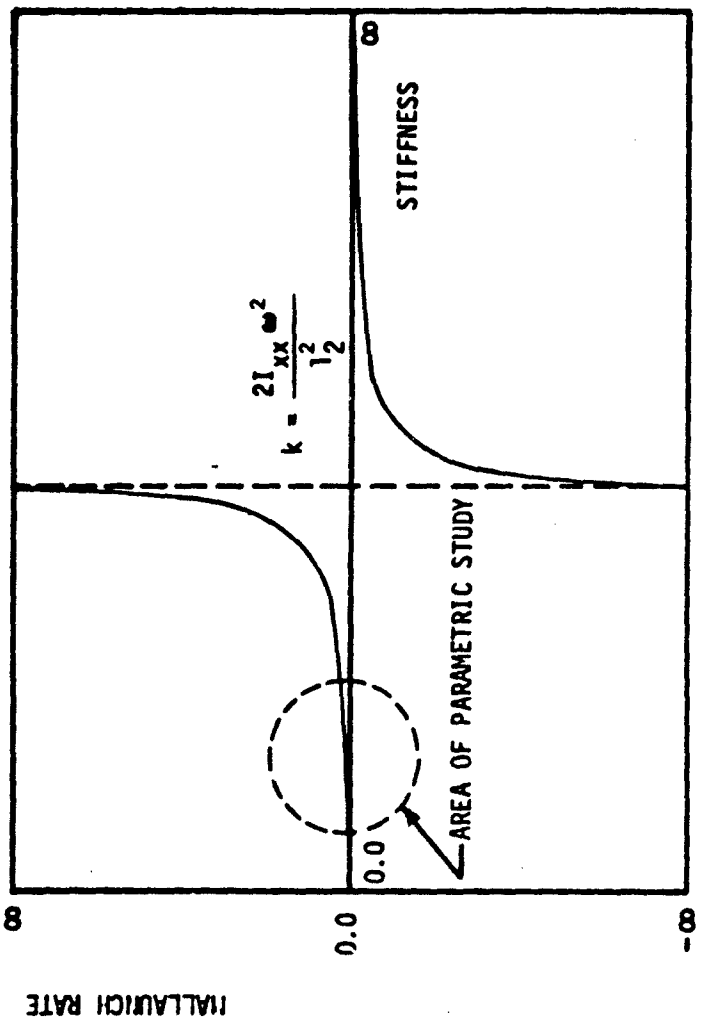

Figure 13. Mallaunch Rate versus Stiffness at End of Guidance

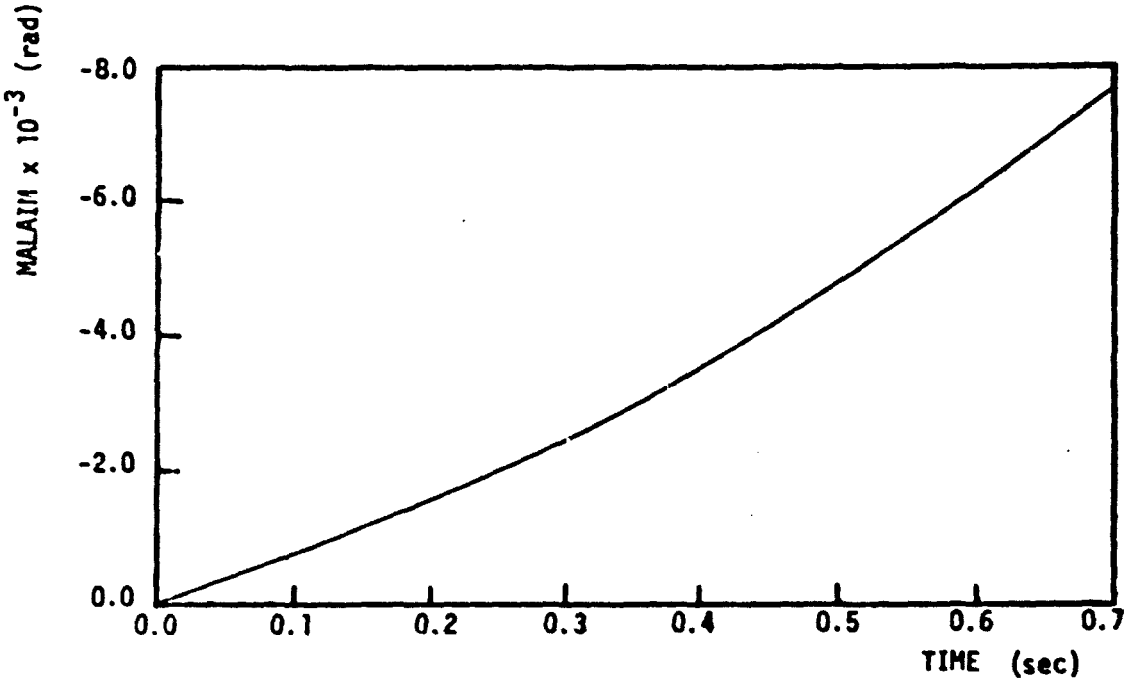

Figure 14. Malaim versus Time for k = 0.0

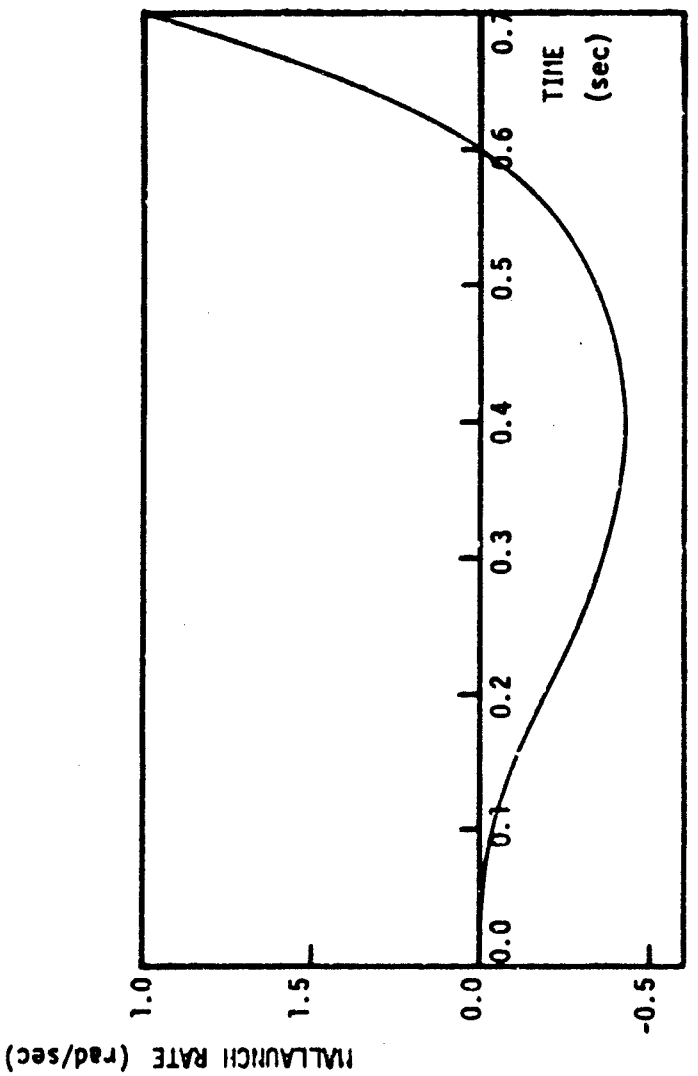

Figure 15. Mallaunch Rate versus Time at k = 0.0

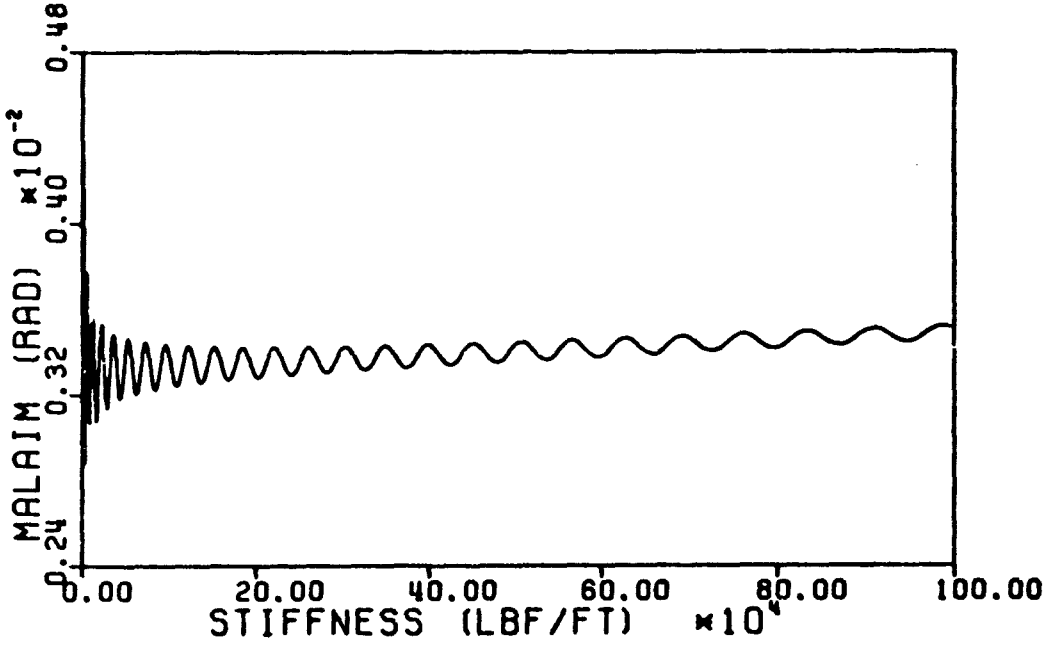

Figure 16. Malaim versus Stiffness at End of Guidance
(ω = 158 cps, a = 3122.316 ft/sec^2)

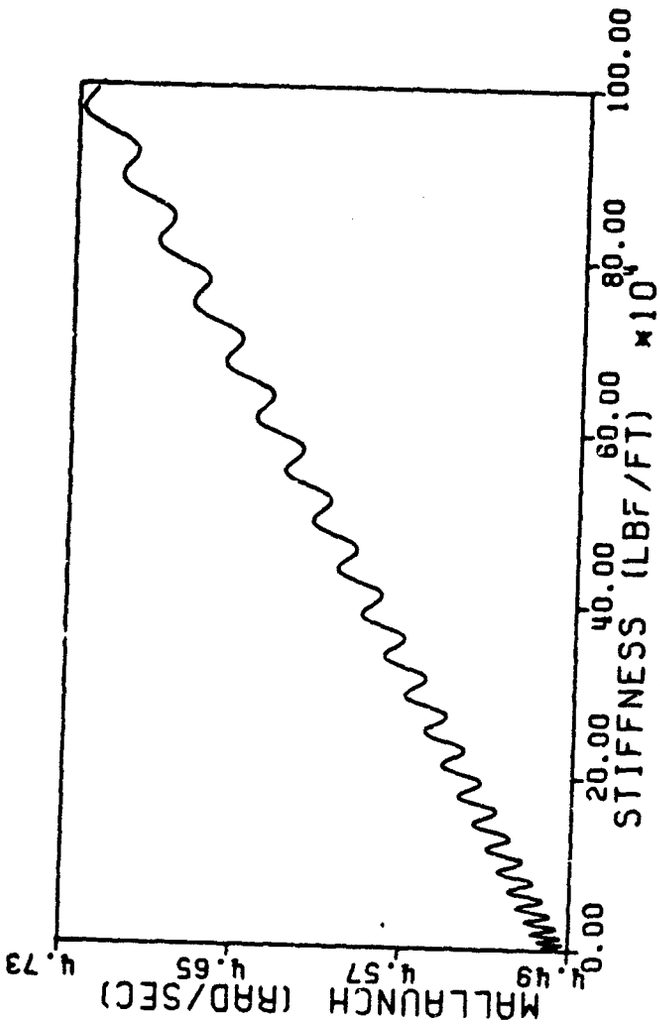

Figure 17. Mallaunch Rate versus Stiffness at End of Guidance (ω = 158 cps, a = 3122.316 ft/sec^2)

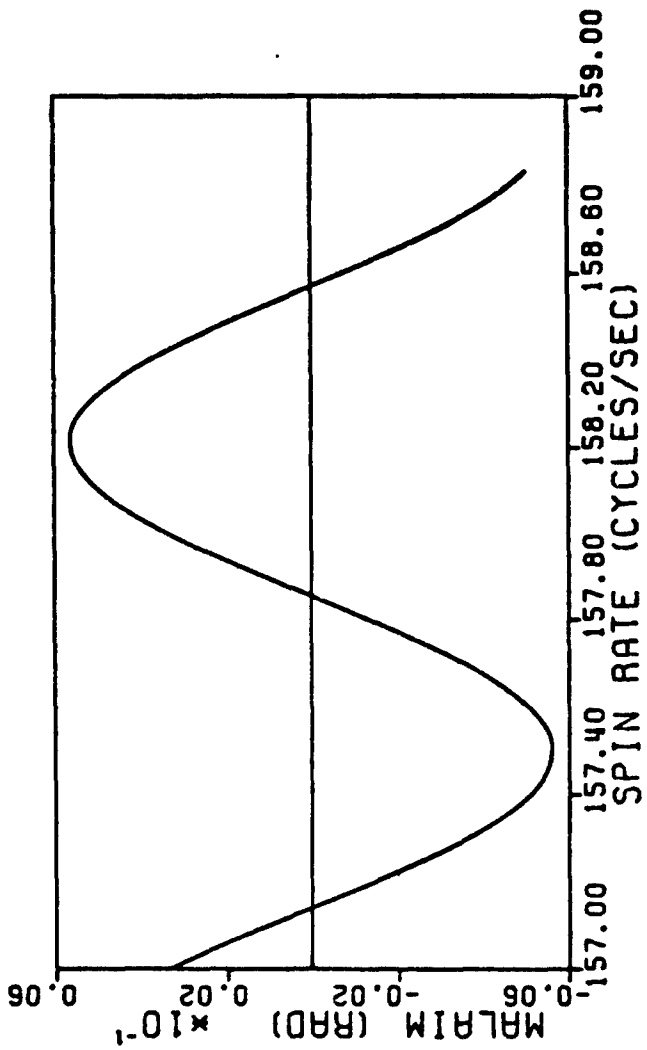

Figure 18. Malaim versus Spin Rate at End of Guidance
(a = 3122.316 ft/sec^2, P_B = 50 lbf)

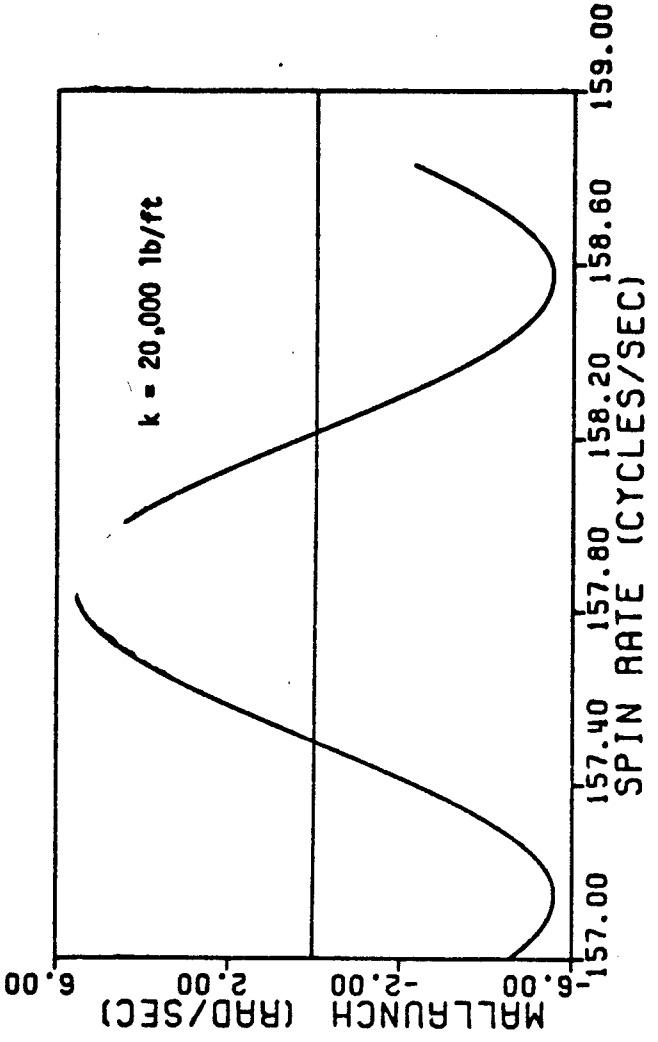

Figure 19. Mallaunch Rate versus Spin Rate at End of Guidance (P_B = 50 lbf, a = 3122.316 ft/sec^2)

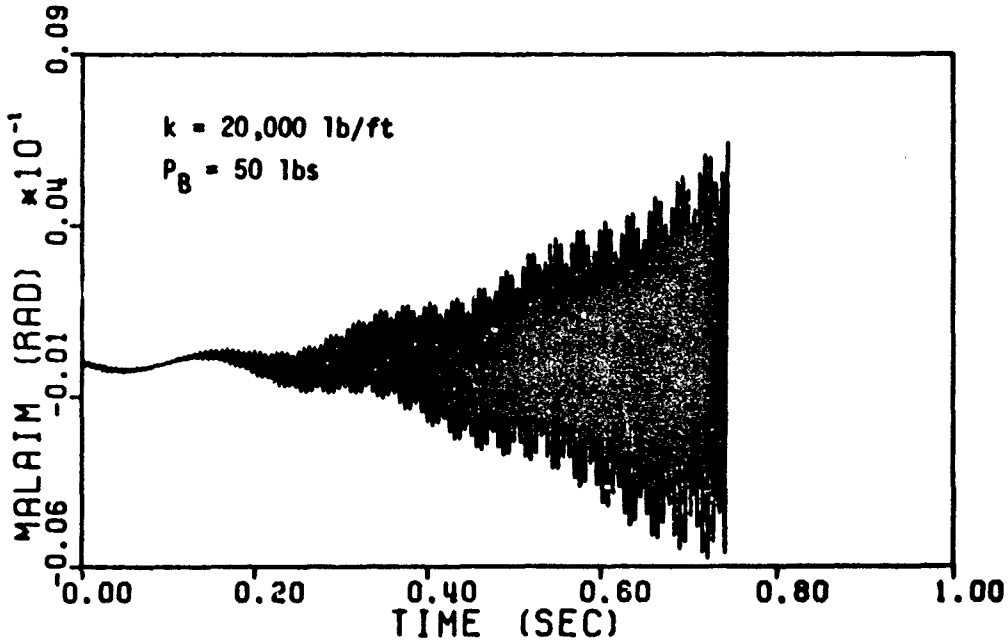

Figure 20. Malaim versus Time
(a = 3122.316 ft/sec^2, ω = 158 cps)

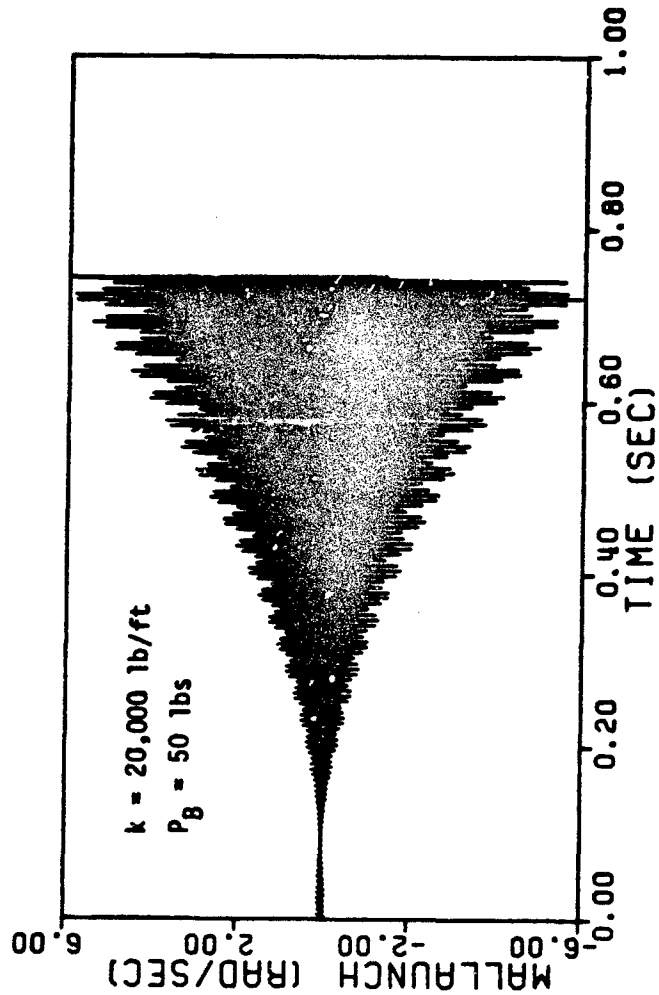

Figure 21. Mallaunch Rate versus Time
(a = 3122.316 ft/sec^2, ω = 158 cps)

E. REFERENCES

1. Robert H. Cannon, Jr., Dynamics of Physical Systems, McGraw-Hill Book Company, New York, 1967.

2. William E. Boyce and Richard C. DiPrima, Elementary Differential Equations and Boundary Value Problems, John Wiley & Sons, Inc., New York, 1969.

3. Murray R. Spiegel, Applied Differential Equations, Prentice-Hall, Inc., Englewood Cliffs, N. J., 1967.

4. William R. Longley, Percey F. Smith, and Wallace A. Wilson, Analytic Geometry and Calculus, Blaisdell Publishing Company, New York, 1965.

F. APPENDIX A COMPUTER PROGRAM

```
C     MAIN--MALAIM AND MALLAUNCH VERSUS STIFFNESS
      DIMENSION PITCHD(1,498), PITCH1(1,498), AK1(1,498),
     1PB1(1,498)
   26 FORMAT(4E15.4)
C
C     OM IS THE OPERATIONAL SPIN RATE OF THE ROCKET. (RAD/SEC)
C
      OM=158.0*2.*3.14159
C
C
C     PF AND PB ARE THE MAGNITUDES OF THE BEARING FORCES
C     OF THE ROCKET'S FRONT AND REAR BEARINGS RESPECTIVELY.
C     (LBF)
C
      PB=50.0
      PF=50.0
C
C
C     AM IS THE MASS OF THE  MULTITUBE LAUNCHING ASSEMBLY.
C     (SLUGS)
C
      AM=223.5/32.2
C
C
C     AJ IS THE MOMENT OF INERTIA ABOUT THE X-AXIS.
C     (SLUGS-FT-FT)
C
      AJ=13.6
C
C
C     D2 IS THE DISTANCE BETWEEN THE MOUNTING LUGS OF THE
C     LAUNCHER ASSEMBLY. (FT)
C
      D2=14./12.
C
C
C     D3 IS THE DISTANCE FROM THE AFT END OF THE ROCKET TO
C     THE CENTER OF GRAVITY. (FT)
C
      D3=24.493 /12.
C
C
C     D4 IS THE CENTER TO CENTER DISTANCE BETWEEN THE
C     BEARINGS. (FT)
C
      D4=25.69/12.
C
C
```

```
C     A IS  THE AVERAGE ACCELERATION OF THE ROCKET AS IT IS
C     PROPELLED OUT THE  TUBE. (FT/SEC/SEC)
C
      A=3122.316
C
      DO 15 K=1,1
C
C     AK IS THE STIFFNESS OF THE MOUNTING LINKS. (LBF/FT)
C
      AK=1000.0
C
      DO 11 J=1,498
C     T IS THE ELAPSED TIME FROM INITIAL BOOST. (SEC)
C
      T=0.7
C
      AB=2.*AJ/(D2**2*AK)
      AC=(D3-D4)*PF+D3*PB
      AD=A*(PB+PF)
      AE=D2**2*AK-2.*AJ*OM**2
C
C     Z IS THE VERTICAL DISPLACEMENT. (FT)
C
      Z=-SQRT(AM/(2.*AK))*((PB-PF)*OM/(2.*AK-AM*OM**2))*SIN(
     1SQRT(2.*AK/AM)*T)+((PB-PF)/(2.*AK-AM*OM**2))*SIN(OM*T)
C
C     DZ IS THE RATE OF VERTICAL DISPLACEMENT. (FT/SEC)
C
      DZ    =(PB-PF)*OM/(2.*AK-AM*OM**2)*(COS(OM*T)-COS(SQRT
     1(2.*AK/AM)*T))
C
C     PITCH IS THE MALAIM. (RAD)
C
      PITCH=SQRT(AB)*(2.*OM*AC/AE+12.*OM*AJ*AD/AE**2+32.*AJ
     1**2*OM**3*AD/AE**3)*SIN(SQRT(1./AB)*T)+AD/AE*T**2*SIN
     2(OM*T)-8.*AJ*OM*AD/AE**2*T*COS(OM*T)-(2.*AC/AE+4.*AJ*
     3AD/AE**2+32.*AJ**2*OM**3*AD/AE**3)*SIN(OM*T)
C
C     DPITCH IS THE MALLAUNCH RATE. (RAD/SEC)
C
      DPITCH    =(2.*OM*AC/AE+12.*OM*AJ*AD/AE**2+32.*AJ**2*
     1OM**3*AD/AE**3)*COS(SQRT(1./AB)*T)+2.*AD/AE*T*SIN(OM*T
     2)+OM*AD*T**2/AE*COS(OM*T)+(8.*AD*AJ*OM/AE**2)*(OM*T*
     3SIN(OM*T)-COS(OM*T))-(2.*AC/AE+4.*AJ*AD/AE**2+32.*AJ**
     42*OM**3*AD/AE**3)*OM*COS(OM*T)
      PITCHD(K,J)=DPITCH
      PITCH1(K,J)=PITCH
      PB1(K,J)=PB
```

```
      AK1(K,J)=AK
      AK =AK+2000.0
   11 CONTINUE
      PB=PB+225.0
   15 CONTINUE
      DO 16 K=1,1
      DO 16 J=1,498
   16 WRITE(6,26)PITCHD(K,J),PITCH1(K,J),PB1(K,J),AK1(K,J)
      CALL SPPLOT(AK1,'STIFFNESS (LBF/FT)',18,PITCH1,
     1'MALAIM (RAD)',12,
     2'FIGURE 8 MALAIM VS. STIFFNESS AT EOG',36,5.0,3.0,0,
     11,498)
      CALL SPPLOT(AK1,'STIFFNESS (LBF/FT)',18,PITCHD,
     1'MALLAUNCH (RAD/SEC)',19,
     2'FIGURE 14 MALLAUNCH RATE VS. STIFFNESS AT EOG',45,
     35.0,3.0,0,1,498)
       CALL PLOT(0.0,0.0,999)
      STOP
      END
```

```
      SUBROUTINE SPPLOT(X,XHDR,KX,Y,YHDR,KY,FHDR,KF,
     1ALENX,ALENY,LINTYP,NROW,NCOL)
C
C
C     SPPLOT IS A SUBROUTINE THAT WILL PLOT NROW NUMBER OF
C     LINES PER GRAPH.
C
C      THE ARGUMENTS OF THE LIST AREO
C         X   NAME OF THE ARRAY CONTAINING THE ABSCISSA OR X
C         VALUES.
C         Y   NAME OF THE ARRAY CONTAINING THE ORDINATE OR Y
C         VALUES.
C         XHDR AND KX DESCRIBE THE DESIRED LEGEND FOR THE
C         X-AXIS.
C         XHDR IS THE LITERAL EXPRESSION OF THE LEGEND TO BE
C         PRINTED.
C         KX IS THE INTEGER NUMBER OF CHARACTERS IN XHDR.
C         YHDR AND KY DESCRIBE THE DESIRED LEGEND FOR THE
C         Y-AXIS.
C         YHDR IS THE LITERAL EXPRESSION OF THE LEGEND TO BE
C         PRINTED.
C         KY IS THE INTEGER NUMBER OF CHARACTERS IN YHDR.
C         ALENX IS THE DESIRED LENGTH OF THE X-AXIS.
C         ALENY IS THE DESIRED LENGTH OF THE Y-AXIS.
C         LINTYP DETERMINES THE TYPE OF LINE YOU GET.
C         IF LINTYP GREATER THAN 0, YOU GET A STRAIGHT LINE
C           CONNECTING A SYMBOL PUT DOWN AT EVERY LINTYPTH
C         POINT.
C          THUS, IF LINTYP WERE EQUAL TO 2, YOU WOULD GET A
C         LINE CONNECTING EVERY SECOND POINT.
C          IF LINTYP WERE EQUAL TO 0, YOU WILL GET A LINE
C         ONLY.
C          IF LINTYP LESS THAN 0, YOU WOULD GET A SYMBOL
C         EVERY LINTYPTH POINT.
C
C
      DIMENSION X(NROW,NCOL), Y(NROW,NCOL), XHDR(20),
     1YHDR(20),FHDR(100)
      CALL GSIZE(11.0,11.0,1121)
      CALL SYMBOL(2.5,1.0,.15,FHDR,0.0,KF)
      CALL PLOT(2.5,5.5,3)
      CALL PLOT(7.5,5.5,2)
      CALL PLOT(7.5,2.5,2)
      CALL PLOT(2.5,2.5,-3)
      CALL SCALE2(X,ALENX,NROW,NCOL,FRX,DLX)
      CALL SCALE2(Y,ALENY,NROW,NCOL,FRY,DLY)
      CALL AXIS(0.0,0.0,XHDR,-KX,ALENX,0.0,FRX,DLX)
      CALL AXIS(0.0,0.0,YHDR,KY,ALENY,90.0,FRY,DLY)
```

```
      DO 32 J=1,NROW
      IF(J .NE. 1) CALL PLOT(0.0,0.0,3)
      INTEQ=J
      IPEN = 3
      ICODE = -1
      NT =IABS(LINTYP)
      IF (LINTYP)7,6,7
    6 NT=1
    7 NF=1
      NA = NT
      KK=1
      IF (LINTYP) 11,12,13
   11 IPENA = 3
      ICODEA = -1
      LSW = 1
      GO TO 15
   12 NA=NCOL
   13 IPENA = 2
      ICODEA = -2
      LSW=0
   15 DO 30 I=1,NCOL
      XN=(X(J,I)-FRX)/DLX
      YN=(Y(J,I)-FRY)/DLY
      IF (NA-NT) 20,21,22
   20 IF (LSW) 23,22,23
   21 CALL SYMBOL (XN,YN,0.08,INTEQ,0.0,ICODE)
      NA = 1
      GO TO 25
   22 CALL PLOT (XN,YN,IPEN)
   23 NA = NA + 1
   25 NF = NF+KK
      ICODE = ICODEA
   30 IPEN = IPENA
   31 CONTINUE
   32 CONTINUE
      RETURN
      END
```

```
      SUBROUTINE SCALE2(ARRAY,AXLEN,NROW,NCOL,FIRST,DEL)
C          ARRAY    NAME OF ARRAY CONTAINING VALUES TO BE
C                   SCALED.
C          AXLEN    LENGTH IN INCHES OVER WHICH ARRAY IS TO
C                   BE SCALED.
C          NPTS     NUMBER OF POINTS TO BE SCALED.
C          INC      INCREMENT OF LOCATION OF SUCCESSIVE
C                   POINTS.
      DIMENSION ARRAY(NROW,NCOL),SAVE(7)
      SAVE(1)=1.0
      SAVE(2)=2.0
      SAVE(3)=4.0
      SAVE(4)=5.0
      SAVE(5)=8.0
      SAVE(6)=10.0
      SAVE(7)=20.
      FAD=0.01
      INC=1
      NPTS=NCOL
      K=IABS(INC)
      N=NPTS*K
      Y1=1.0E60
      YF=-1.0E-60
      DO 26 JJ=1,NROW
      YO=ARRAY(JJ,1)
      YN=YO
      DO 26 I=1,N,K
      YS=ARRAY(JJ,I)
      IF  (YO-YS)  22,22,21
   21 YO=YS
      GO  TO  25
   22 IF  (YS-YN)  25,25,24
   24 YN=YS
   25 IF(YN .GT. YF)YF=YN
      IF(YO .LT. Y1)Y1=YO
   26 CONTINUE
      YO=Y1
      YN=YF
      FIRSTV=YO
      IF  (YO)  34,35,35
   34 FAD=FAD-1.0
   35 DELTAV=(YN-FIRSTV)/AXLEN
      IF (DELTAV) 70,70,40
   40 I=ALOG10(DELTAV)+1000.0
      P=10.0**(I-1000)
      DELTAV=DELTAV/P-0.01
      DO  45  I=1,6
      IS=I
```

```
      IF  (SAVE(I)-DELTAV)  45,50,50
   45 CONTINUE
   50 DELTAV=SAVE(IS)*P
      FIRSTV=DELTAV*AINT(YO/DELTAV+FAC)
      T=FIRSTV+(AXLEN+0.01)*DELTAV
      IF (T-YN)  55,57,57
   55 FIRSTV=P*AINT(YO/P+FAC)
      T=FIRSTV+(AXLEN+.01)*DELTAV
      IF (T-YN) 56,57,57
   56 IS=IS+1
      GO  TO  50
   57 FIRSTV=FIRSTV-AINT((AXLEN+(FIRSTV-YN)/DELTAV)/2.0)*
     1DELTAV
      IF (YO*FIRSTV) 58,58,59
   58 FIRSTV=0.0
   59 IF  (INC) 61,61,65
   61 FIRSTV=FIRSTV+AINT(AXLEN+.5)*DELTAV
      DELTAV=-DELTAV
   65 FIRST=FIRSTV
      DEL=DELTAV
   67 RETURN
   70 DELTAV=2.0*FIRSTV
      DELTAV=ABS(DELTAV/AXLEN)+1.
      GO TO 40
      END
```